Polymer Chemistry, **2021** DOI: 10.1039/d1py00843a

ELECTRONIC SUPPORTING INFORMATION

OF THE ARTICLE

THERMORESPONSIVE PROPERTIES OF POLYACRYLAMIDES IN PHYSIOLOGICAL SOLUTIONS

*Kristýna Kolouchová,[1] Volodymyr Lobaz,[1] Hynek Beneš,[1] Victor R. de la Rosa,[2,3] David Babuka,[1,4] Pavel Švec,[1,5] Peter Černoch,[1] Martin Hrubý,[1] Richard Hoogenboom,[2,]*Petr Štěpánek,[1] and Ondřej Groborz[1,6,7,]**

[1]Institute of Macromolecular Chemistry, Czech Academy of Sciences, Heyrovsky square 2, 162 06 Prague 6, Czech Republic
[2]Department of Organic and Macromolecular Chemistry, Ghent University, Krijgslaan 281-S4, 9000 Ghent, Belgium
[3]AVROXA BV, Technologiepark-Zwijnaarde 82, B-9052 Ghent, Belgium
[4]Department of Biophysics, Institute of Physics, Faculty of Mathematics and Physics, Charles University, Ke Karlovu 3, Prague 2, 121 16, Czech Republic
[5]Department of Physical and Macromolecular Chemistry, Faculty of Science, Charles University, Hlavova 8, Prague 2, 128 00, Czech Republic
[6]Institute of Biophysics and Informatics, Charles University, First Faculty of Medicine, Salmovská 1, 120 00 Prague 2, Czech Republic
[7]Department of Organic and Medicinal Chemistry, Charles University, Faculty of Science, Hlavova 8, 128 43 Prague 2, Czech Republic

*corresponding authors: O. Groborz: ondrej.groborz@seznam.cz, richard.hoogenboom@ugent.be

Table of Content – List of Chapters

Table of Content – List of Schemes

Table of Content – List of Tables

Table of Content – List of Figures

Nuclear magnetic resonance data

Size exclusion chromatographs

Turbidimetry measurements

S1. Materials

N,N-dimethylformamide (DMF) and tetrahydrofuran (THF) were purchased from Lach-Ner s.r.o. (Neratovice, Czech Republic) in analytical quality, dried using molecular sieves 3.0 Å and distilled before their use. MeOH-4d (99.80% D) was purchased from Eurisotope (Saint-Aubin, France). 2,2-Difluoroethylamine (97%) was purchased from Fluorochem (Derbyshire, UK). Argon 5.0 ($c_{Ar} \geq 99.999\%$) was purchased from Messer Technogas s.r.o. (Prague, Czech Republic). Foetal bovine serum (FBS, qualified, heat inactivated, 10500-064, LOT 2165873H) was purchased from Thermo Fisher Scientific (Waltham, MA, USA). Triethylamine (TEA, ≥ 99%), acryloyl chloride (99%, ≈ 400 ppm phenothiazine), pyrrolidine (≥ 99.0%), *N*,*N*-diethylacrylamide (99%, < 200 ppm MeHQ), and *N*-isopropylacrylamide (≥ 99.0%) were purchased from Sigma-Aldrich s.r.o. (Prague, Czech Republic). Foetal bovine serum was stored at –22 °C; monomers, their precursors and NMR solvents were stored at 4 °C; the remaining chemicals were stored a dry, dark storage at room temperature. All chemicals were used without any additional purification, unless stated otherwise.

S2. Experimental

S2.1. Monomer synthesis

(*N*-acryloyl)pyrrolidine and ***N*-(2,2-difluoroethyl)acrylamide** were synthesised from acryloyl chloride and the corresponding amines (**Scheme S1**) as previously published in the literature,[S1,S2] with slight modification. The remaining monomers were purchased.

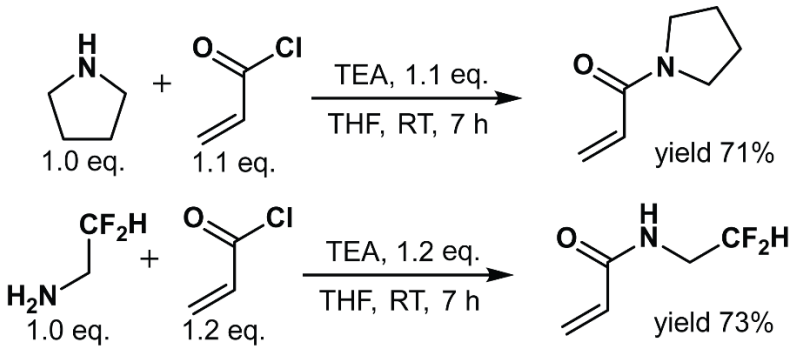

Scheme S1. Synthesis of **(*N*-acryloyl)pyrrolidine** and ***N*-(2,2-difluoroethyl)acrylamide** from acryloyl chloride and the corresponding amines

Pyrrolidine (18.7 mL, 16.2 g, 228 mmol) or 2,2-difluoroethylamine (14.0 mL, 16.8 g, 207 mmol), respectively, were mixed with triethylamine (34.0 mL, 24.8 g, 245 mmol), dissolved in dry tetrahydrofuran (THF, 250 mL), and cooled down to 0 °C on a water/ice bath. Acryloyl chloride (freshly distilled at atmospheric pressure, 20.0 mL, 22.4 g, 247 mmol) was dissolved in dry THF (40 mL), and this solution was added dropwise to the amine solution under constant stirring until cooling to 0 °C. After this step, the reaction mixture was stirred at room temperature for 7 h and subsequently diluted with diethyl ether (500 mL) and filtered. The filtrate was washed with an aqueous $NaHCO_3$ solution, water, and saline using a separatory funnel. The organic phases were dried with $MgSO_4$, the solvent was removed using a rotary evaporator, and the product was purified by flash chromatography in multiple batches (mobile phase: ethyl acetate/hexane 1:2). The yields were 20.2 g (71%) for (*N*-acryloyl)pyrrolidine and 20.4 g (73%) for *N*-(2,2-difluoroethyl)acrylamide.

***N*-acryloylpyrrolidine**: ^{1}H (MeOH-4d): 6.62 (dd, J = 16.8, 10.4 Hz, 1H), 6.27 (dd, J = 16.8, 2.0 Hz, 1H), 5.74 (dd, J = 10.4, 2.0 Hz, 1H), 3.62 (t, J = 6.8 Hz, 1H), 3.50 (t, J = 6.9 Hz, 1H), 2.07-1.85 (m, 4H). ^{13}C: 165.1, 128.7, 126.6, 46.5, 45.7, 25.6, 23.8 ppm. (**Figure S1** to **S3**)

***N*-(2,2-difluoroethyl)acrylamide**: ^{1}H (DMSO-6d): 8.48 (t, J = 4.9 Hz, 1H), 6.28 (dd, J = 17.1, 10.1 Hz, 1H), 6.14 (dd, J = 17.1, 2.2 Hz, 1H), 6.04 (tt, J = 55.8, 3.8 Hz, 1H), 5.65 (dd, J = 10.1, 2.2 Hz, 1H),

3.57 ppm (tdd, J = 16.1, 6.0, 3.9 Hz, 2H). ^{13}C: 165.66, 131.40, 126.67, 114.95 (t, J = 239.7 Hz), 41.29 ppm (t, J = 25.6 Hz). ^{19}F: –121.79 ppm (dt, J = 55.9, 16.1 Hz). (**Figure S4** to **S7**)

S2.2. Polymer synthesis

Poly[*N*-(2,2-difluoroethyl)acrylamide] (**pDFEA**), poly(*N*-isopropylacrylamide) (**pNIPAM**), poly(*N*-diethylacrylamide) (**pDEA**) and poly(*N*-acryloylpyrrolidine) (**pAP**) were prepared by reversible addition−fragmentation chain-transfer polymerisation (RAFT)[S3] with 4-cyano-4-[(dodecylsulfanylthiocarbonyl)sulfanyl]pentanoic acid as the RAFT polymerisation chain transfer agent (CTA)[S4] and 4,4′-azobis(4-cyanovaleric acid) (ACVA) as the initiator (**Figure 2**).[S3]

The polymerisation mixture consisted of a specific monomer (1.50 to 2.00 g), CTA and ACVA in various molar ratios and dried DMF (**Table S1**). The mixture was bubbled with argon in an oven-dried Schlenk flask, heated to 70 °C in an oil bath and stirred with a magnetic stirring bar overnight. Subsequently, the product was precipitated in diethyl ether, filtered, and the polymer was re-dissolved in methanol and purified using a Sephadex™ LH-20 column and methanol as the eluent. The polymer-containing fractions were evaporated in a rotatory evaporator under reduced pressure, and the polymer was re-dissolved in water and isolated by freeze-drying.

Table S1. Volumes/ mass/ molar amount of solvent (V_{DMF}), monomers (m_{mon}, n_{mon}), charge transfer agent (m_{CTA}, n_{CTA}) and initiator (m_{ini}, n_{ini}) used in polymer synthesis

Polymer/code		V_{DMF} (mL)	m_{mon} (g)	n_{mon} (mmol)	m_{CTA} (mg)	n_{CTA} (µmol)	m_{ini} (mg)	n_{ini} (µmol)
pDFEA	F1	4.00	1.50	11.1	21.2	52.5	4.41	15.8
	F2				14.1	35.0	2.94	10.5
	F3				8.5	21.0	1.77	6.3
pNIPAM	I1	6.00	2.00	17.7	56.5	140	11.8	42.0
	I2				28.3	70.0	5.89	21.0
	I3				18.8	46.7	3.92	14.0
pDEA	E1	6.00	2.00	15.7	28.3	70.0	5.89	21.0
	E2				14.1	35.0	2.94	10.5
	E3				11.3	28.0	2.35	8.4
pAP	P1	4.00	1.50	12.0	42.4	105	8.82	31.5
	P2				21.2	52.5	4.41	15.8
	P3				14.1	35.0	2.94	10.5

After polymerisation, the CTA group was removed by aminolysis using propylamine ($PrNH_2$), followed by nucleophilic addition of methyl acrylate to the thiol end-group in dry DMF under an argon atmosphere, as previously reported (**Figure 2**).[S5] Polymer-CTA, propylamine, and tris(2-carboxyethyl)phosphine hydrochloride (to prevent the oxidation of thiols to disulphides[S6]) were dissolved in DMF (5.00 mL). The reaction mixture was stirred for 120 min at room temperature under a nitrogen atmosphere. Methyl acrylate was added to the reaction mixture and stirred at room temperature for 24 h. The polymers were purified using the procedure mentioned above. Yields and reactant amounts are summarised in **Table S1** and **Table S2**.

pDFEA: ^{1}H (MeOH-4d): 8.00 (1H), 5.95 (t, J = 56.1, 1H), 3.58 (t, J = 14.4 Hz, 2H), 2.18 (1H), 1.67 ppm (2H); ^{13}C: 176.2, 114.2 (J = 239.5 Hz), 41.8 (t, J = 28.1 Hz), 35.1 ppm; ^{19}F: –123.8 ppm (2F). (**Figure S8** to **S11**)

pNIPAM: ^{1}H (MeOH-4d): 7.63 (1H), 3.98 (1H), 2.11 (1H), 1.60 (2H), 1.17 ppm (6H); ^{13}C: 174.8, 42.9, 41.1-41.9, 35.0, 21.4 ppm. (**Figure S12** to **S14**)

pDEA: ^{1}H (MeOH-4d): 3.52-3.36 (4H), 2.65 (1H), 1.74-1.81 (2H), 1.13 ppm (6H); ^{13}C: 174.2, 40.2-41.8, 36.6, 36.1, 12.0-13.8 ppm. (**Figure S15** to **S17**)

pAP: ^{1}H (MeOH-4d): 3.1-3.8 (4H), 2.3-2.7 (1H), 1.96 (4H), 1.68 ppm (2H); ^{13}C: 173.7, 45.9-46.5, 39.0, 35.0, 24.0-25.7 ppm. (**Figure S18** to **S20**)

Table S2. Mass and molar amount of previously prepared polymers (m_{pol}, n_{pol}), propylamine (V_{PA}, n_{PA}), tris(2-carboxyethyl)phosphine hydrochloride (m_{TCEP}, n_{TCEP}), and methyl acrylate (V_{MA}, n_{MA})

Polymer/code		m_{pol} (g)	n_{pol} (µmol)	n_{PA} (mmol)	V_{PA} (µL)	n_{TCEP} (µmol)	m_{TCEP} (mg)	n_{MA} (mmol)	V_{MA} (mL)
pDFEA	F1	1.00	38.2	1.91	81.2	38.2	11.0	6.69	550
	F2		27.6	1.38	58.7	27.6	7.9	4.83	400
	F3		20.2	1.01	42.9	20.2	5.8	3.54	290
pNIPAM	I1	1.00	49.5	2.48	105.2	49.5	14.1	8.66	710
	I2		31.6	1.58	67.2	31.6	9.1	5.53	450
	I3		20.6	1.03	43.8	20.6	5.9	3.61	290
pDEA	E1	1.00	44.8	2.24	95.2	44.8	12.8	7.84	640
	E2		28.8	1.44	61.2	28.8	8.3	5.04	410
	E3		24.2	1.21	51.4	24.2	6.9	4.24	350
pAP	P1	1.00	51.0	2.55	108.4	51.0	14.6	8.93	730
	P2		27.8	1.39	59.1	27.8	8.0	4.87	400
	P3		19.5	0.98	41.4	19.5	5.6	3.41	280

S2.3. NMR spectroscopy

All NMR spectra were measured on a Bruker Avance III HD 400 MHz spectrometer (Bruker, Billerica, MA, USA) equipped with a broadband probe. All compounds (5 to 10 mg) were dissolved in MeOH-4d or DMSO-6d (0.50 to 0.80 mL). The following spectra were assessed: ^{1}H NMR (32 scans, relaxation delay 30.0 s), ^{13}C NMR (^{1}H decoupled, 1024 scans, relaxation delay 2.00 s), ^{19}F NMR (64 scans, relaxation delay 5.00 s), ^{1}H-^{13}C multiplicity-edited HSQC (heteronuclear single quantum coherence spectroscopy)[S7,S8] (2 scans, relaxation delay 1.50 s, size of the fid 2048 by 256, spectral width 14.0 by 200 ppm, using ^{1}H and ^{13}C external projections), see **Figure S1 to S20**. These spectra were used for polymer structure confirmation and peak-matching. In addition, we used ^{1}H NMR spectra of all polymers (256 scans, relaxation delay 5.00 s) to determine polymer purity and end-moiety conversion. The spectra were processed in TopSpin 3.6.1 (Bruker, Billerica, MA, USA) and MestReNova 6.0.2 (Mestrelab Research S.L., Santiago de Compostela, Spain), trace contaminates were assigned according to reference.[S9] Both processes and non-processed NMR spectra of all polymers are available from the **NMR.rar** file on the website of the journal.

All 1D spectra were processed in MestReNova 6.0.2 (Mestrelab Research S.L., Santiago de Compostela, Spain), and all 2D spectra were processed in TopSpin 3.6.1 (Bruker, Billerica, MA, USA).

S2.4. Size exclusion chromatography

The number-average molar mass (M_n), weight-average molar mass (M_w), and polymer dispersity ($Đ_M = M_w/M_n$) were determined by SEC using an HPLC Ultimate 3000 system (Dionex, Sunnyvale, CA, USA) equipped with an SEC column (TSKgel SuperAW3000 150 × 6 mm, 4 µm). Three detectors, UV/VIS, refractive index (RI) Optilab®-rEX and multiangle light scattering (MALS) DAWN® EOS (Wyatt Technology Co., Santa Barbara, CA, USA), were employed with a methanol (A) and sodium acetate buffer (B, 0.3 M, pH 6.5) mixture (A:B = 80:20 v/v, flow rate of 0.6 mL·min^{-1}) as the mobile phase (**Figure S21** to **S24**). The dn/dc of the mobile phase and polymers was 0.1100 (**pDFEA**), 0.1540 (**pNIPAM**), 0.2015 (**pDEA**), and 0.1646 mL·g^{-1} (**pAP**) at 620 nm and 20 °C.

S2.5. Turbidimetry

Turbidimetry was measured on a Crystal16™ parallel crystalliser turbidimeter (Avantium Technologies, Ontario, Canada) connected to a recirculation chiller and dry compressed air. Aqueous polymer solutions were heated from 10.0 °C to 55.0 °C (in some cases to 80.0 °C) with a heating rate of 0.5 $K \cdot min^{-1}$, followed by cooling to 10 °C and maintaining this temperature for 30 min. Each measurement was repeated 6 times; the samples were stirred at 700 rpm.

All polymers were dissolved in ultrapure water, phosphate buffered saline (PBS, 140 mM, pH = 7.40, Dulbecco type[S10]) or foetal bovine serum (FBS) at a concentration of 1.25, 2.50, 5.00, 10.0, 20.0 and 40.0 mg/mL. The samples were stored at 4°C before their measurements. Transmittance was monitored at λ = 600 nm. A sudden decrease of transmittance below 50% indicated the cloud point temperature. [S11]

S2.6. Refractive index increment (d*n*/d*c*)

We measured the refractive index increment (d*n*/d*c*) of all study polymers (in PBS in five different concentrations (*ca.* ≈ 0.12 to ≈ 2.3 mg/mL) on a PSS DnDc-2010/620 differential refractometer (Polymer Standard Service, Mainz, Germany) at 620 nm and 29.0 °C. The data were processed using Differential Refractometer Software (version 5.32, Brookhaven Instruments Corp., Holtsville, NY, USA), see **Figure S57 to S68**. The refractometer was calibrated using a series of aqueous solutions of potassium chloride according to the user manual.

S2.7. Dynamic light scattering (DLS)

We determined the size of the polymer assemblies by dynamic light scattering (DLS) on a Zetasizer Nano-ZS, Model ZEN3600 (Malvern Instruments, Malvern, UK) at θ = 173° scattering angle and at 15.0 to 60.0 °C with 0.5 °C increment and 2 min of temperature equilibration per step. The measurement was repeated 3 times at each step. All samples were filtered using 0.45 μm PVDF filters before the measurements. The data were evaluated using the Zetasizer software (Nano, version 7.10, Malvern, UK), JMalgen (v.2.0, Institute of Macromolecular Chemistry, Prague, Czech Republic), Genr (v.11, Institute of Macromolecular Chemistry, Prague, Czech Republic)[S12] and Matlab (v.9.9.0.1467703 (R2020b), The MathWorks, Inc., Natick, MA, USA). We present the DLS results as intensity-based size distributions because they entail smaller calculation errors than volume or number-based size distributions.

S2.8. Isothermal titration calorimetry

F1, **F2**, **F3**, **I3**, **E3** or **P3** polymer solutions (10 mg/mL, 201 μL) in ultrapure water were titrated with PBS or FBS using ITC 200 titration calorimeter (Malvern Panalytical, Malvern, UK). In each run, 40 μL of PBS or FBS was added in consecutive injections (the first injection was always 0.1 μL; then with increment 0.5 or 1.0 μL). All samples were stirred at 1000 rpm and titrated at three temperatures: (i) below T_{CP}, 293 K for all polymers in all media; (ii) below T_{CP} in ultrapure water, but above T_{CP} in PBS or FBS, 298 K (**F1**), 301 K (**E3** and **F3**), 303 K (**I3**), 305 K (**F2**) and 323 K (**P3**); and (iii) above T_{CP} in all media, 313 K (**E3** and **I3**), 323 K (**F3**) and 333 K (**P3**). Subsequently, PBS and FBS were titrated to ultrapure water at all experimental temperatures to determine their heat of dilution (as blanks samples). In addition, PBS and FBS were titrated (10×1 μL injections) to the solution of benzoic acid (0.25 mM ≈ concentrations of polymers) at 293, 313 and 333 K to estimate the thermal contribution of the neutralization reaction of terminal carboxylic group (see **Figure S41** for details).

The isotherms of complex shape were fitted to two independent binding sites model (using Wiseman model[S13]). The ionic strength of PBS (162.7 mM) was accepted as the titrant concentration for both PBS and FBS. From the fit, the reaction enthalpy change ΔH for the first binding site (kJ/mol of polymer) was extracted and normalized to the concentration of the monomer units. Other fitting

parameters (stoichiometry n and association constant K, M^{-1}) were not used in the discussion (see **Figures S37** to **S43** for details).

S2.9. Data processing

All data were processed in Microsoft Office 365 Pro Plus 16.0 (Microsoft, Redmond, WA, USA) and OriginPro 8.6.0 (OriginLab Corporation, Northampton, MA, USA) unless stated otherwise. The schemes and structures were drawn in ChemDraw Professional 16.0.1.4 (77) (Perkin Elmer Informatics, Inc., Waltham, MA, USA). The graphics were processed in Adobe Illustrator CS6 16.0.0 (Adobe Systems Inc., San Jose, CA, USA).

DOI: 10.1039/d1py00843a

S3. NMR spectra

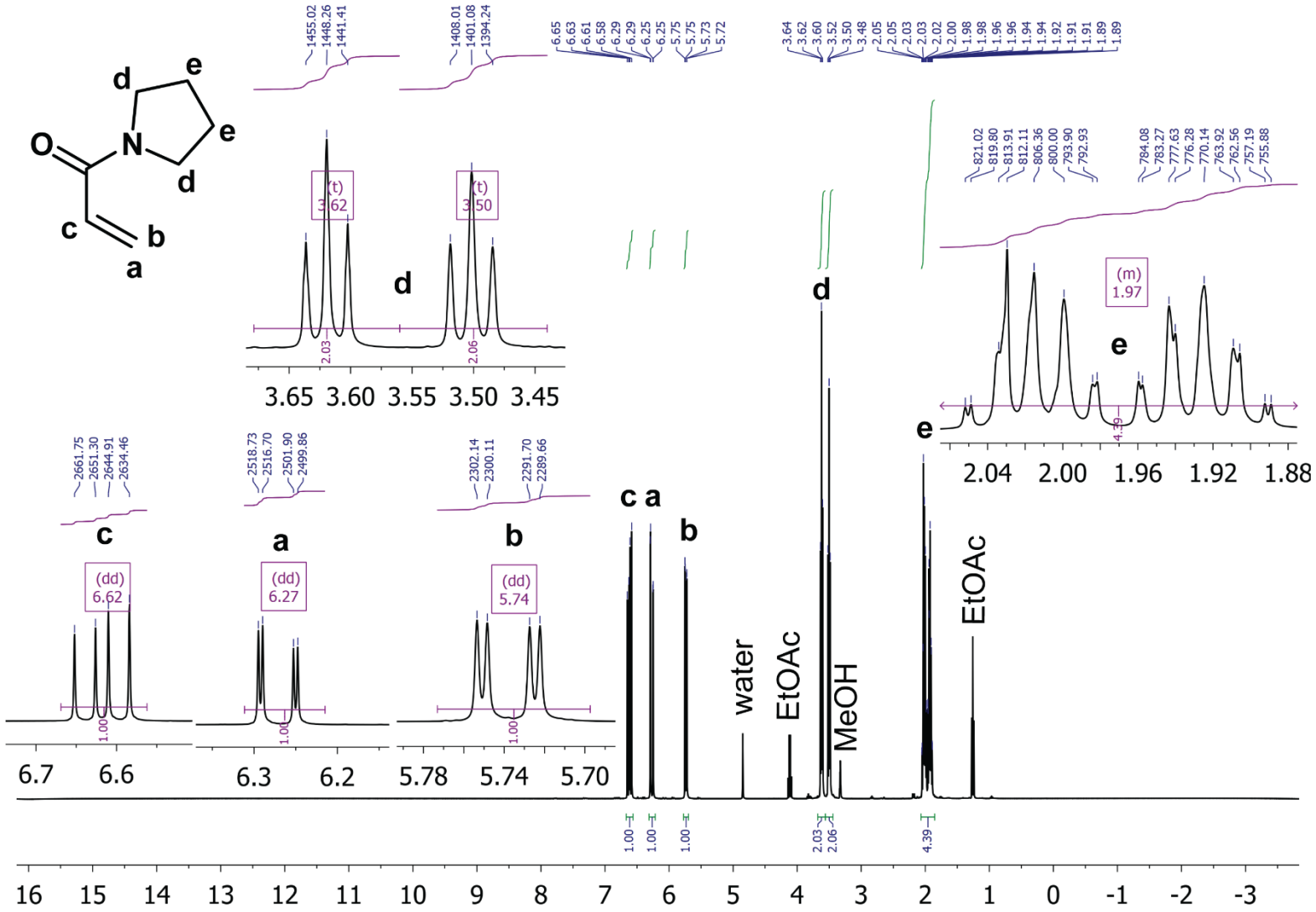

Figure S1. [1]H NMR (400 MHz) spectrum of the ***N*-acryloylpyrrolidine** monomer in MeOH-4d: 6.62 (dd, J = 16.8, 10.4 Hz, 1H), 6.27 (dd, J = 16.8, 2.0 Hz, 1H), 5.74 (dd, J = 10.4, 2.0 Hz, 1H), 3.62 (t, J = 6.8 Hz, 1H), 3.50 (t, J = 6.9 Hz, 1H), and 2.07-1.85 ppm (m, 4H)

DOI: 10.1039/d1py00843a

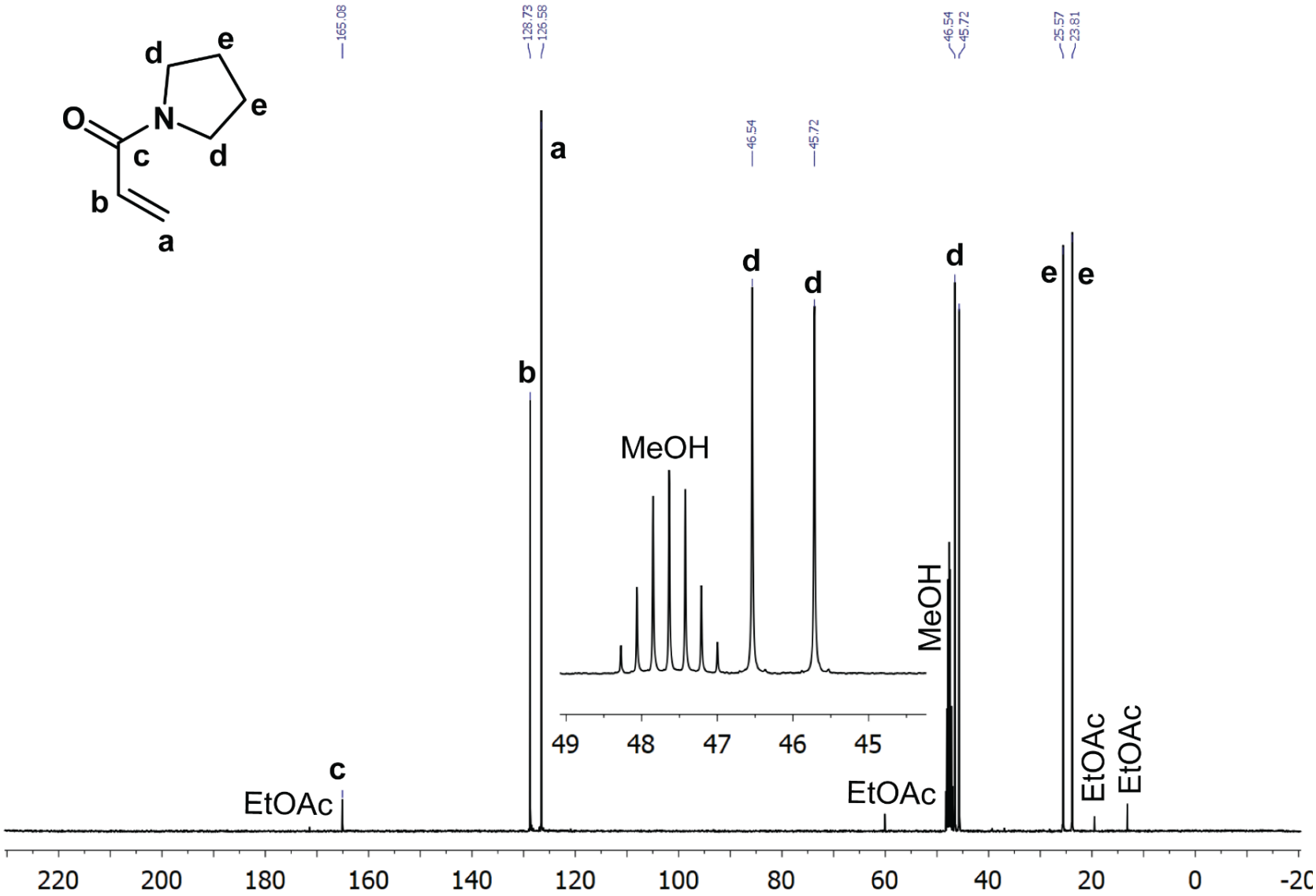

Figure S2. $^{13}C\{^{1}H\}$ NMR (101 MHz) spectrum of the ***N*-acryloylpyrrolidine** monomer in MeOH-4d: 165.1, 128.7, 126.6, 46.5, 45.7, 25.6, and 23.8 ppm

DOI: 10.1039/d1py00843a

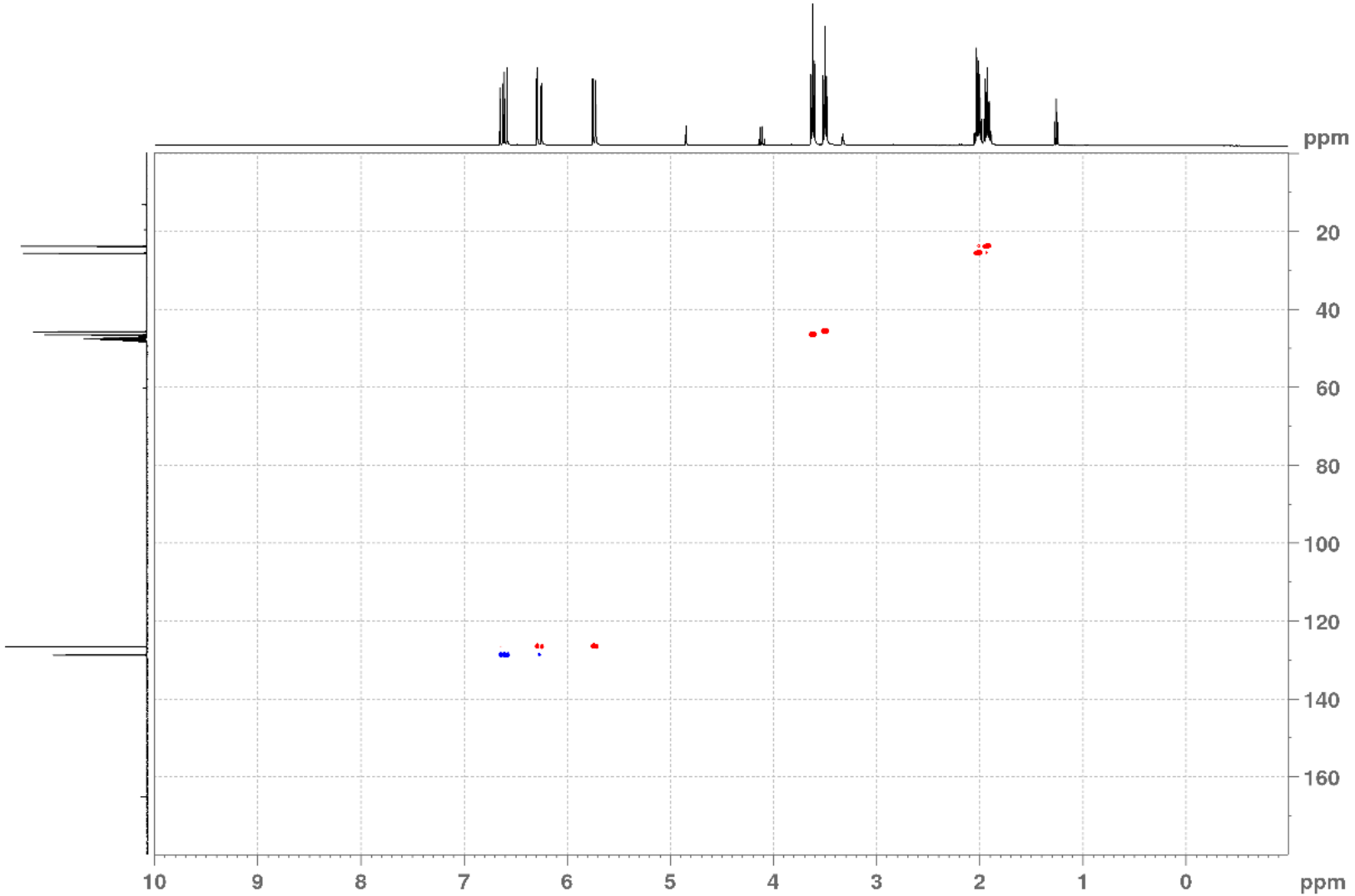

Figure S3. Multiplicity-edited HSQC NMR spectrum (400 MHz) of the ***N*-acryloylpyrrolidine** monomer in MeOH-4d; negative values (**red**) indicate CH_2 moieties, while positive values (**blue**) indicate CH or CH_3 moieties

DOI: 10.1039/d1py00843a

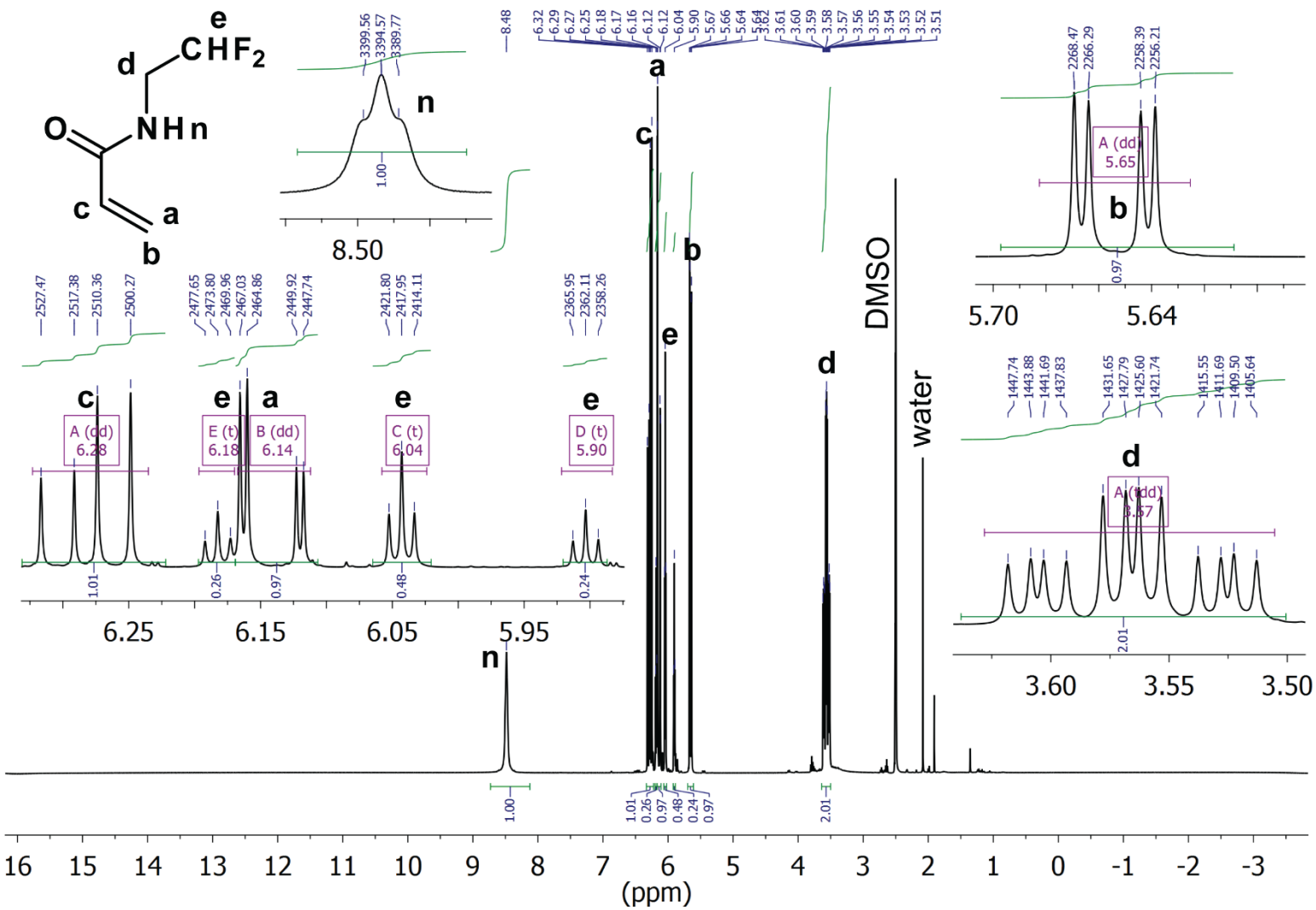

Figure S4. [1]H NMR (400 MHz) spectrum of the ***N*-(2,2-difluoroethyl)acrylamide** monomer in DMSO-6d: 8.48 (t, J = 4.9 Hz, 1H), 6.28 (dd, J = 17.1, 10.1 Hz, 1H), 6.14 (dd, J = 17.1, 2.2 Hz, 1H), 6.04 (tt, J = 55.8, 3.8 Hz, 1H), 5.65 (dd, J = 10.1, 2.2 Hz, 1H), and 3.57 ppm (tdd, J = 16.1, 6.0, 3.9 Hz, 2H). The signal **n** in the zoom area was apodized differently from the rest of this spectrum. As shown in the spectrum, the signal **e** is split into three areas, and the total signal integral of all three areas is ≈ 0.97.

DOI: 10.1039/d1py00843a

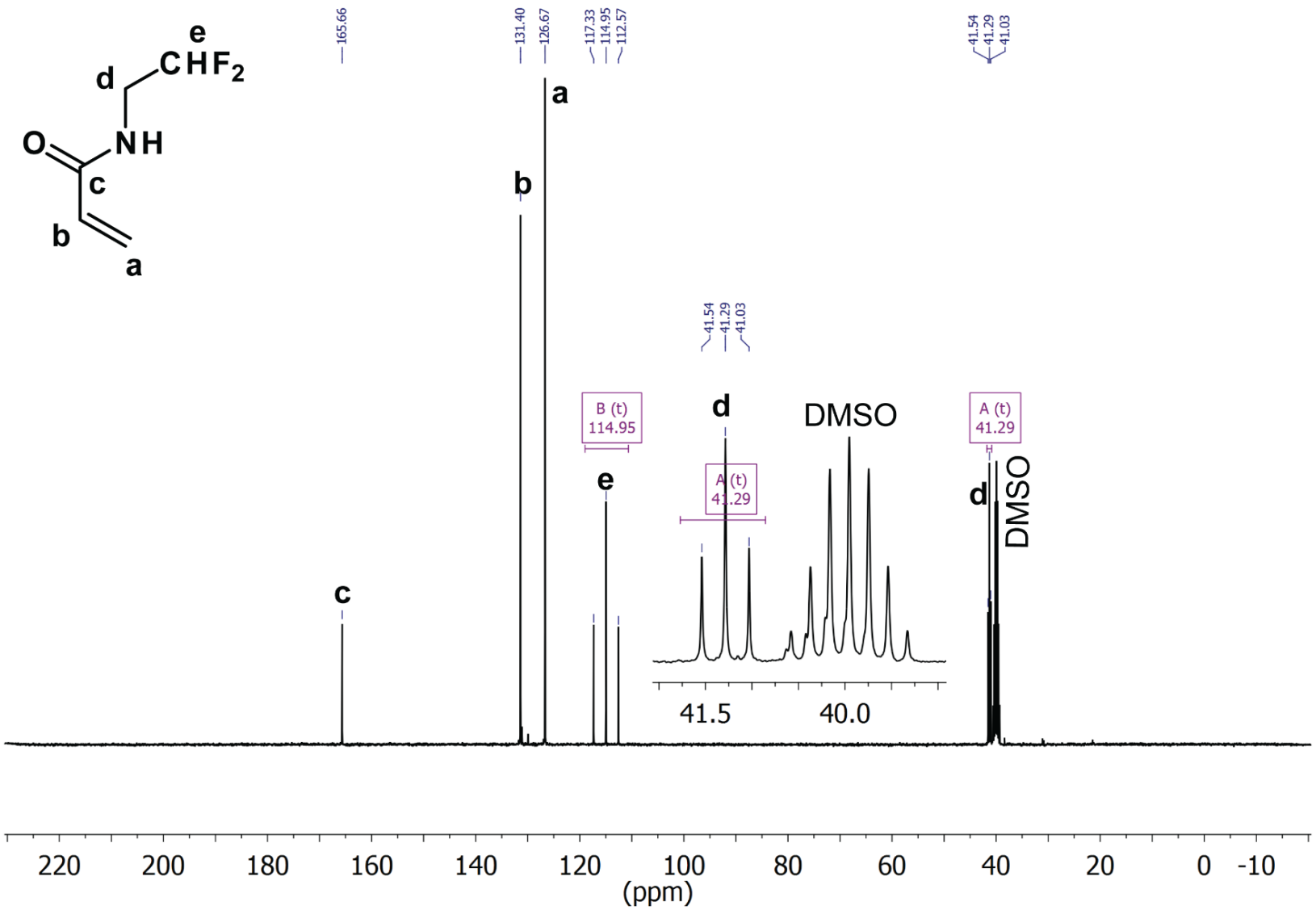

Figure S5. $^{13}C\{^{1}H\}$ NMR (101 MHz) spectrum of the ***N*-(2,2-difluoroethyl)acrylamide** monomer in DMSO-6d: 165.66, 131.40, 126.67, 114.95 (t, J = 239.7 Hz), and 41.29 ppm (t, J = 25.6 Hz)

DOI: 10.1039/d1py00843a

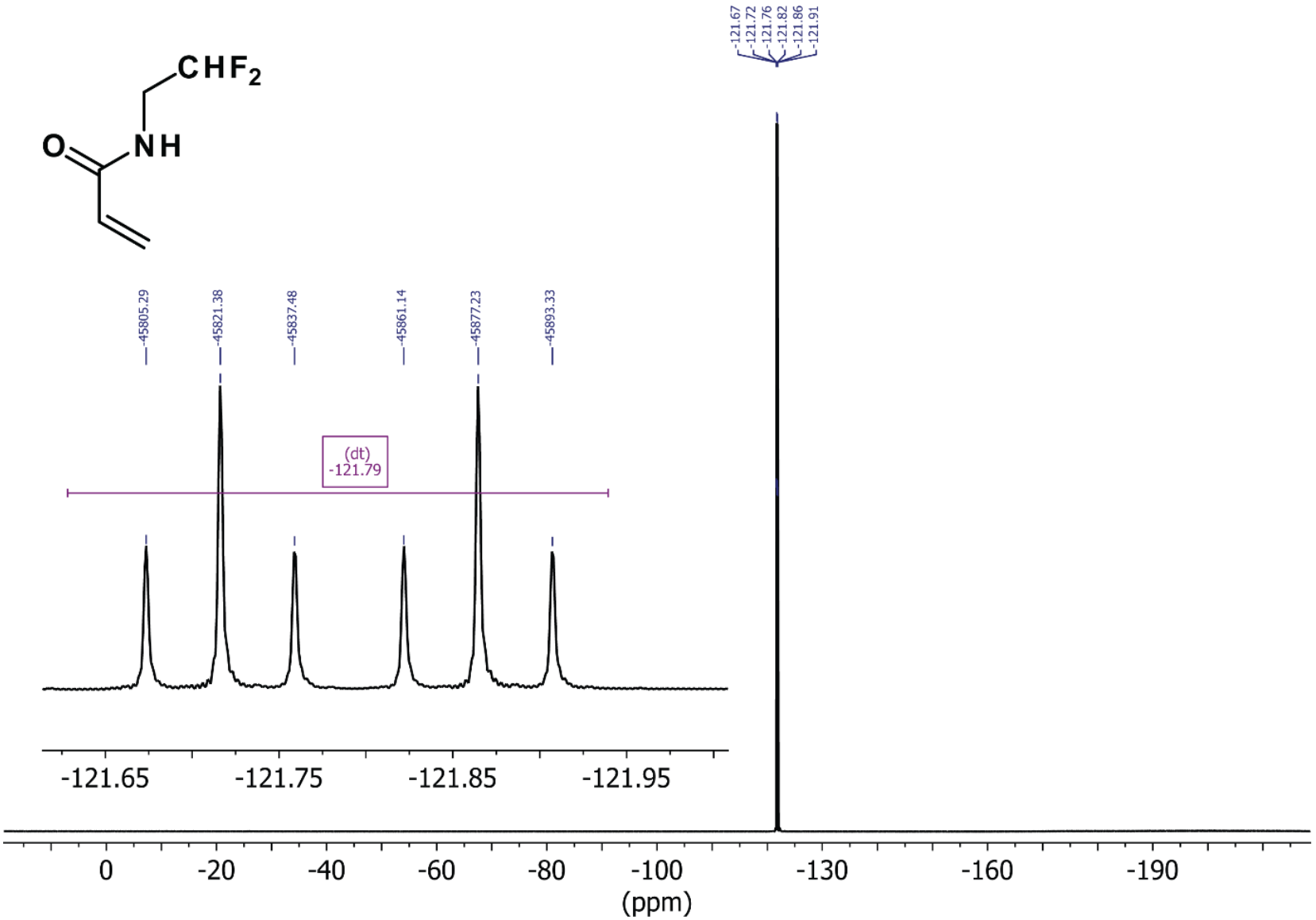

Figure S6. ^{19}F NMR (376 MHz) spectrum of the ***N*-(2,2-difluoroethyl)acrylamide** monomer in DMSO-6d: –121.79 ppm (dt, J = 55.9, 16.1 Hz; 2F)

DOI: 10.1039/d1py00843a

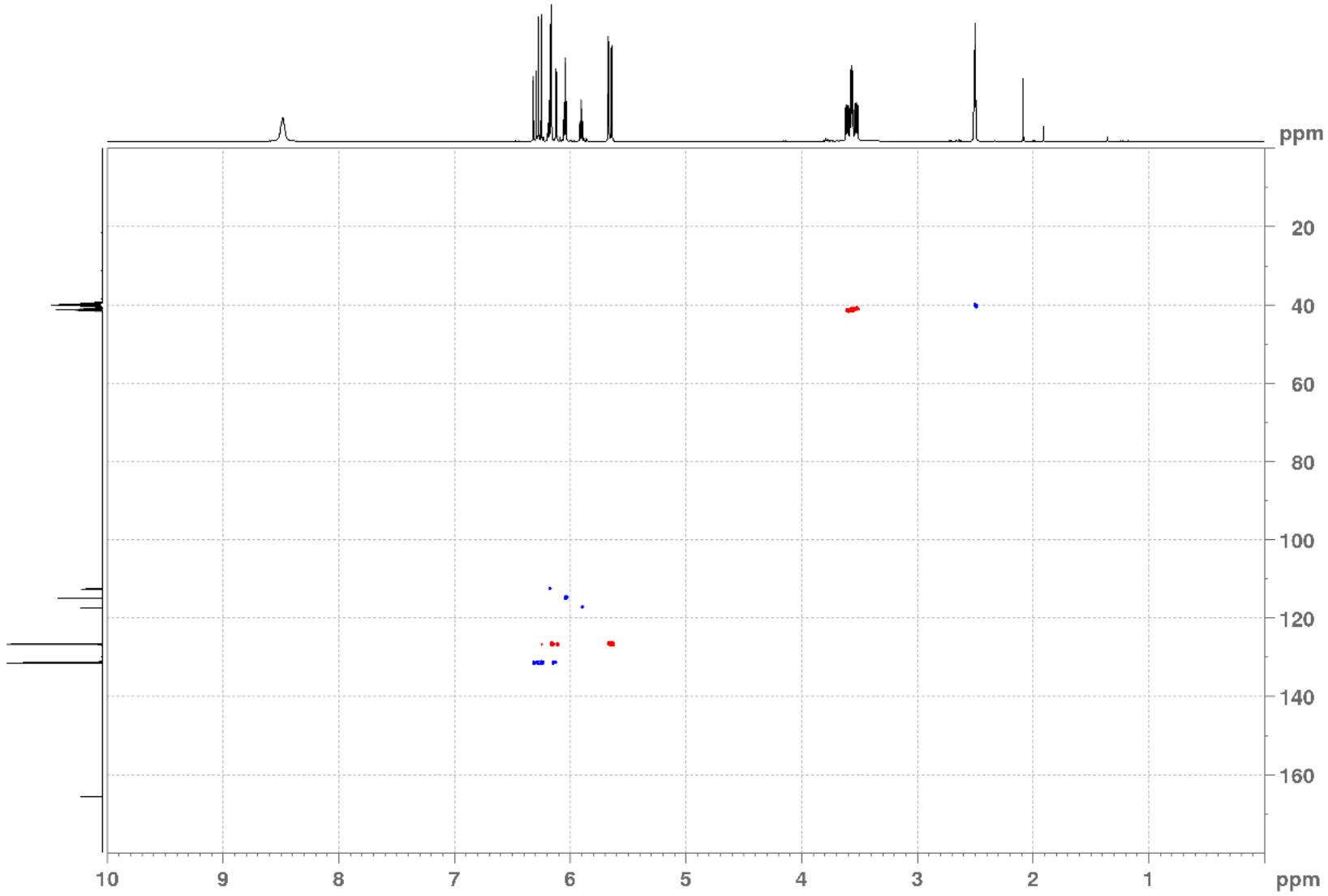

Figure S7. Multiplicity-edited HSQC NMR (400 MHz) spectrum of ***N*-(2,2-difluoroethyl)acrylamide** in DMSO-6d; negative values (**red**) indicate CH_2 moieties, while positive values (**blue**) indicate CH or CH_3 moieties.

DOI: 10.1039/d1py00843a

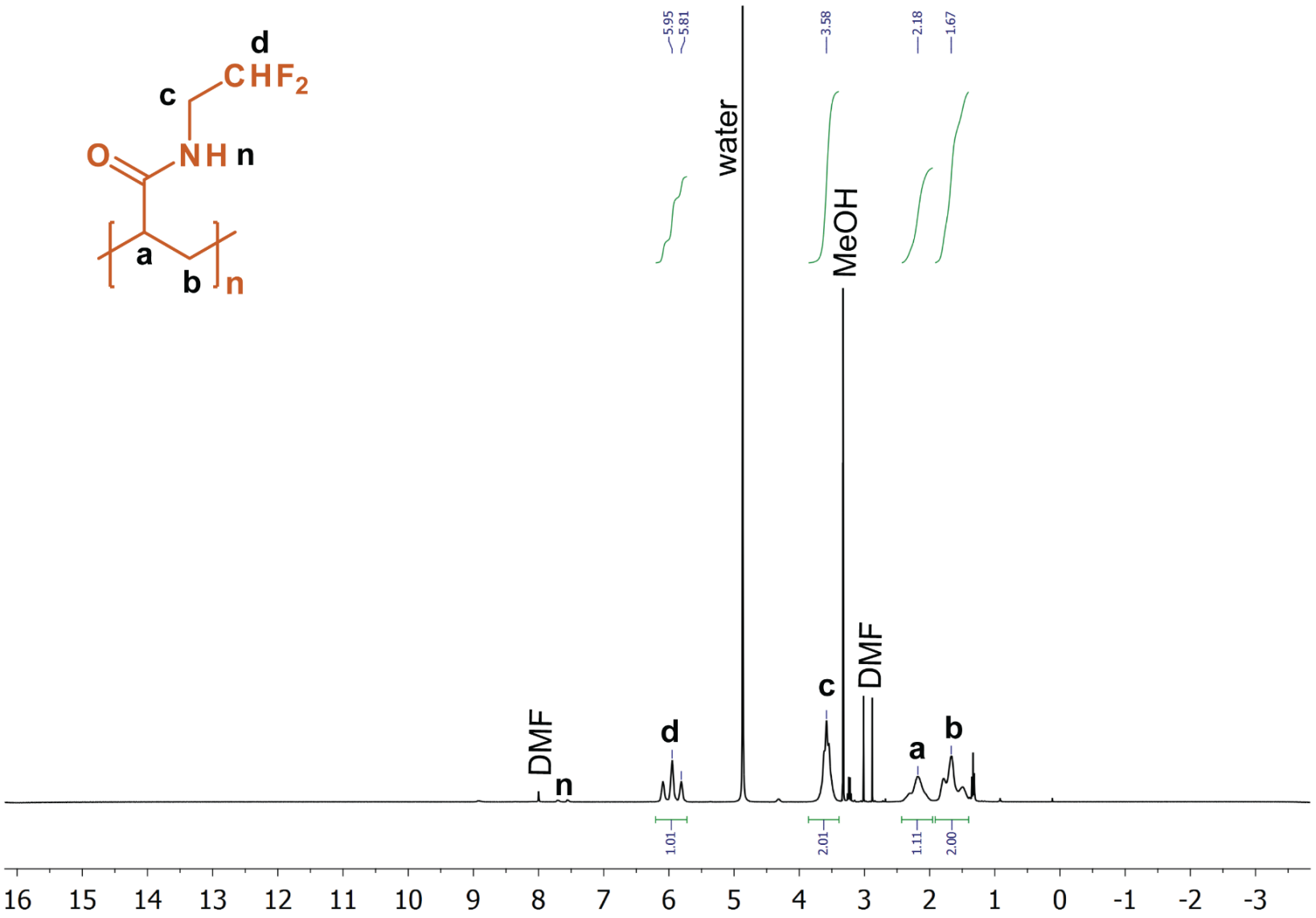

Figure S8. ^{1}H NMR (400 MHz) spectrum of the **pDFEA** polymer in MeOH-4d: 8.00 (1H), 5.95 (t, J = 56.1, 1H), 3.58 (t, J = 14.4 Hz, 2H), 2.18 (1H), and 1.67 ppm (2H).

DOI: 10.1039/d1py00843a

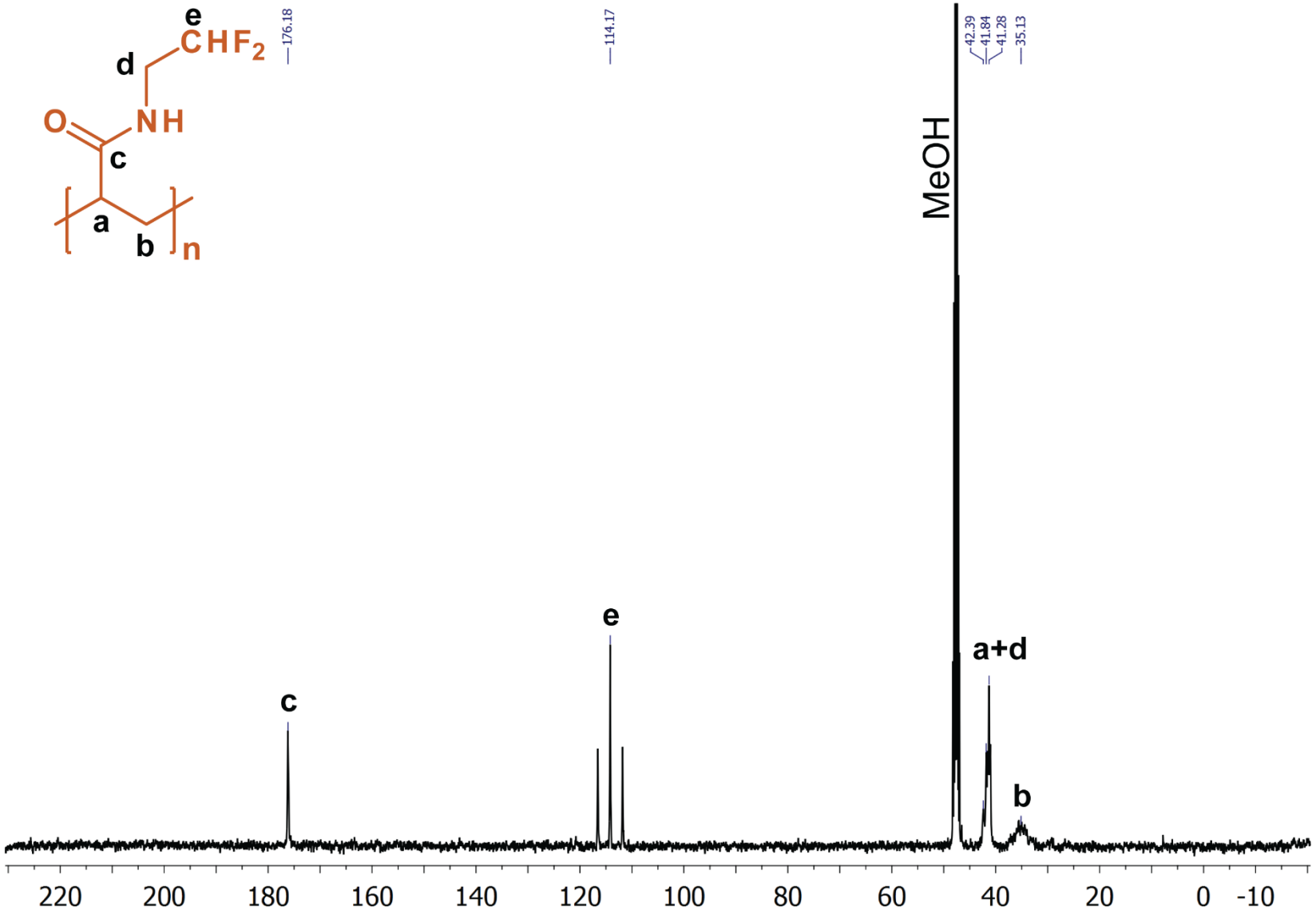

Figure S9. $^{13}C\{^{1}H\}$ NMR (101 MHz) spectrum of the **pDFEA** polymer in MeOH-4d: 176.2, 114.2 (J = 239.5 Hz), 41.8 (t, J = 28.1 Hz), and 35.1 ppm

DOI: 10.1039/d1py00843a

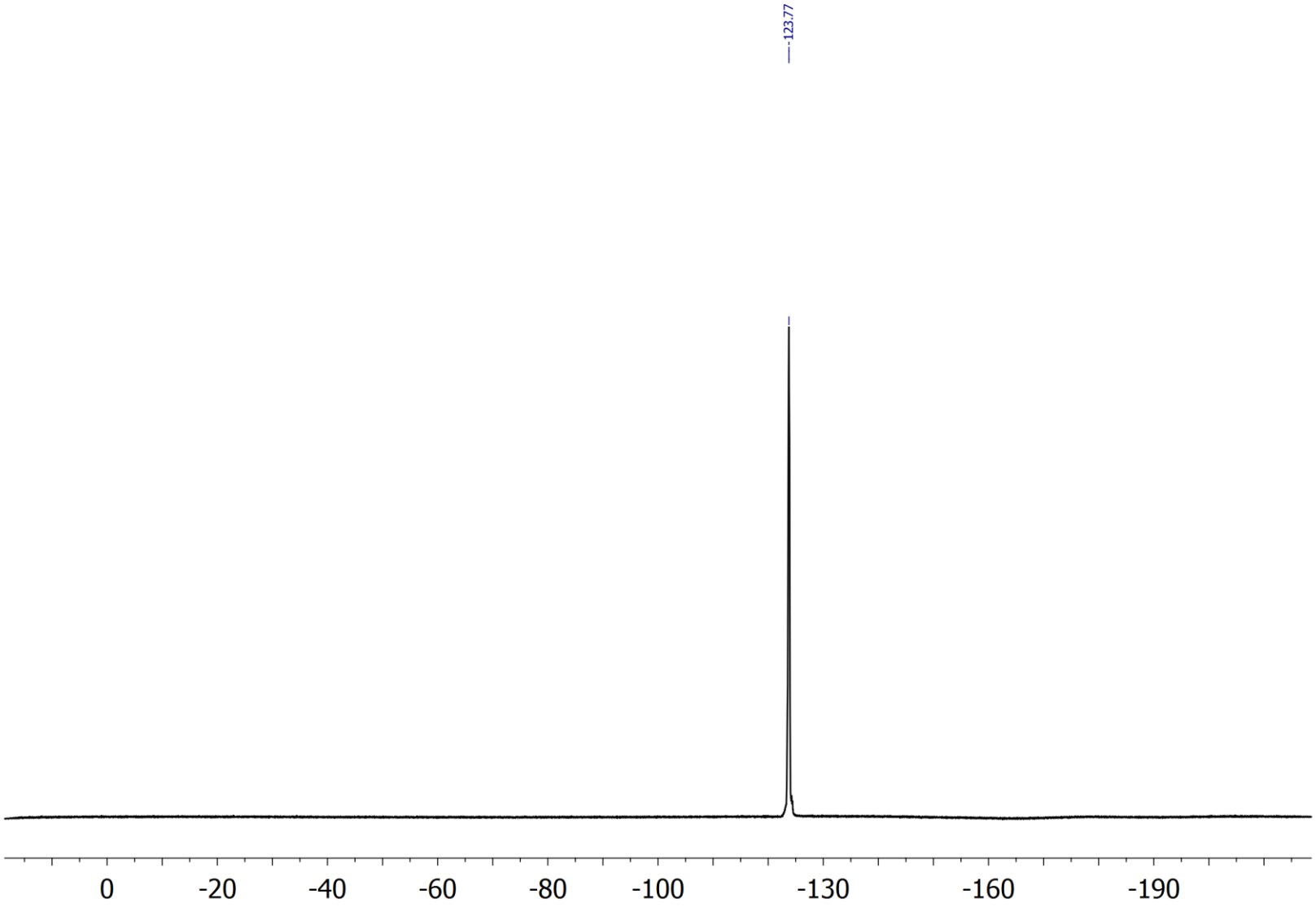

Figure S10. ^{19}F NMR (376 MHz) spectrum of the **pDFEA** polymer in MeOH-4d: –123.8 ppm

DOI: 10.1039/d1py00843a

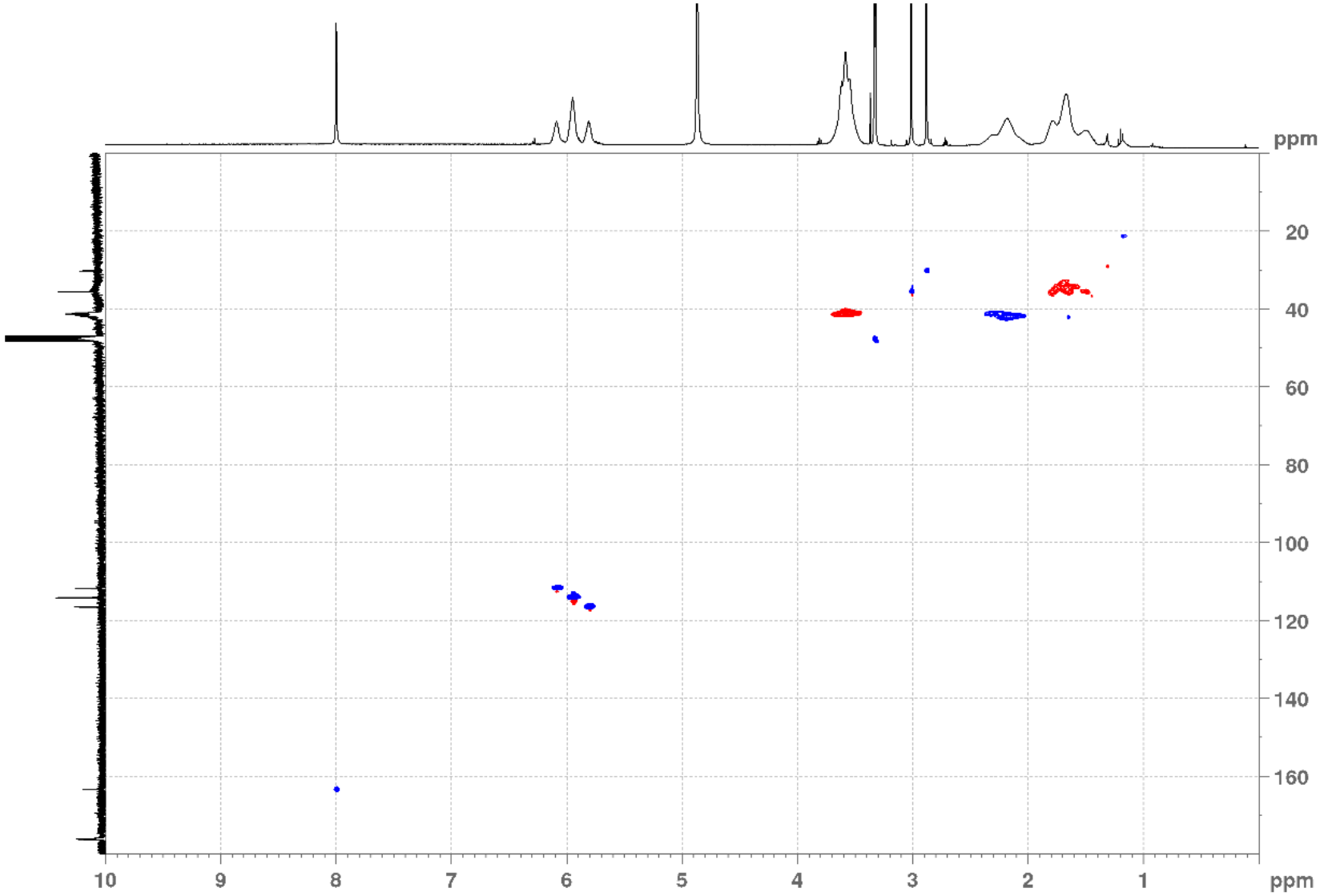

Figure S11. Multiplicity-edited HSQC NMR (400 MHz) spectrum of **pDFEA** polymer in MeOH-4d; negative values (**red**) indicate CH_2 moieties, while positive values (**blue**) indicate CH or CH_3 moieties.

DOI: 10.1039/d1py00843a

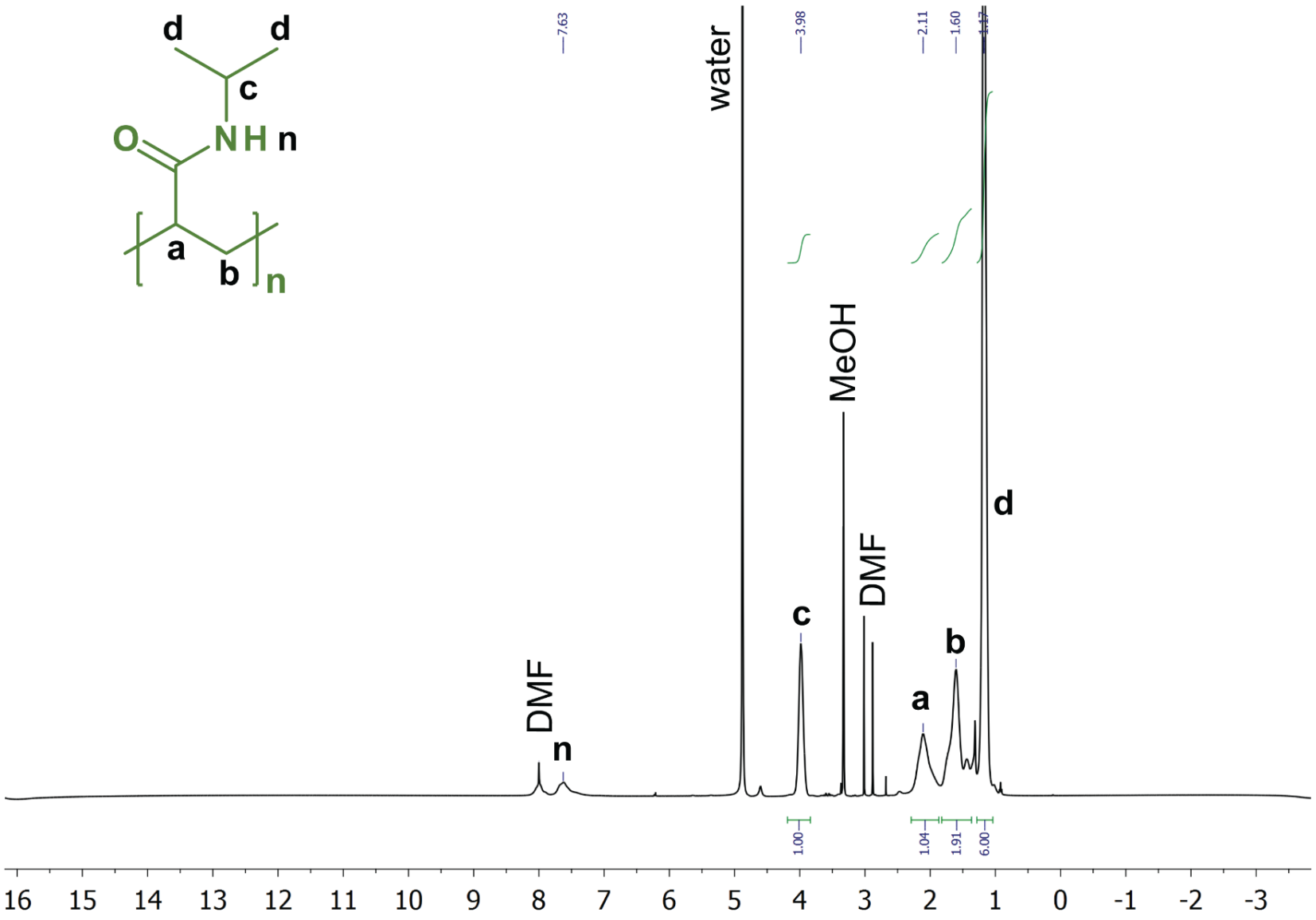

Figure S12. ^{1}H NMR (400 MHz) spectrum of the **pNIPAM** polymer in MeOH-4d: 7.63 (1H), 3.98 (1H), 2.11 (1H), 1.60 (2H), and 1.17 ppm (6H)

DOI: 10.1039/d1py00843a

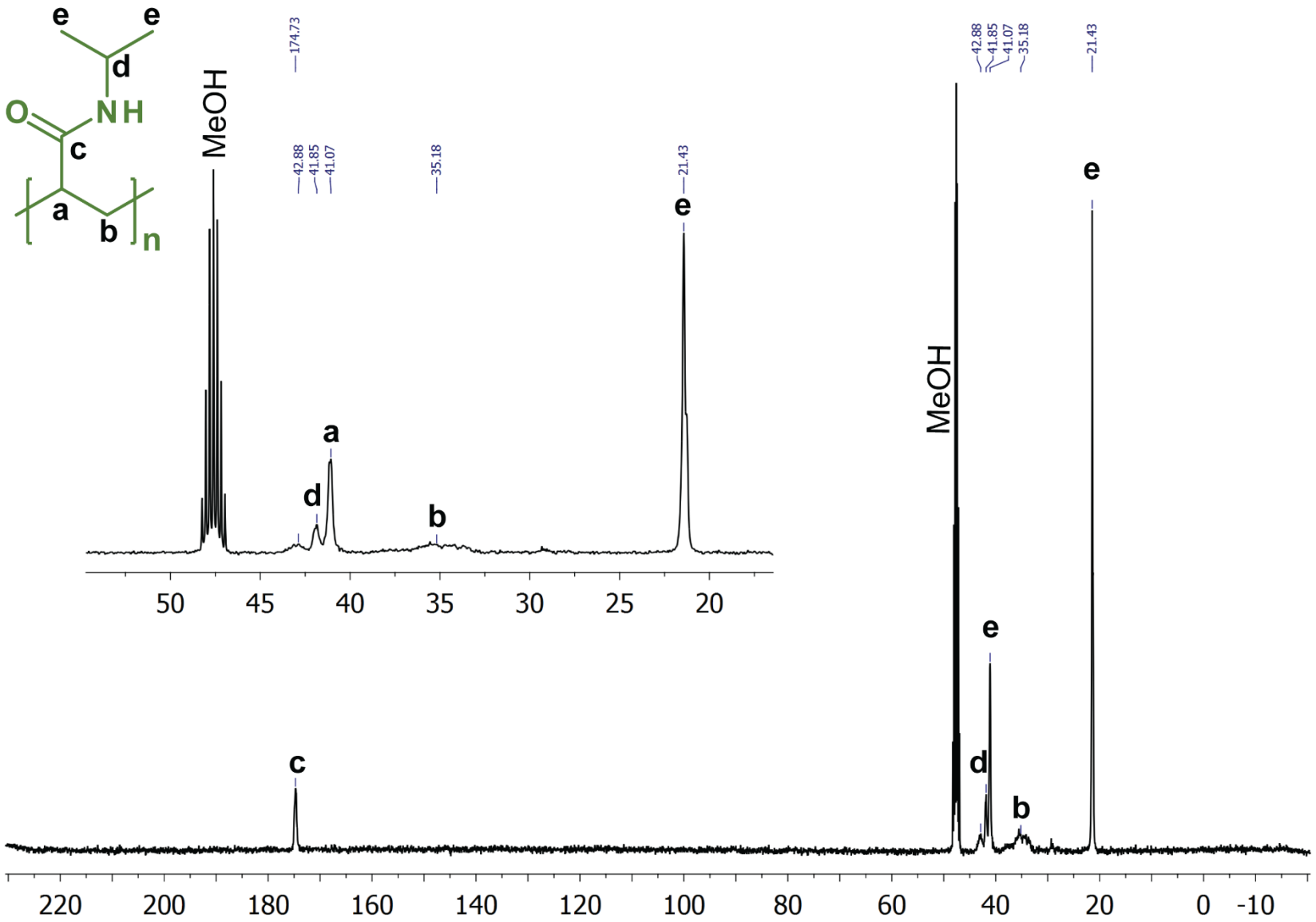

Figure S13. $^{13}C\{^{1}H\}$ NMR (101 MHz) spectrum of the **pNIPAM** polymer in MeOH-4d: 174.8, 42.9, 41.1-41.9, 35.0, and 21.4 ppm

DOI: 10.1039/d1py00843a

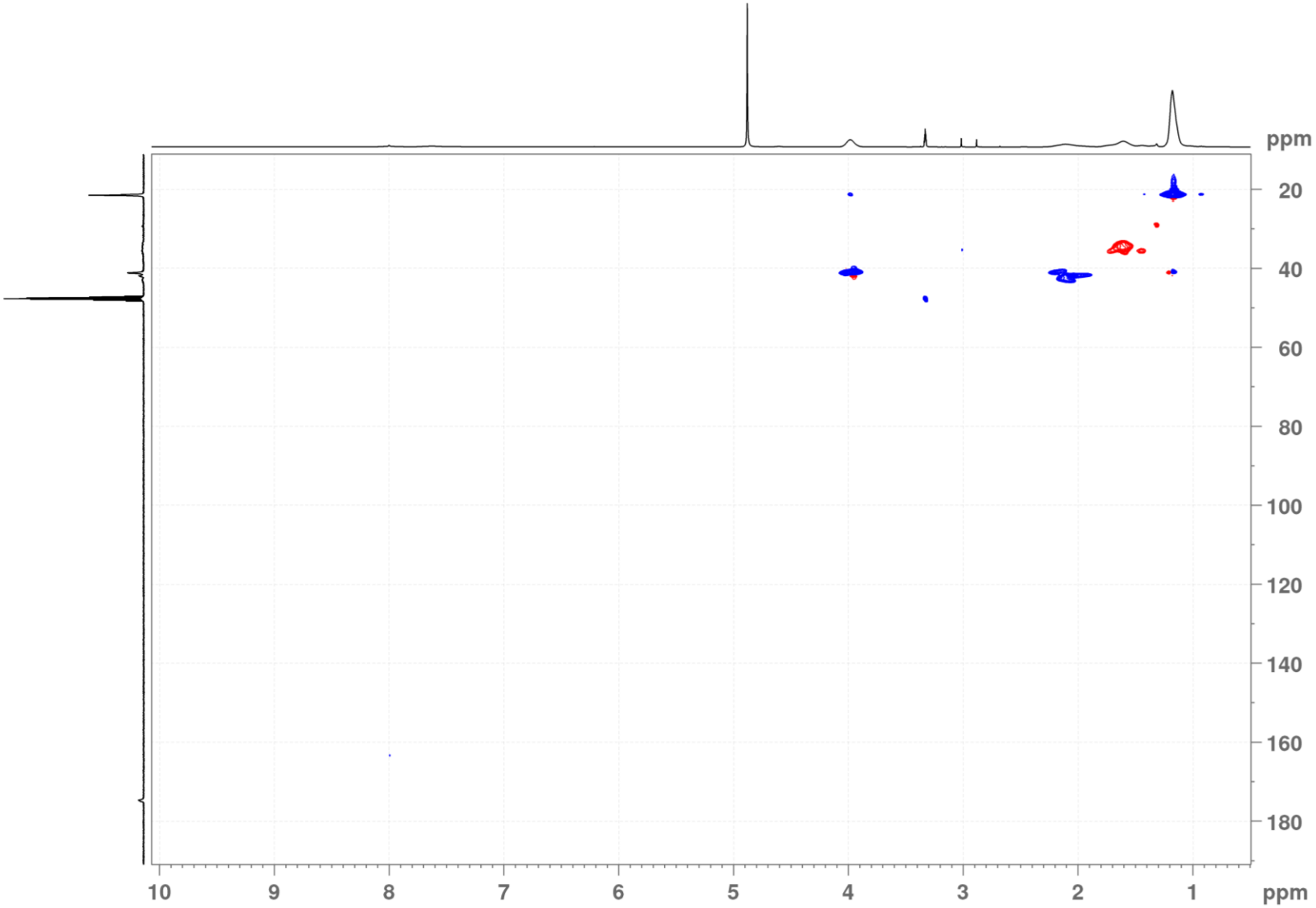

Figure S14. Multiplicity-edited HSQC NMR (400 MHz) spectrum of the **pNIPAM** polymer in MeOH-4d; negative values (**red**) indicate CH_2 moieties, while positive values (**blue**) indicate CH or CH_3 moieties.

DOI: 10.1039/d1py00843a

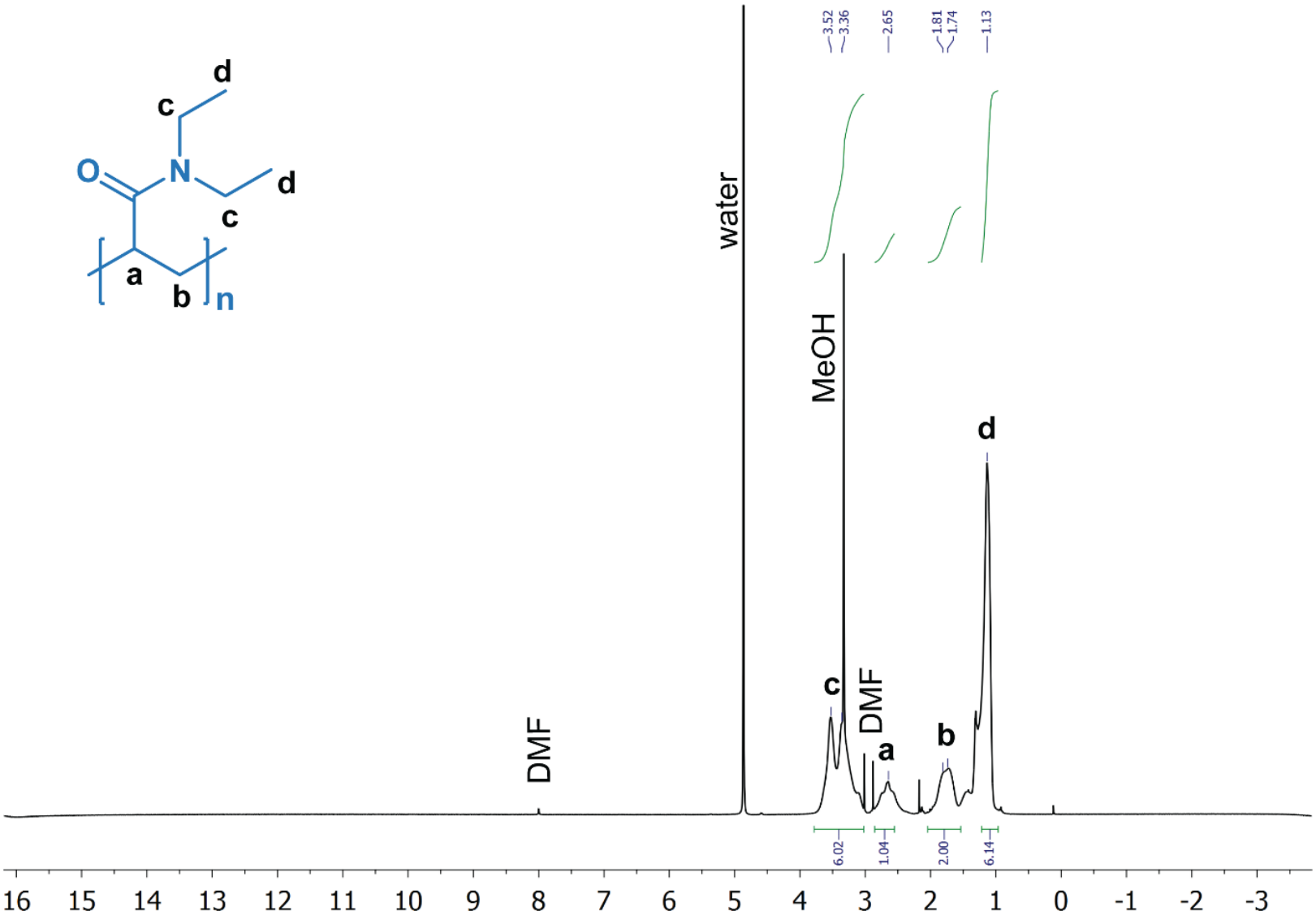

Figure S15. ^{1}H NMR (400 MHz) spectrum of the **pDEA** polymer in MeOH-4d: 3.52-3.36 (4H), 2.65 (1H), 1.74-1.81 (2H), and 1.13 ppm (6H)

DOI: 10.1039/d1py00843a

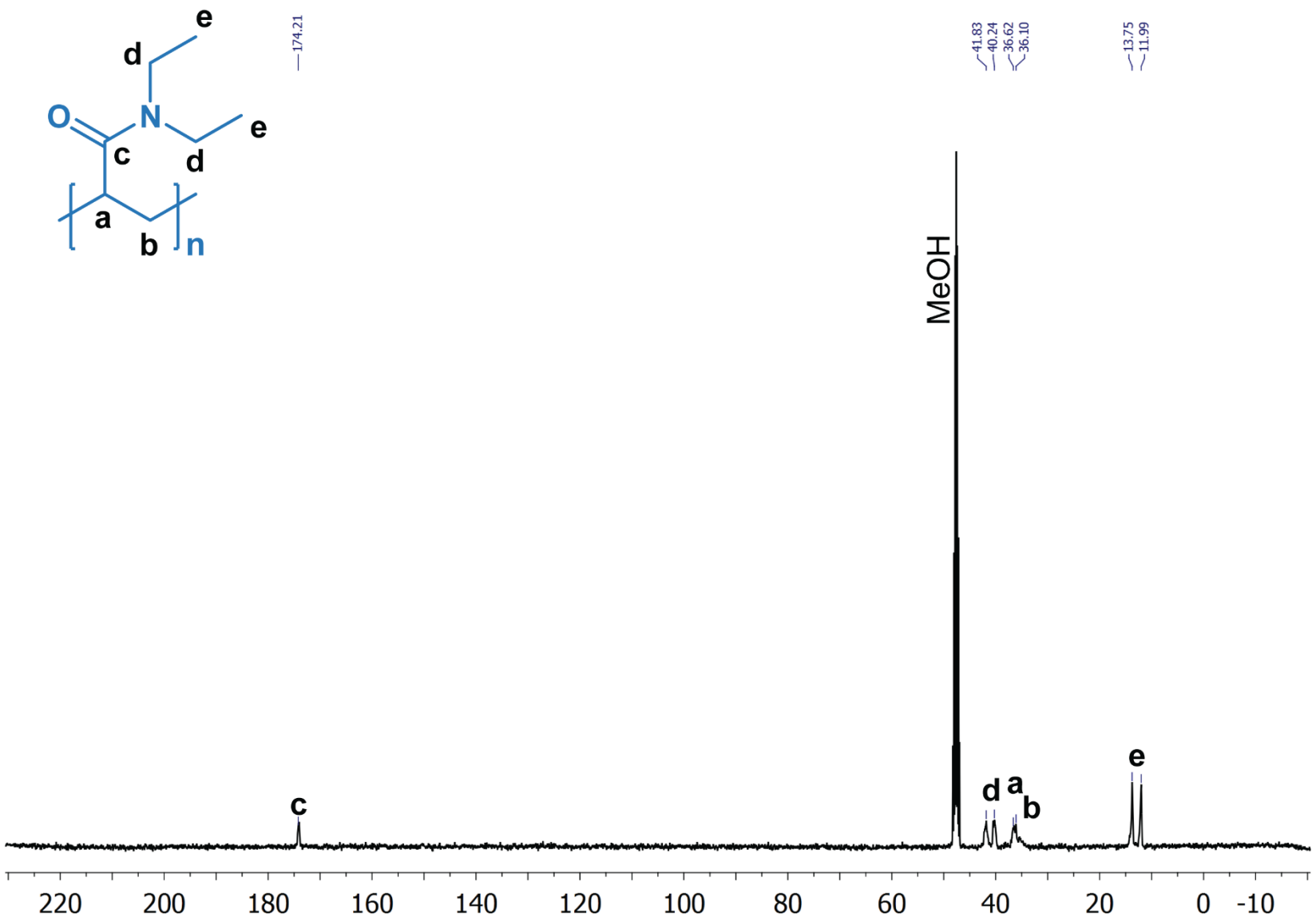

Figure S16. $^{13}C\{^{1}H\}$ NMR (101 MHz) spectrum of the **pDEA** polymer in MeOH-4d: 174.2, 40.2-41.8, 36.6, 36.1, and 12.0-13.8 ppm

DOI: 10.1039/d1py00843a

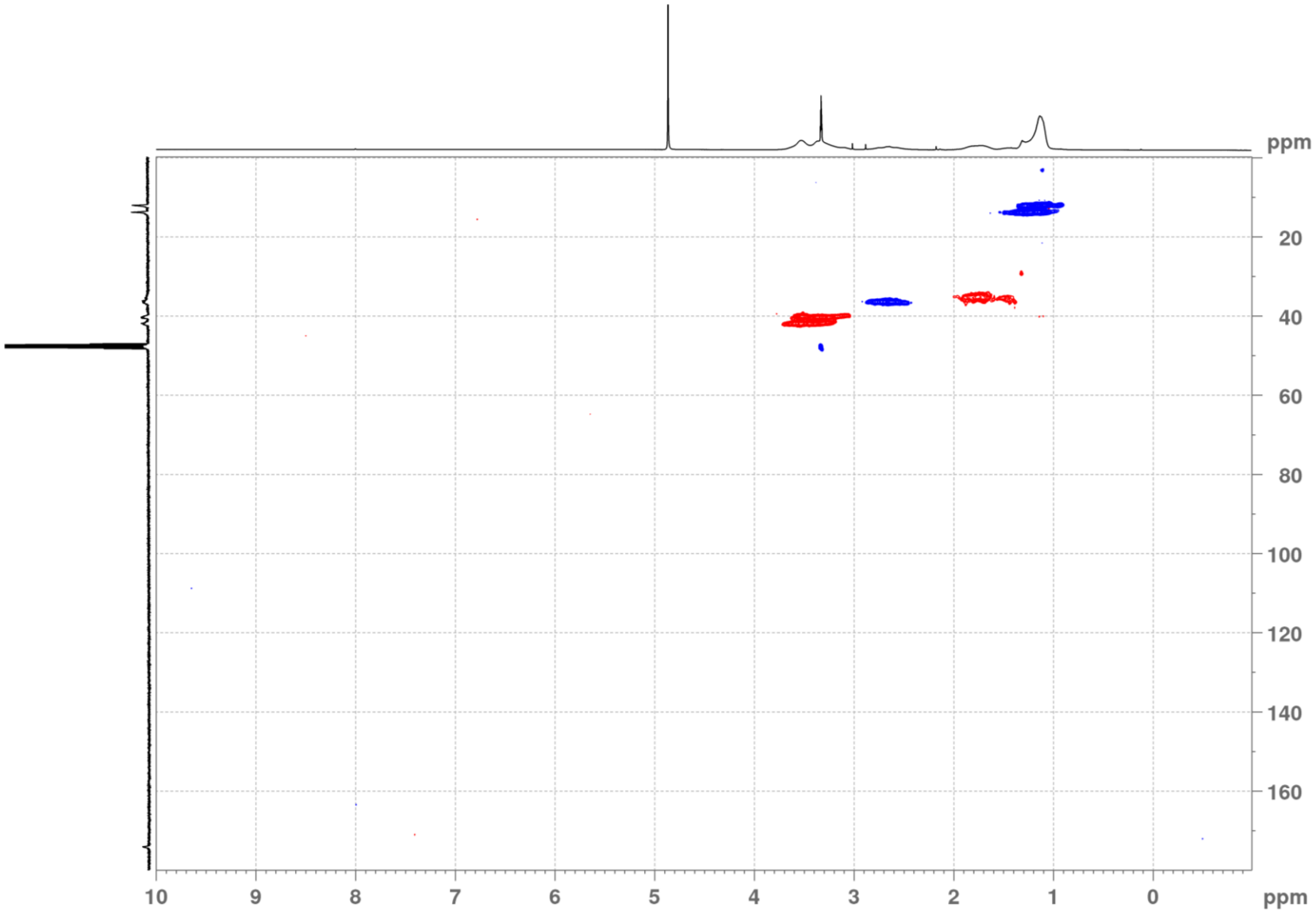

Figure S17. Multiplicity-edited HSQC NMR (400 MHz) spectrum of the **pDEA** polymer in MeOH-4d; negative values (**red**) indicate CH_2 moieties, while positive values (**blue**) indicate CH or CH_3 moieties.

DOI: 10.1039/d1py00843a

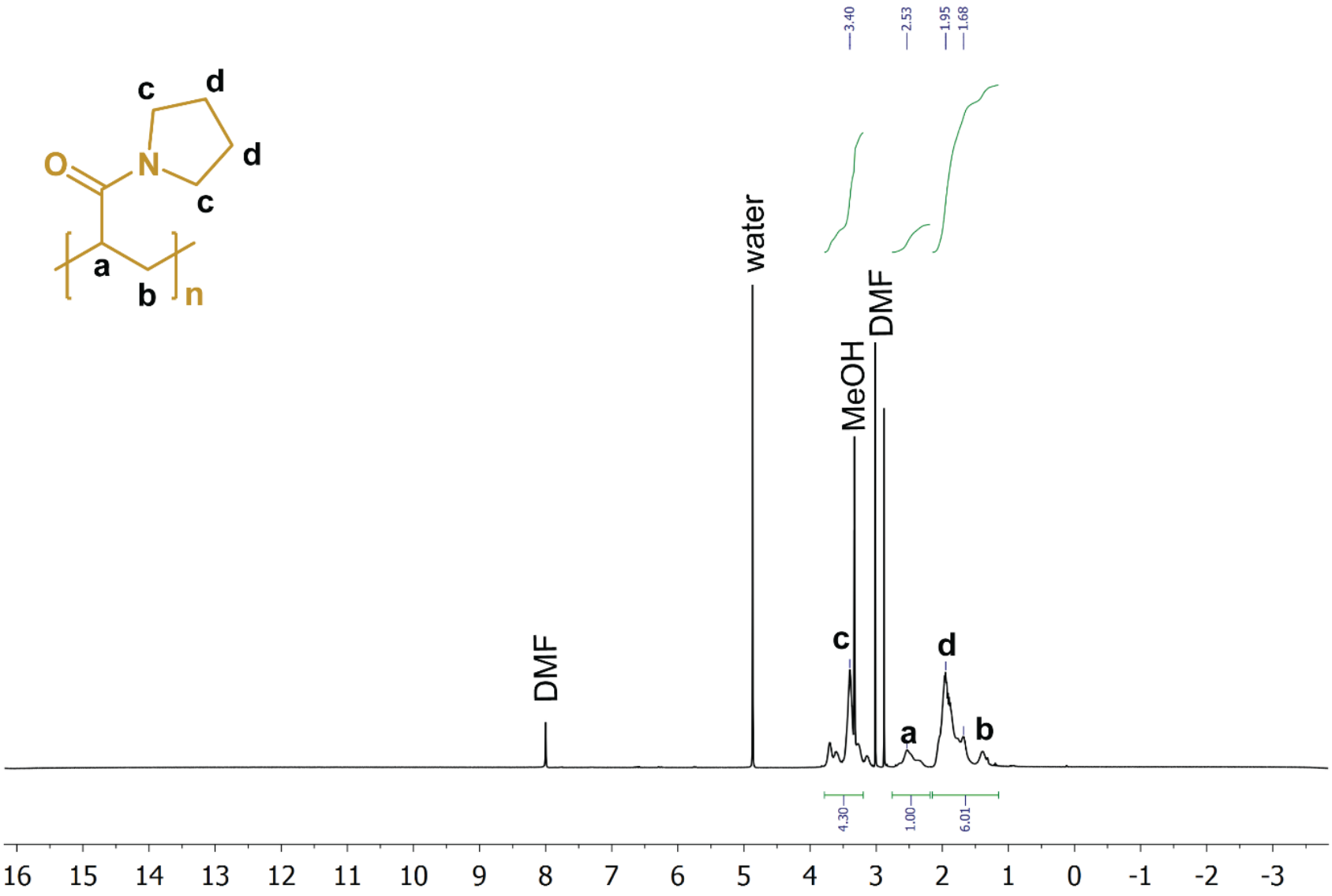

Figure S18. [1]H NMR (400 MHz) spectrum of the **pAP** polymer in MeOH-4d: 3.1-3.8 (4H), 2.3-2.7 (1H), 1.96 (4H), and 1.68 ppm (2H)

DOI: 10.1039/d1py00843a

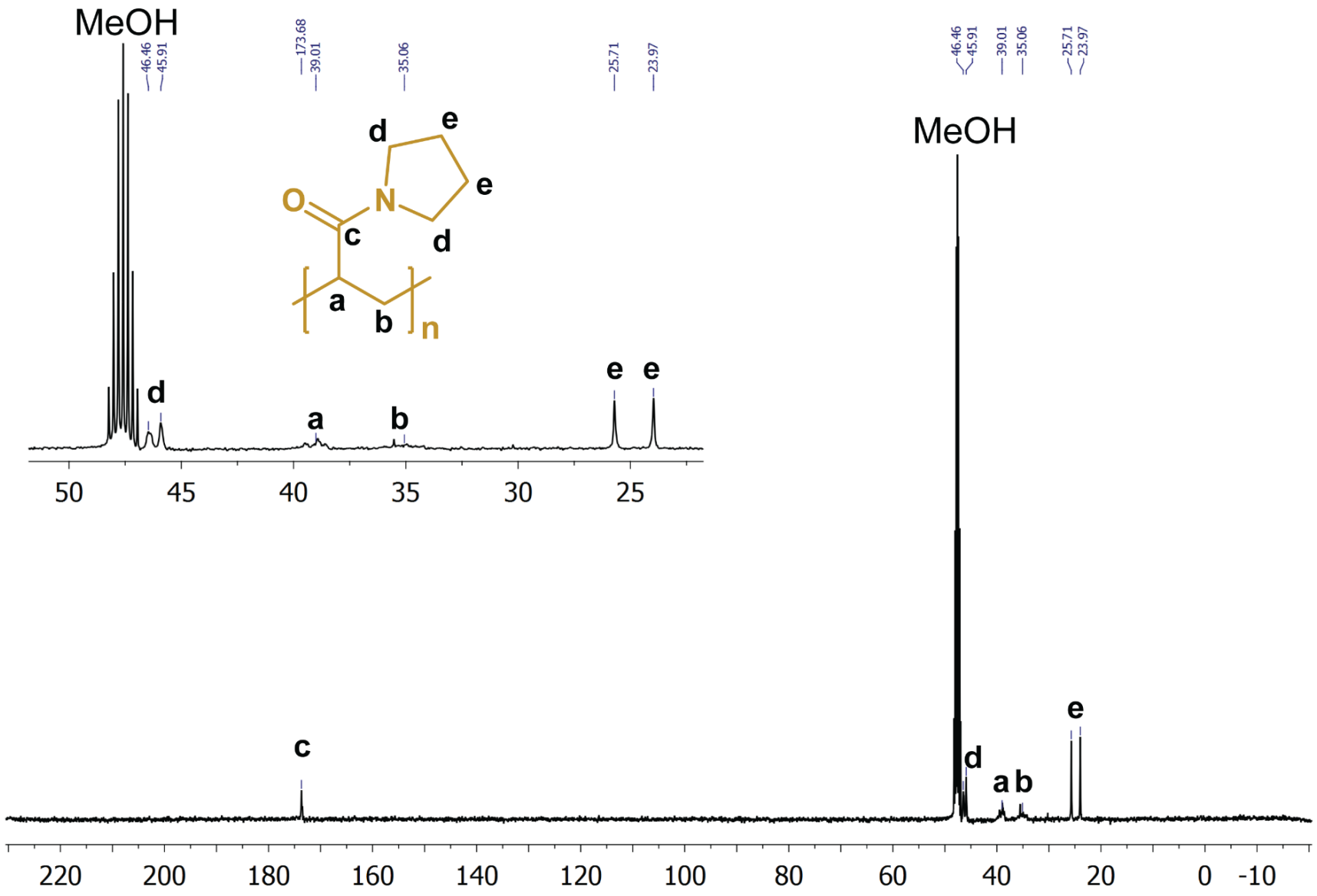

Figure S19. $^{13}C\{^{1}H\}$ NMR (101 MHz) spectrum of the **pAP** polymer in MeOH-4d: 173.7, 45.9-46.5, 39.0, 35.0, 24.0-25.7 ppm

DOI: 10.1039/d1py00843a

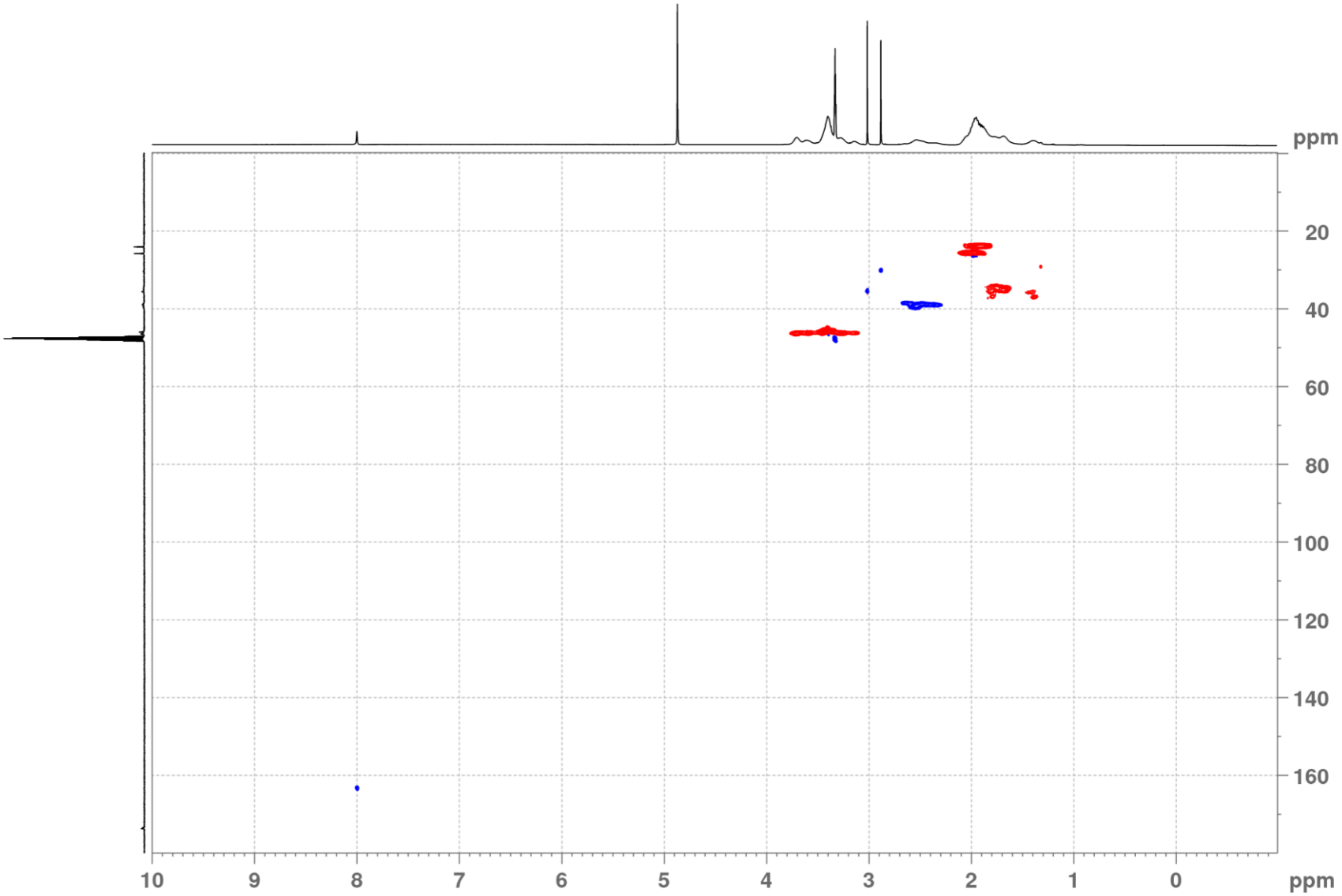

Figure S20. Multiplicity-edited HSQC NMR (400 MHz) spectrum of the **pAP** polymer in MeOH-4d; negative values (**red**) indicate CH_2 moieties, while positive values (**blue**) indicate CH or CH_3 moieties.

S4. Size exclusion chromatograms (SEC traces)

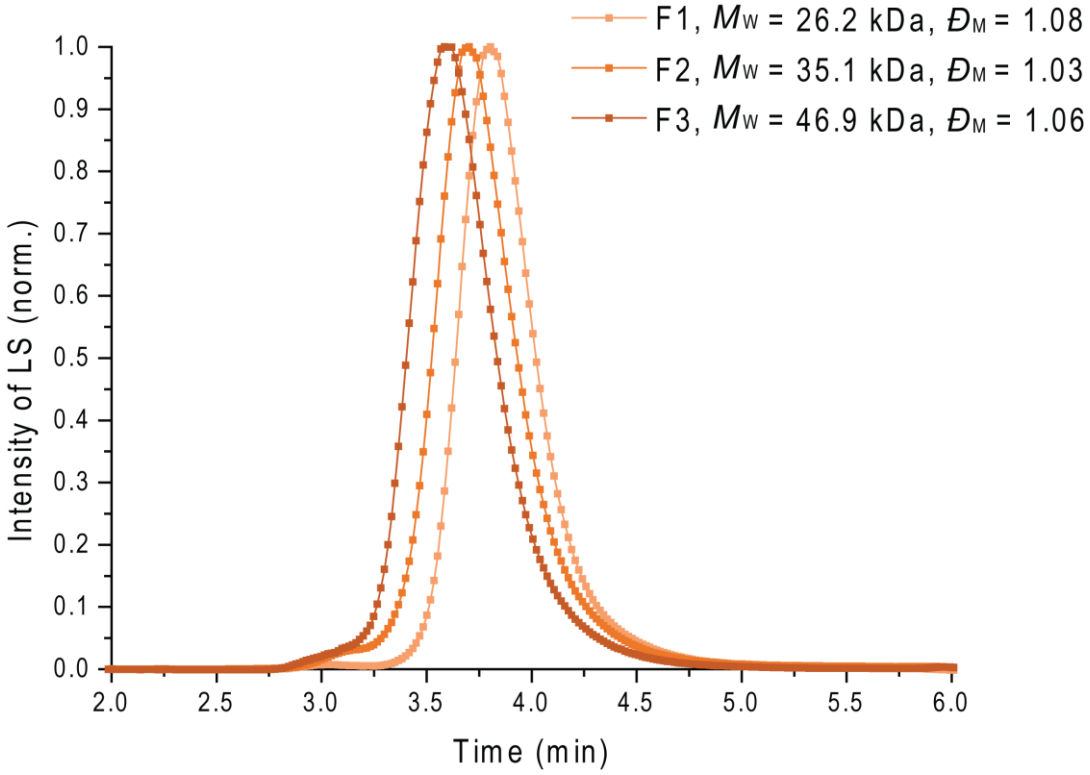

Figure S21. Size exclusion chromatograms of **pDFEA** polymers; mobile phase methanol and sodium acetate buffer (0.3 M, pH 6.5) mixture (80:20 v/v, flow rate of 0.6 mL·min^{-1}). These data were subsequently used to determine the M_w, M_n, and dispersity ($Đ_M$) of the polymers

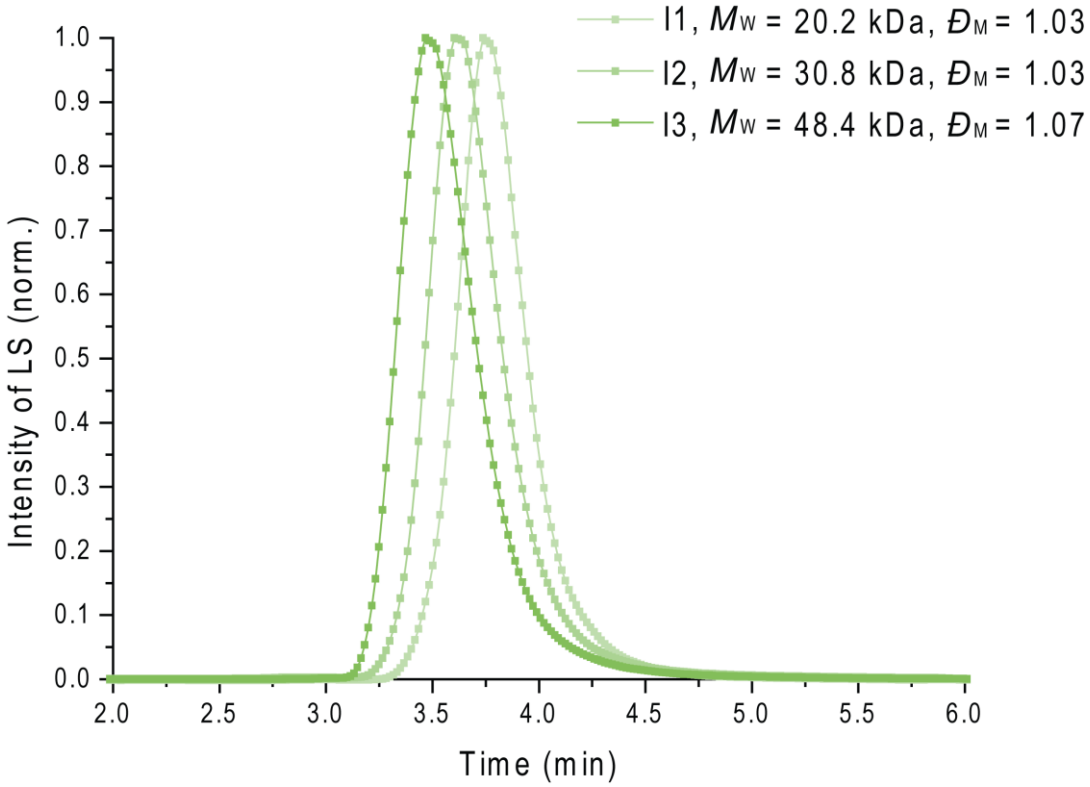

Figure S22. Size exclusion chromatograms of **pNIPAM** polymers; mobile phase methanol and sodium acetate buffer (0.3 M, pH 6.5) mixture (80:20 v/v, flow rate of 0.6 mL·min^{-1}). These data were subsequently used to determine the M_w, M_n, and dispersity ($Đ_M$) of the polymers

.

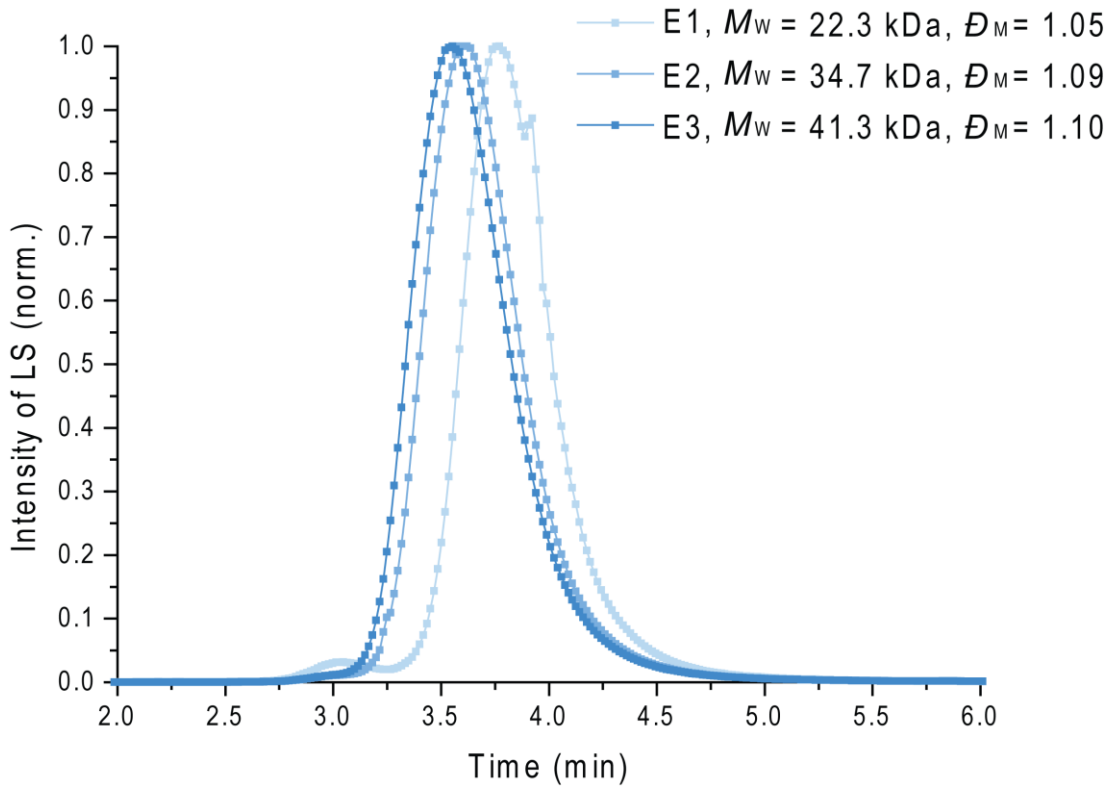

Figure S23. Size exclusion chromatograms of **pDEA** polymers; mobile phase methanol and sodium acetate buffer (0.3 M, pH 6.5) mixture (80:20 v/v, flow rate of 0.6 mL·min^{-1}). These data were subsequently used to determine the M_w, M_n, and dispersity ($Đ_M$) of the polymers

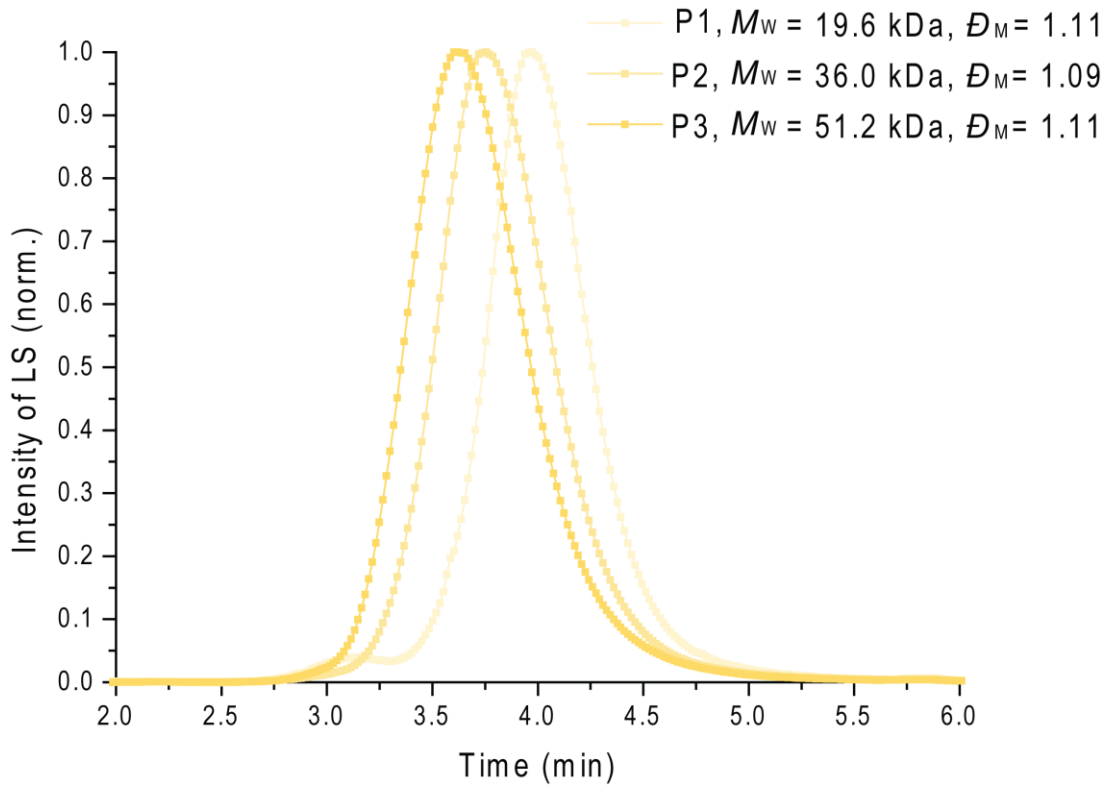

Figure S24. Size exclusion chromatograms of **pAP** polymers; mobile phase methanol and sodium acetate buffer (0.3 M, pH 6.5) mixture (80:20 v/v, flow rate of 0.6 mL·min^{-1}). These data were subsequently used to determine the M_w, M_n, and dispersity ($Đ_M$) of the polymers

 DOI: 10.1039/d1py00843a

S5. Turbidimetric data – tables

Table S3. T_{CP} values in various solvents (water, PBS and FBS) as a function of the concentration of **pDFEA** polymers (**F1**, **F2**, and **F3**); the data are expressed as mean of 6 experiments and their standard deviation (SD). An asterisk (*) indicates concentration points with multiple outlier points, which were discarded.

Polymer *c* **(mg/ml)**	**F1 (°C)** $T_{CP} \pm SD$	**F2 (°C)** $T_{CP} \pm SD$	**F3 (°C)** $T_{CP} \pm SD$	**F1 (°C)** $T_{CP} \pm SD$	**F2 (°C)** $T_{CP} \pm SD$	**F3 (°C)** $T_{CP} \pm SD$	**F1 (°C)** $T_{CP} \pm SD$	**F2 (°C)** $T_{CP} \pm SD$	**F3 (°C)** $T_{CP} \pm SD$
Medium	**Ultrapure water**			**Phosphate saline buffer**			**Foetal Bovine Serum**		
1.25	-	-	-	64.07 ± 0.05	55.25 ± 0.04	52.22 ± 0.04	33.85 ± 0.10	48.00 ± 0.17	49.97 ± 0.35
2.50	-	-	-	27.07 ± 0.23	30.75 ± 0.12	42.32 ± 0.25	28.25 ± 0.19	37.90 ± 0.23	34.60 ± 0.11
5.0	-	-	-	29.17 ± 0.14	29.95 ± 0.10	42.08 ± 0.24	24.58 ± 0.08	32.52 ± 0.10	29.99 ± 0.08
10.0	27.21 ± 0.62	34.00 ± 0.90	27.33 ± 0.68	27.05 ± 0.25	29.30 ± 0.11	42.48 ± 0.43	22.60 ± 0.06	30.10 ± 0.22	28.67 ± 0.10
20.0	-	-	-	25.57 ± 0.05	31.64 ± 0.20	43.88 ± 0.23	24.63 ± 0.15	28.87 ± 0.12	40.35 ± 0.10*
40.0	-	-	-	24.14 ± 0.10	24.96 ± 0.36	26.73 ± 0.29	24.90 ± 0.35	28.41 ± 0.08	43.80 ± 0.14

Table S4. T_{CP} values in various solvents (water, PBS and FBS) as a function of the concentration of **pNIPAM** polymers (**I1**, **I2**, and **I3**); the data are expressed as mean of 6 experiments and their standard deviation (SD). An asterisk (*) indicates concentration points with multiple outlier points, which were discarded.

Polymer *c* **(mg/ml)**	**I1 (°C)** $T_{CP} \pm SD$	**I2 (°C)** $T_{CP} \pm SD$	**I3 (°C)** $T_{CP} \pm SD$	**I1 (°C)** $T_{CP} \pm SD$	**I2 (°C)** $T_{CP} \pm SD$	**I3 (°C)** $T_{CP} \pm SD$	**I1 (°C)** $T_{CP} \pm SD$	**I2 (°C)** $T_{CP} \pm SD$	**I3 (°C)** $T_{CP} \pm SD$
Medium	**Ultrapure water**			**Phosphate saline buffer**			**Foetal Bovine Serum**		
1.25	-	-	-	33.42 ± 0.04	30.98 ± 0.04	29.65 ± 0.10	33.62 ± 0.08	30.88 ± 0.04	29.72 ± 0.04
2.50	-	-	-	32.25 ± 0.18	30.18 ± 0.11	29.13 ± 0.05	30.90 ± 0.15	28.62 ± 0.10	27.64 ± 0.05
5.0	-	-	-	31.08 ± 0.10	29.48 ± 0.08	28.75 ± 0.05	28.98 ± 0.10	26.30 ± 0.11	25.70 ± 0.06
10.0	29.98 ± 0.27	31.39 ± 0.17	31.59 ± 0.43	29.25 ± 0.10	28.30 ± 0.06	28.05 ± 0.10	25.67 ± 0.10	24.39 ± 0.10	24.60 ± 0.06
20.0	-	-	-	28.95 ± 0.05	26.80 ± 0.00	28.29 ± 0.04	28.90 ± 0.09	29.23 ± 0.15	33.05 ± 0.32
40.0	-	-	-	26.90 ± 0.34	28.37 ± 0.05	28.28 ± 0.04	28.82 ± 0.34	28.43 ± 0.16	31.03 ± 0.13

Table S5. T_{CP} values in various solvents (water, PBS and FBS) as a function of the concentration of **pDEA** polymers (**E1**, **E2**, and **E3**); the data are expressed as mean of 6 experiments and their standard deviation (SD). An asterisk (*) indicates concentration points with multiple outlier points, which were discarded.

Polymer *c* **(mg/ml)**	**E1 (°C)** $T_{CP} \pm SD$	**E2 (°C)** $T_{CP} \pm SD$	**E3 (°C)** $T_{CP} \pm SD$	**E1 (°C)** $T_{CP} \pm SD$	**E2 (°C)** $T_{CP} \pm SD$	**E3 (°C)** $T_{CP} \pm SD$	**E1 (°C)** $T_{CP} \pm SD$	**E2 (°C)** $T_{CP} \pm SD$	**E3 (°C)** $T_{CP} \pm SD$
Medium	**Ultrapure water**			**Phosphate saline buffer**			**Foetal Bovine Serum**		
1.25	-	-	-	31.88 ± 0.04	31.72 ± 0.04	31.17 ± 0.05	35.77 ± 0.25	32.60 ± 0.24	31.53 ± 0.23
2.50	-	-	-	29.58 ± 0.08	30.85 ± 0.08	29.30 ± 0.09	31.90 ± 0.14	30.00 ± 0.20	29.12 ± 0.15
5.0	-	-	-	28.20 ± 0.06	29.98 ± 0.04	28.35 ± 0.08	28.03 ± 0.20	27.97 ± 0.16	27.07 ± 0.15
10.0	29.28 ± 0.04	30.16 ± 0.11	29.92 ± 0.12	27.37 ± 0.08	28.47 ± 0.10	27.60 ± 0.11	23.95 ± 0.12	25.82 ± 0.17	25.27 ± 0.19
20.0	-	-	-	28.92 ± 0.16*	29.17 ± 0.06*	29.18 ± 0.05*	27.93 ± 0.13	29.47 ± 0.09	29.34 ± 0.07
40.0	-	-	-	28.85 ± 1.34*	28.75 ± 0.07*	28.87 ± 0.06*	27.57 ± 0.23	28.33 ± 0.05	27.88 ± 0.08

Table S6. T_{CP} values in various solvents (water, PBS and FBS) as a function of the concentration of **pAP** polymers (**P1**, **P2**, and **P3**); the data are expressed as mean of 6 experiments and their standard deviation (SD). An asterisk (*) indicates concentration points with multiple outlier points, which were discarded.

Polymer *c* **(mg/ml)**	**P1 (°C)** $T_{CP} \pm SD$	**P2 (°C)** $T_{CP} \pm SD$	**P3 (°C)** $T_{CP} \pm SD$	**P1 (°C)** $T_{CP} \pm SD$	**P2 (°C)** $T_{CP} \pm SD$	**P3 (°C)** $T_{CP} \pm SD$	**P1 (°C)** $T_{CP} \pm SD$	**P2 (°C)** $T_{CP} \pm SD$	**P3 (°C)** $T_{CP} \pm SD$
Medium	**Ultrapure water**			**Phosphate saline buffer**			**Foetal Bovine Serum**		
1.25	-	-	-	64.06 ± 0.05	55.28 ± 0.06	52.22 ± 0.04	75.02 ± 0.79	59.18 ± 0.08	55.31 ± 0.08
2.50	-	-	-	58.35 ± 0.16	52.68 ± 0.08	50.23 ± 0.10	70.70 ± 0.57	53.67 ± 0.19	50.55 ± 0.14
5.0	-	-	-	55.15 ± 0.08	49.15 ± 0.10	47.73 ± 0.08	60.85 ± 0.37	51.83 ± 0.08	48.53 ± 0.08
10.0	58.10 ± 0.10	56.78 ± 0.42	56.2 ± 0.58	53.65 ± 0.10	47.30 ± 0.17	46.27 ± 0.10	56.72 ± 0.34	48.63 ± 0.14	45.73 ± 0.08
20.0	-	-	-	54.65 ± 0.04	50.09 ± 0.02	50.13 ± 0.05	54.62 ± 0.40	58.40 ± 0.14*	49.57 ± 0.08
40.0	-	-	-	54.00 ± 0.14	48.38 ± 0.22	48.08 ± 0.12	49.53 ± 0.38	33.65 ± 0.20	48.98 ± 0.12

Note: At high polymer concentrations (20 and 40 mg/mL), the cloud point temperatures were poorly reproducible and unreliable, and the inter-run-differences were up to 20°C (particularly in **pDFEA** in PBS). At low concentrations (1.25 to 10.0 mg/mL), multiple independent experiments provided the same value of T_{CP} (within a margin of 0.5°C). We kept repeating measurements until two independent runs provided *similar* results and reliable turbidimetry-as-a-function-of-temperature graphs (*i.e.*, the turbidity decreased monotonously and relatively quickly with no sudden or inexplicable changes in trends). Therefore, we concluded that turbidimetry is not a reliable method for determining T_{CP}s at high polymer concentrations and these data were accordingly disregarded from further interpretations. Nevertheless, we present the complete set of our results in **Tables S3** to **S6**.

S6. Turbidimetric data

Every polymer solution was measured at least 6 times. If the data from all runs were similar, the data was processed: we calculated the mean values and standard deviations of T_{CPS} (**Table S3 to S6**). Only one cycle is shown in **Figures S25** to **S36** for clarity.

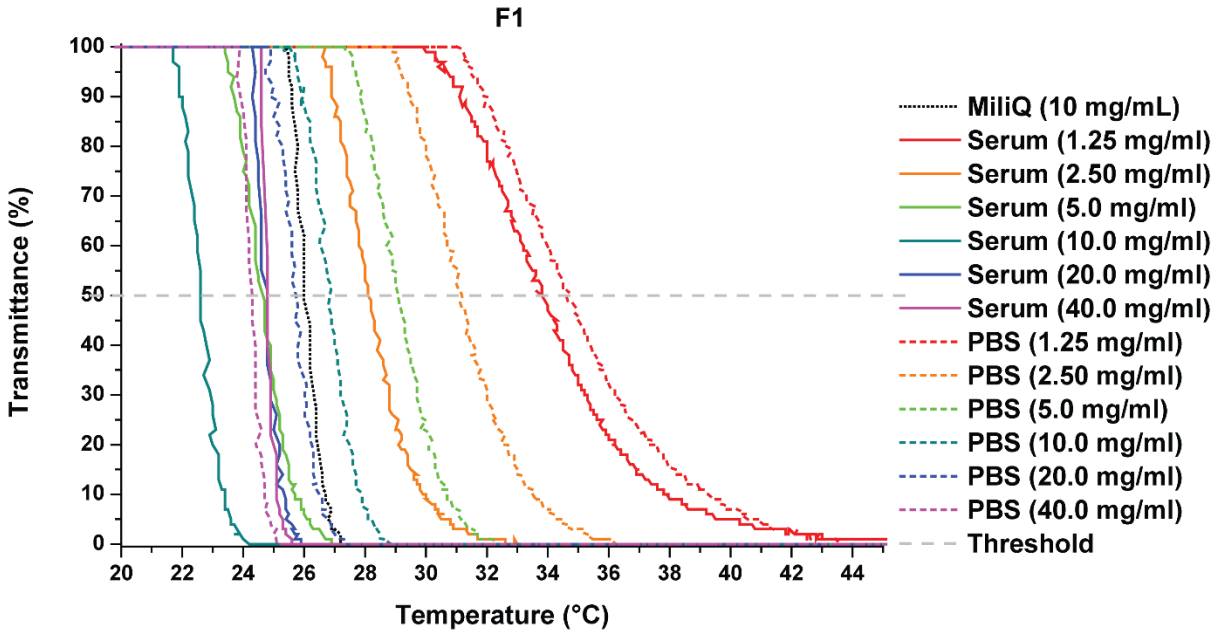

Figure S25. Transmittance of the **F1** (**pDFEA**) solution in ultrapure water (MiliQ), PBS, and FBS (serum), respectively, as a function of temperature

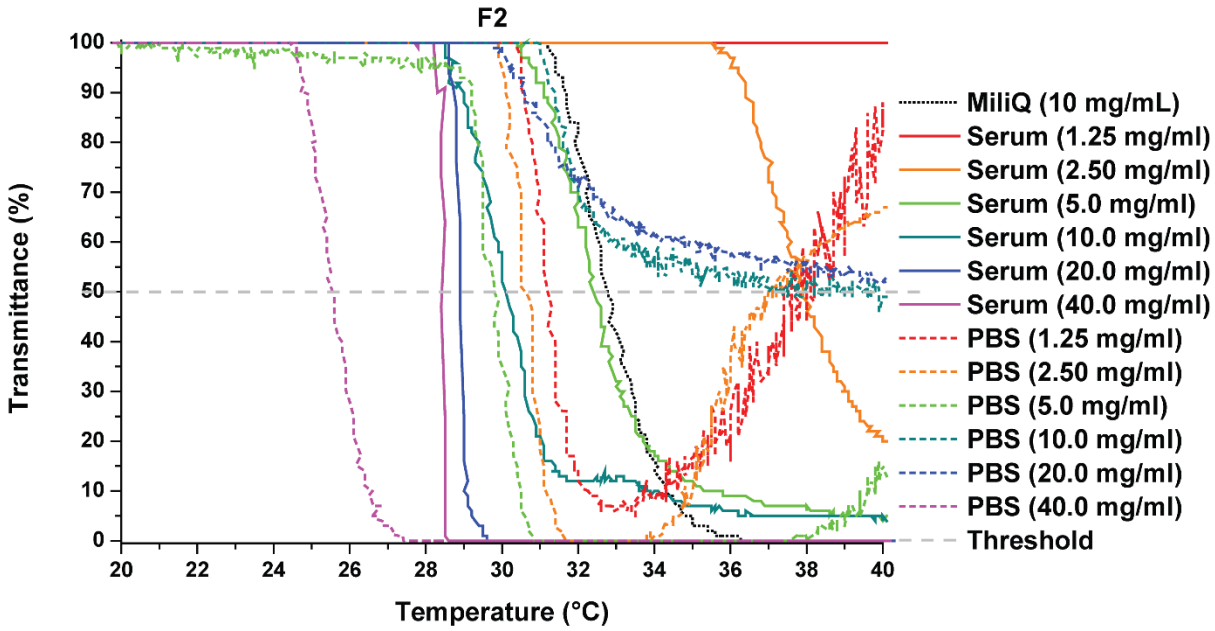

Figure S26. Transmittance of the **F2** (**pDFEA**) solution in ultrapure water (MiliQ), PBS, and FBS (serum), respectively, as a function of temperature

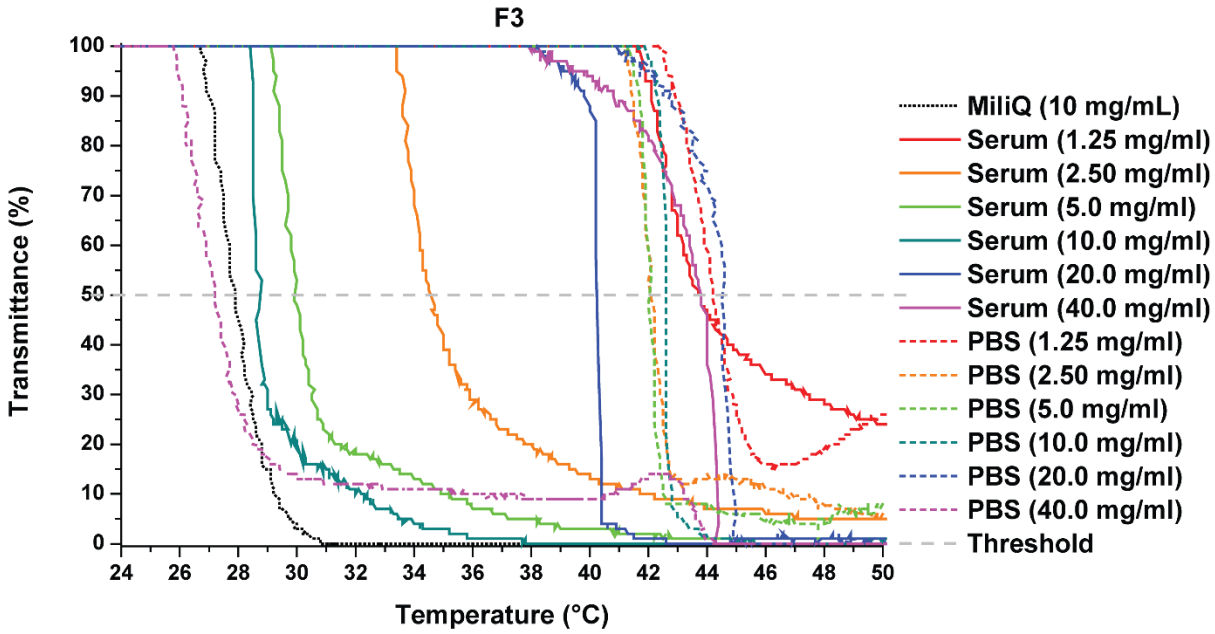

Figure S27. Transmittance of the **F3** (**pDFEA**) solution in ultrapure water (MiliQ), PBS, and FBS (serum), respectively, as a function of temperature

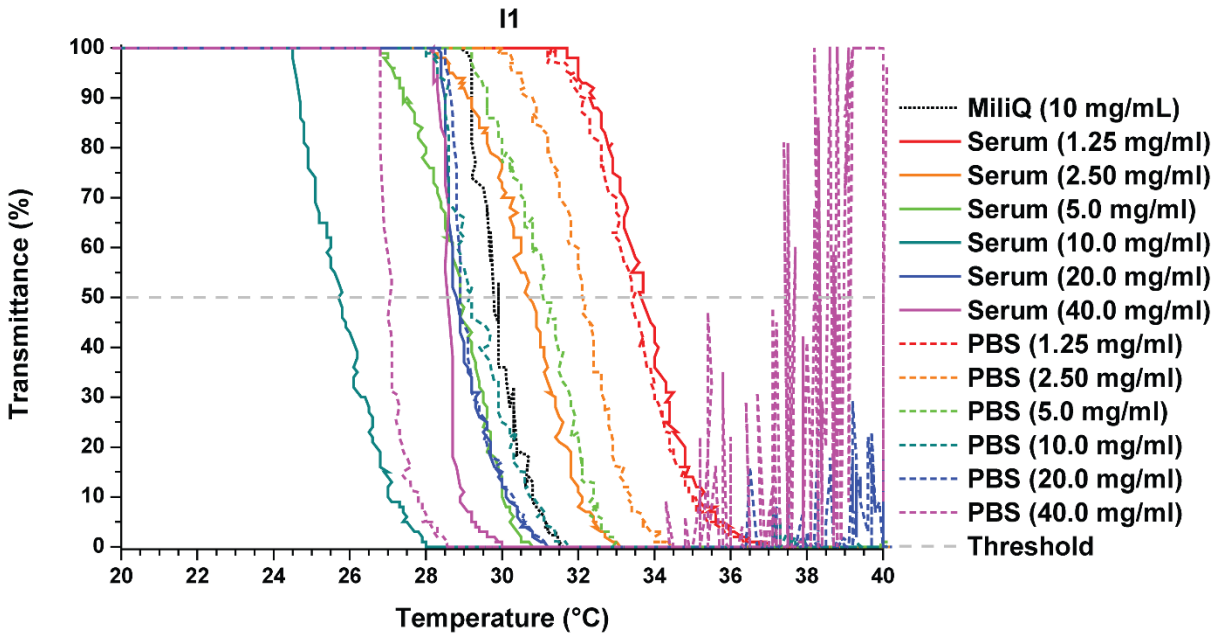

Figure S28. Transmittance of the **I1** (**pNIPAM**) solution in ultrapure water (MiliQ), PBS, and FBS (serum), respectively, as a function of temperature

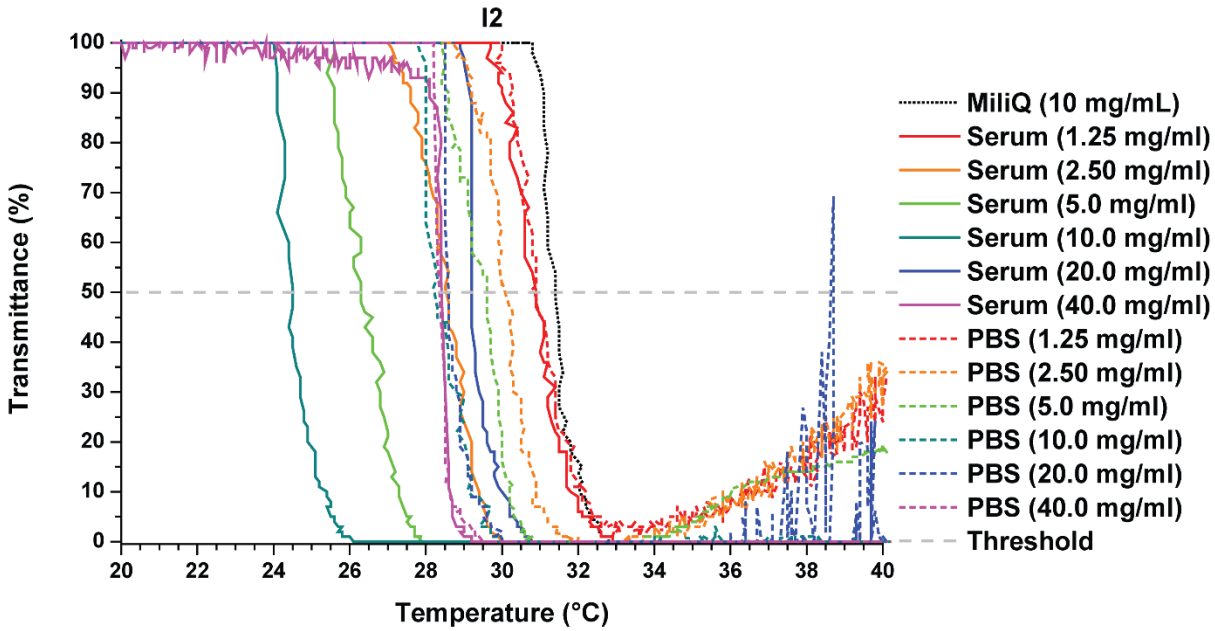

Figure S29. Transmittance of the **I2** (**pNIPAM**) solution in ultrapure water (MiliQ), PBS, and FBS (serum), respectively, as a function of temperature

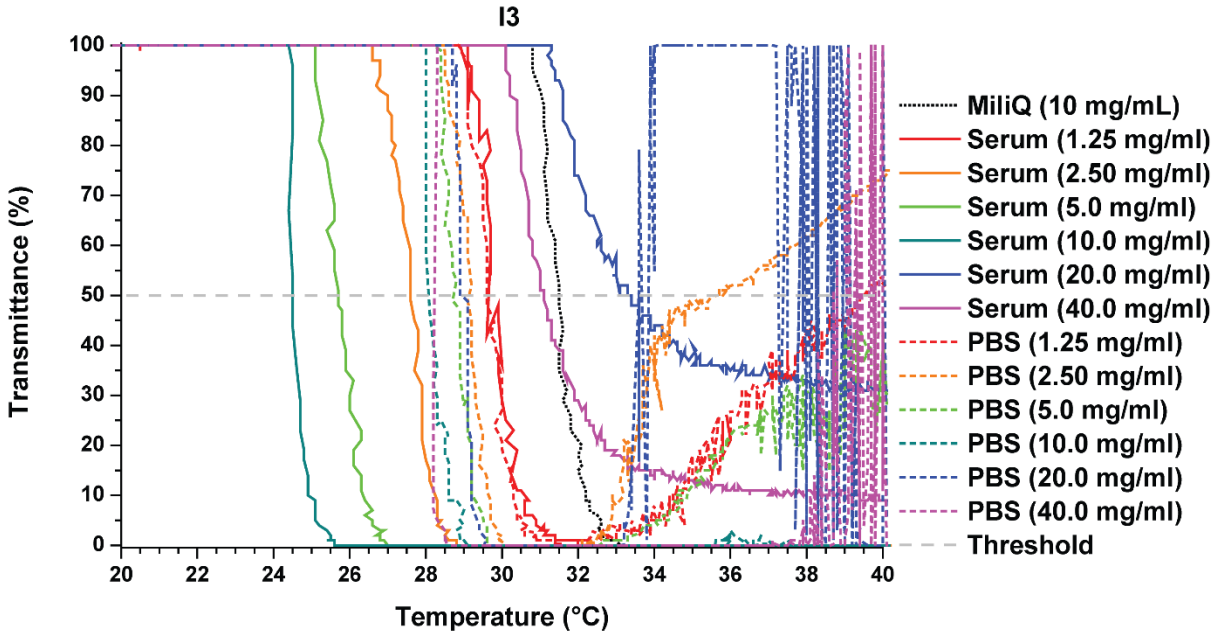

Figure S30. Transmittance of the **I3** (**pNIPAM**) solution in ultrapure water (MiliQ), PBS, and FBS (serum), respectively, as a function of temperature

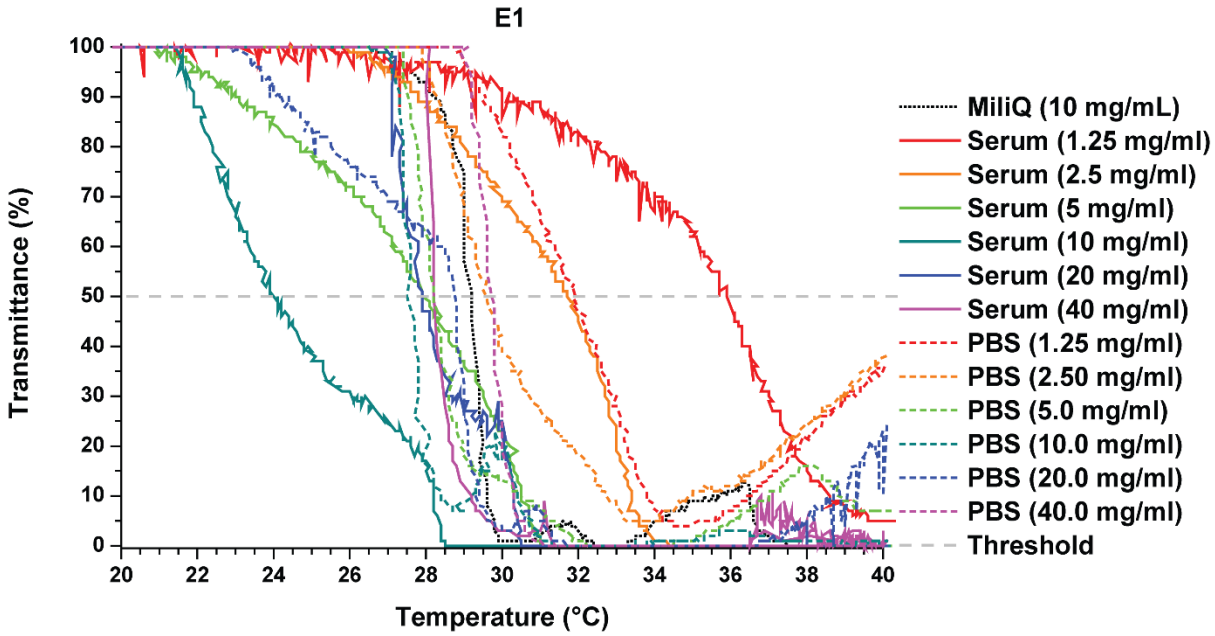

Figure S31. Transmittance of the **E1** (**pDEA**) solution in ultrapure water (MiliQ), PBS, and FBS (serum), respectively, as a function of temperature

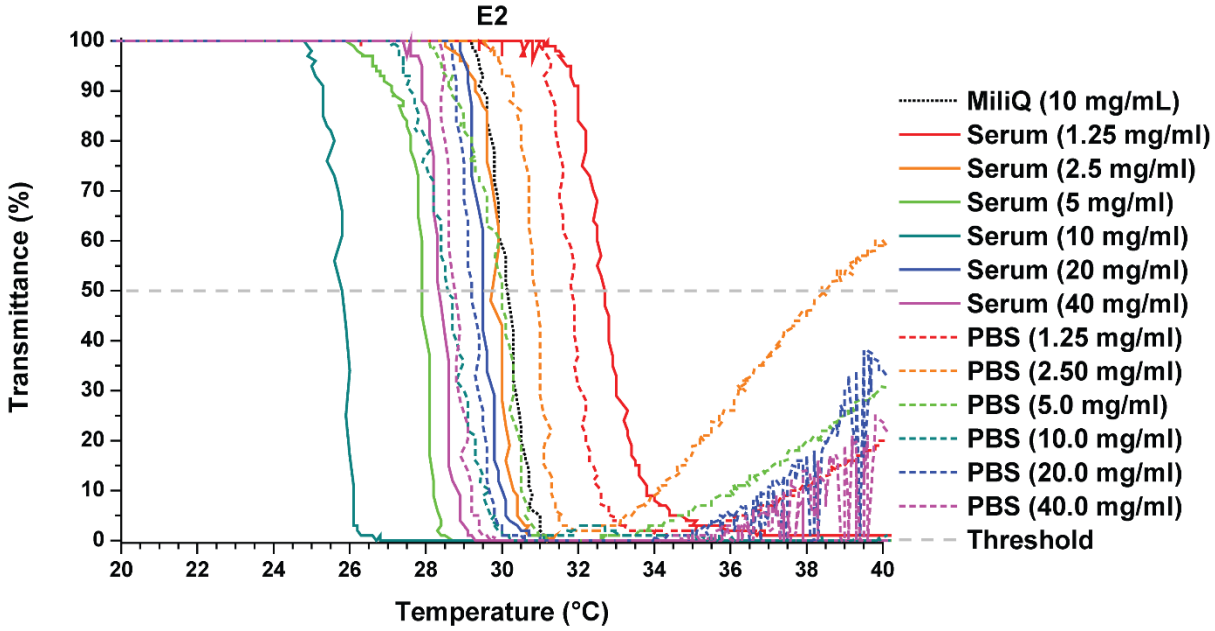

Figure S32. Transmittance of the **E2** (**pDEA**) solution in ultrapure water (MiliQ), PBS, and FBS (serum), respectively, as a function of temperature

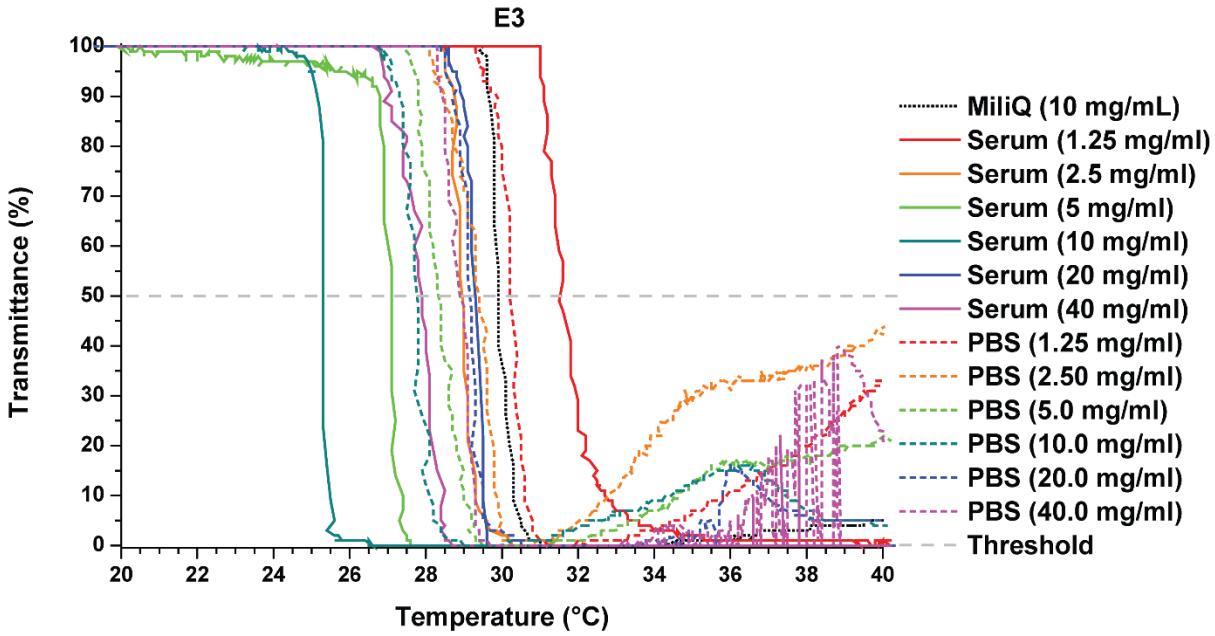

Figure S33. Transmittance of the **E3** (**pDEA**) solution in ultrapure water (MiliQ), PBS, and FBS (serum), respectively, as a function of temperature

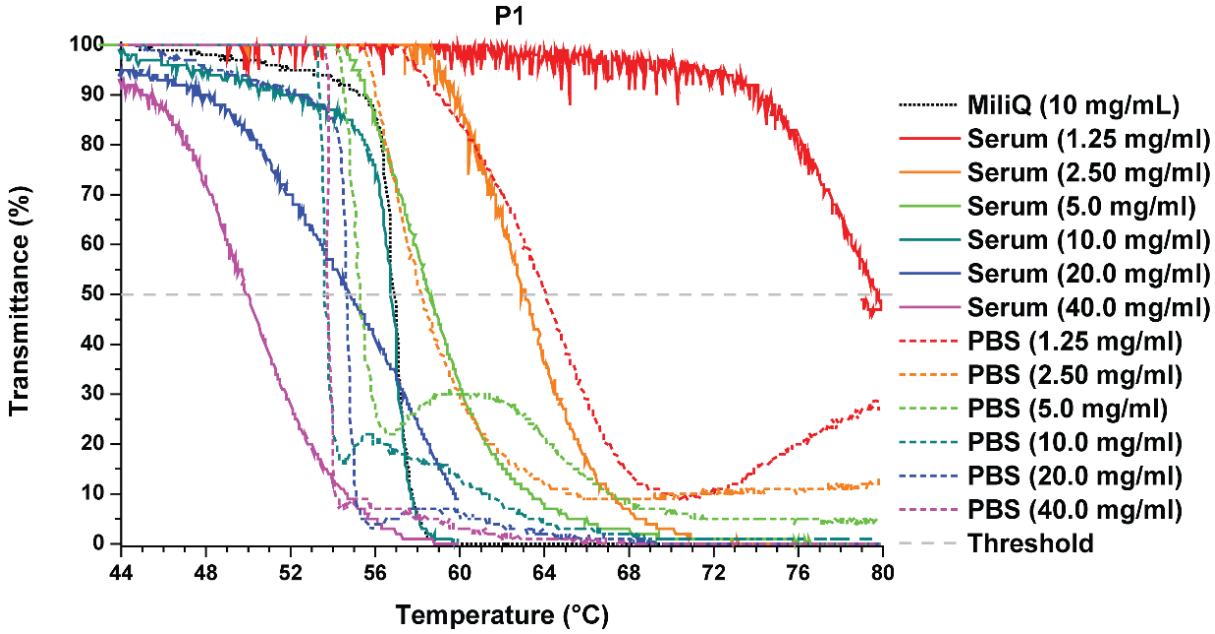

Figure S34. Transmittance of the **P1** (**pAP**) solution in ultrapure water (MiliQ), PBS, and FBS (serum), respectively, as a function of temperature

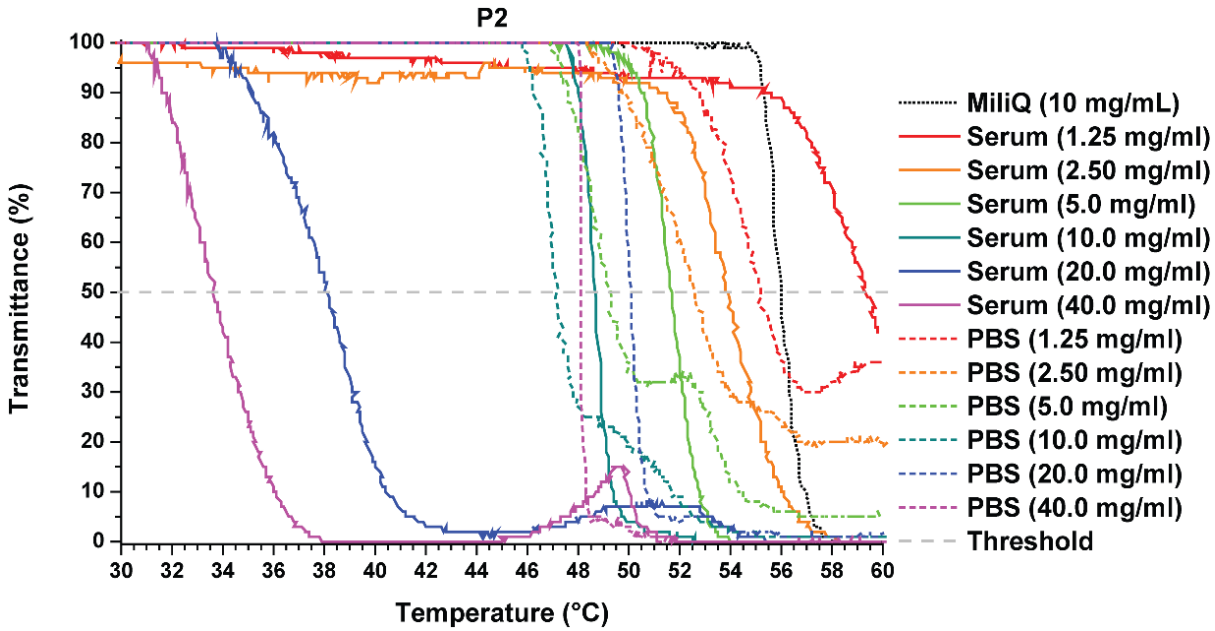

Figure S35. Transmittance of the **P2** (**pAP**) solution in ultrapure water (MiliQ), PBS, and FBS (serum), respectively, as a function of temperature

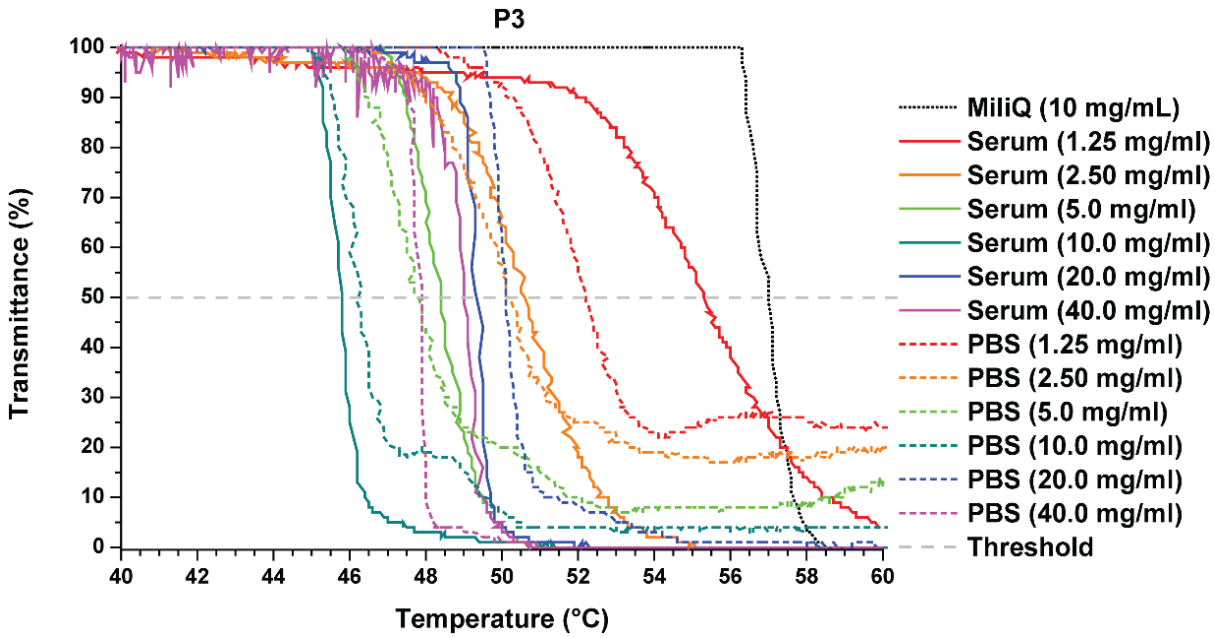

Figure S36. Transmittance of the **P3** (**pAP**) solution in ultrapure water (MiliQ), PBS, and FBS (serum), respectively, as a function of temperature

S7. Isothermal titration calorimetry

Polymers **F1**, **F2**, **F3**, **I3**, **E3**, or **P3** were dissolved in ultrapure water and thermally equilibrated at 3 specific temperatures: (i) below the T_{CP} of the study polymers in all solvents (no aggregates were visible to the naked eye neither before nor after the titration); (ii) above the T_{CP} of the polymer in PBS and FBS, but below the T_{CP} of the polymer in water (titration triggered aggregation); and (iii) above the T_{CP} of polymer in all solvents (the polymer aggregates were titrated). Subsequently, we disrupted the system equilibrium by consecutively adding small portions of PBS or FBS and measuring the heat flux caused by the establishment of a new equilibrium (see *e.g.* **Figure 5A**, black line). Then, we measured the heat flux corresponding to the PBS or FBS addition to ultrapure water (no added polymer, blank samples; **Figure 5A**, red line) to subtract the heat flux caused by PBS/ FBS dilution. After subtracting the heat flux of the blank sample from the heat flux of the sample solution, we obtained a complex titration isotherm[S13] (**Figure 5B**), with three phases: **I**, **II** and **III** (**Figure 5A**).

S7.1. ITC – titration of polymers F3, I3, E3, and P3

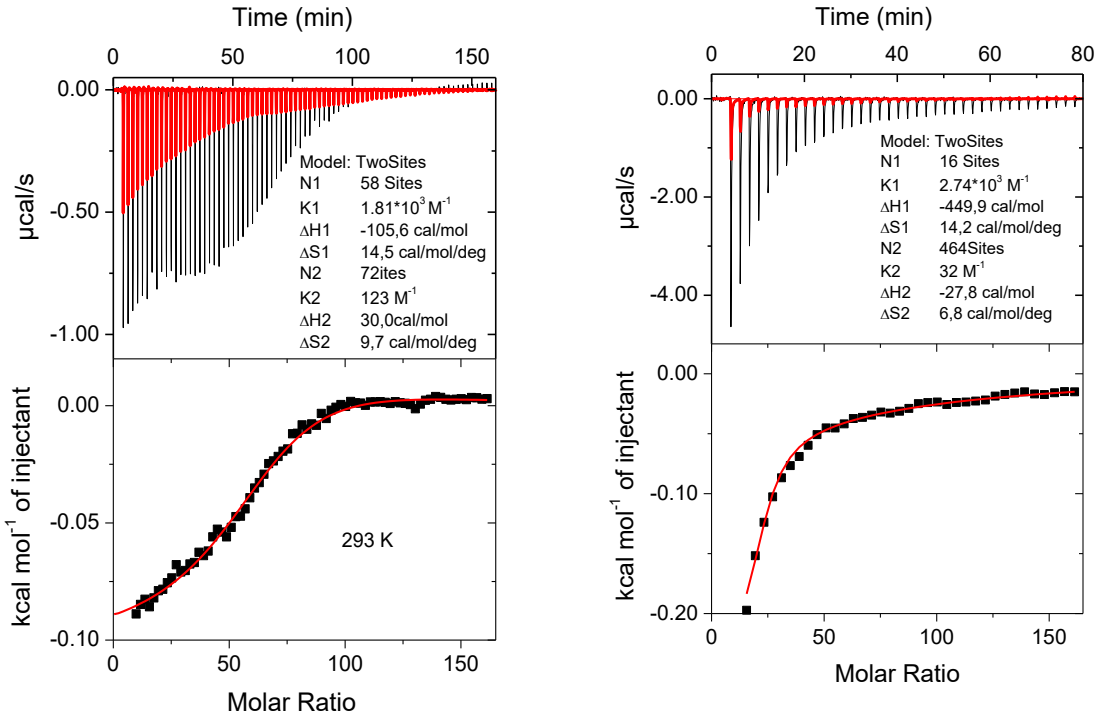

a **b**

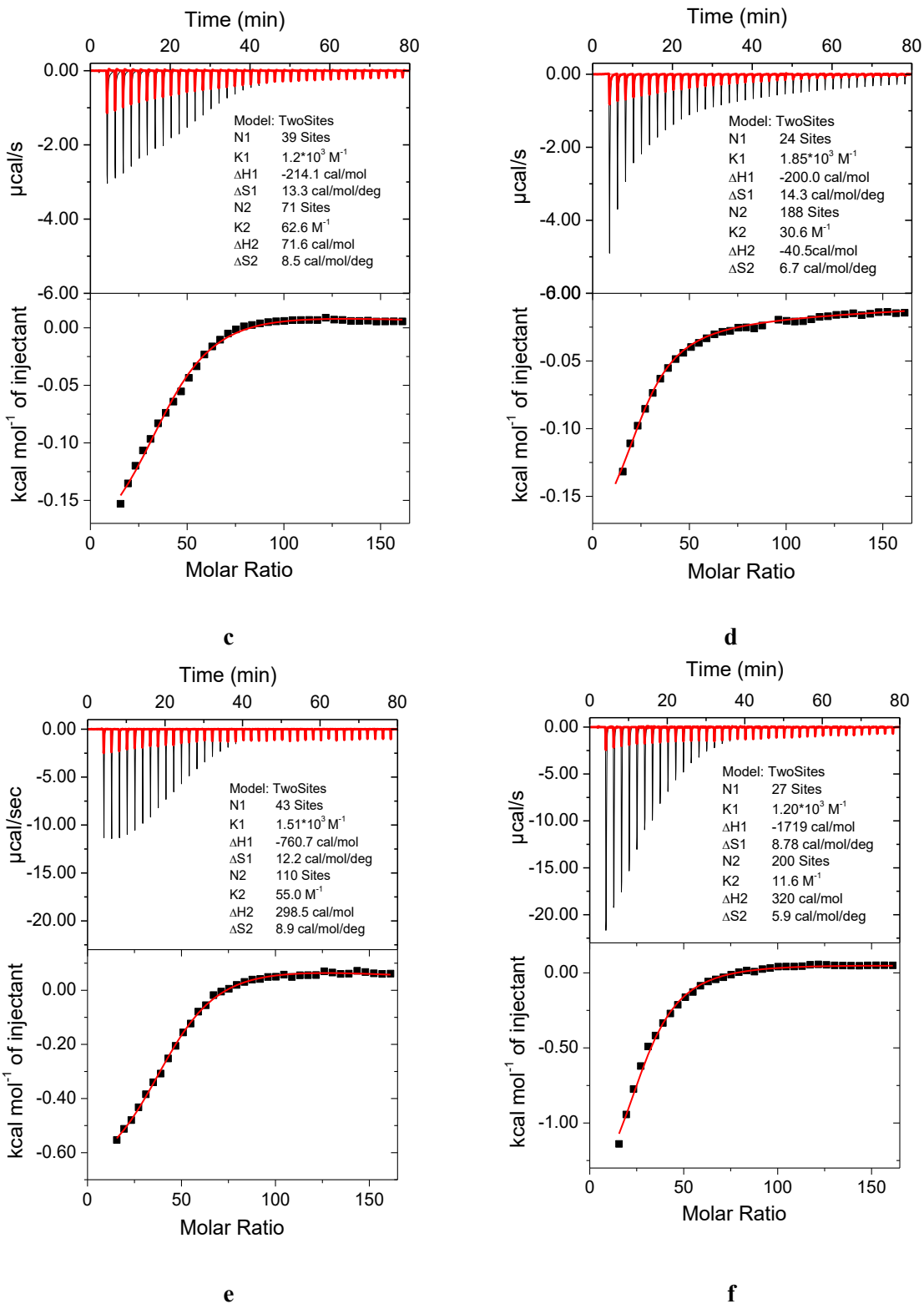

Figure S37. Titration of the **F3** (**pDFEA**) solution in ultrapure water with PBS (a,c,e) and FBS (b,d,f) respectively; 293 K (a,b), 301 K (c,d) and 323 K (e,f). Upper graph – heat flux as a function of time; red line – titration of PBS or FBS, respectively, into ultrapure water; black line – titration into polymer solution. Lower graph – integrated heat per 1 mol of titrant (scatter); fit to a two-site model (line).

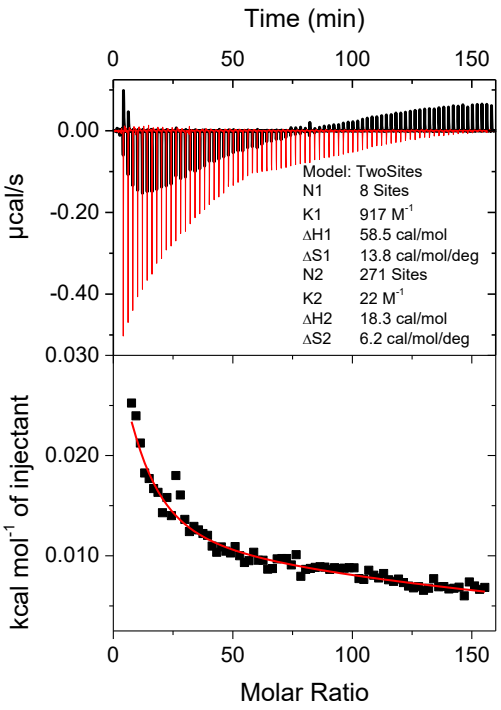
Time (min)
µcal/s
kcal mol^{-1} of injectant
Molar Ratio
Model: TwoSites
N1 8 Sites
K1 917 M^{-1}
ΔH1 58.5 cal/mol
ΔS1 13.8 cal/mol/deg
N2 271 Sites
K2 22 M^{-1}
ΔH2 18.3 cal/mol
ΔS2 6.2 cal/mol/deg

a

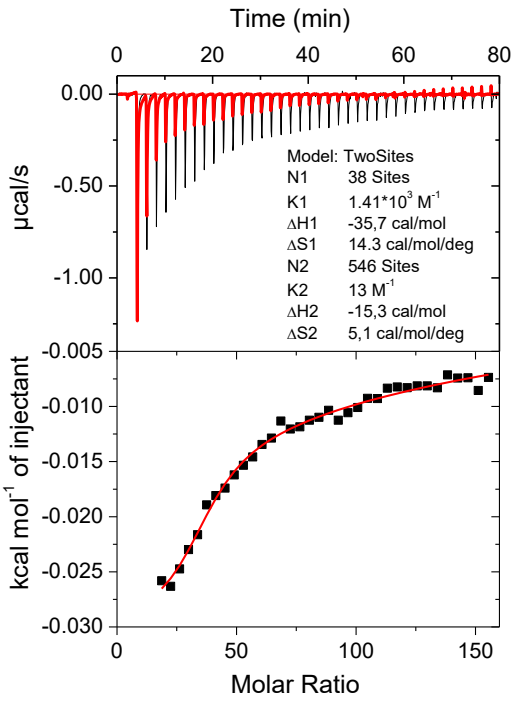
Time (min)
µcal/s
kcal mol^{-1} of injectant
Molar Ratio
Model: TwoSites
N1 38 Sites
K1 1.41*10^{3} M^{-1}
ΔH1 -35,7 cal/mol
ΔS1 14.3 cal/mol/deg
N2 546 Sites
K2 13 M^{-1}
ΔH2 -15,3 cal/mol
ΔS2 5,1 cal/mol/deg

b

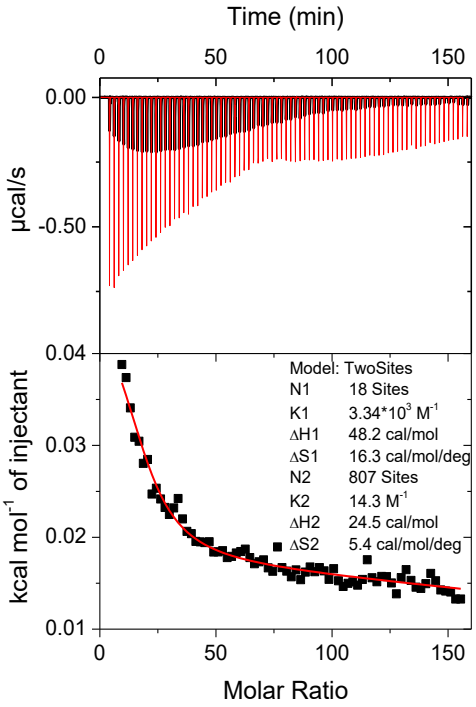
Time (min)
µcal/s
kcal mol^{-1} of injectant
Molar Ratio
Model: TwoSites
N1 18 Sites
K1 3.34*10^{3} M^{-1}
ΔH1 48.2 cal/mol
ΔS1 16.3 cal/mol/deg
N2 807 Sites
K2 14.3 M^{-1}
ΔH2 24.5 cal/mol
ΔS2 5.4 cal/mol/deg

c

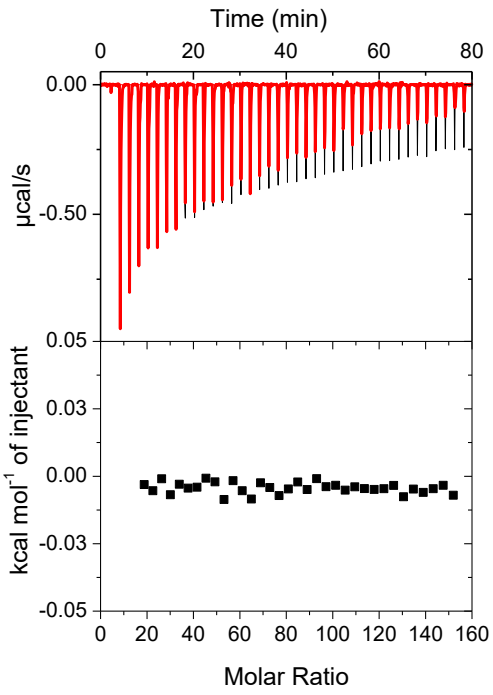
Time (min)
µcal/s
kcal mol^{-1} of injectant
Molar Ratio

d

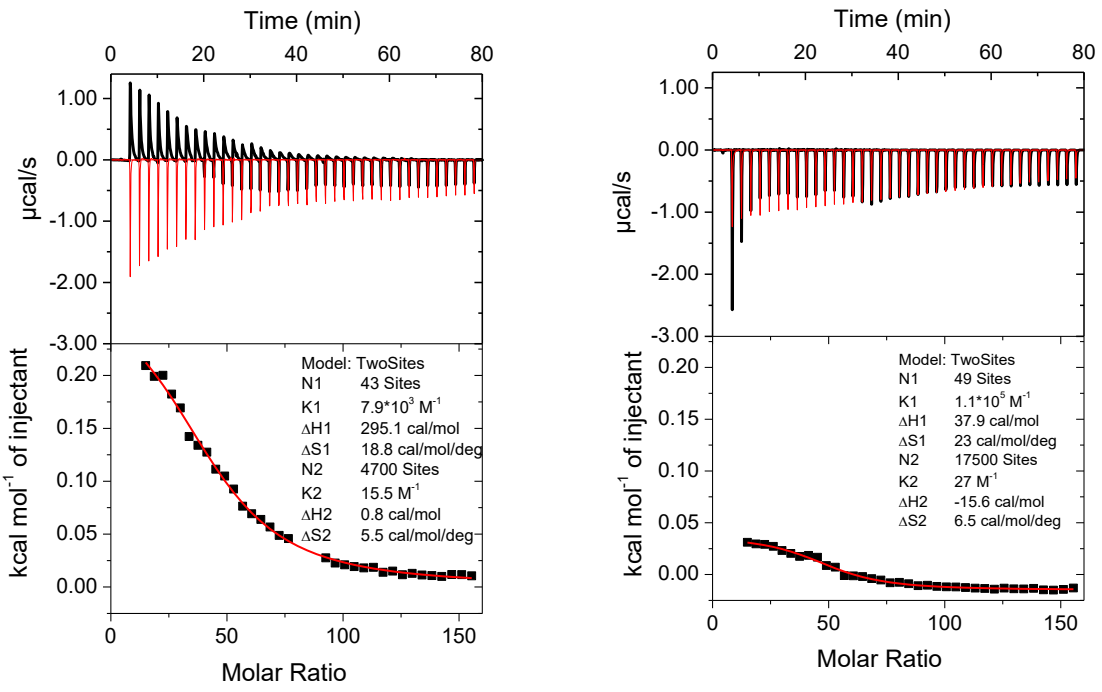

e **f**

Figure S38. Titration of the **I3** (**pNIPAM**) solution in ultrapure water with PBS (**a**,**c**,**e**) and FBS (**b**,**d**,**f**) respectively; 293 K (**a**,**b**), 303 K (**c**,**d**) and 313 K (**e**,**f**). Upper graph – heat flux as a function of time; red line – titration of PBS or FBS, respectively, into ultrapure water; black line – titration into polymer solution. Lower graph – integrated heat per 1 mol of titrant (scatter); fit to the two-site model (line).

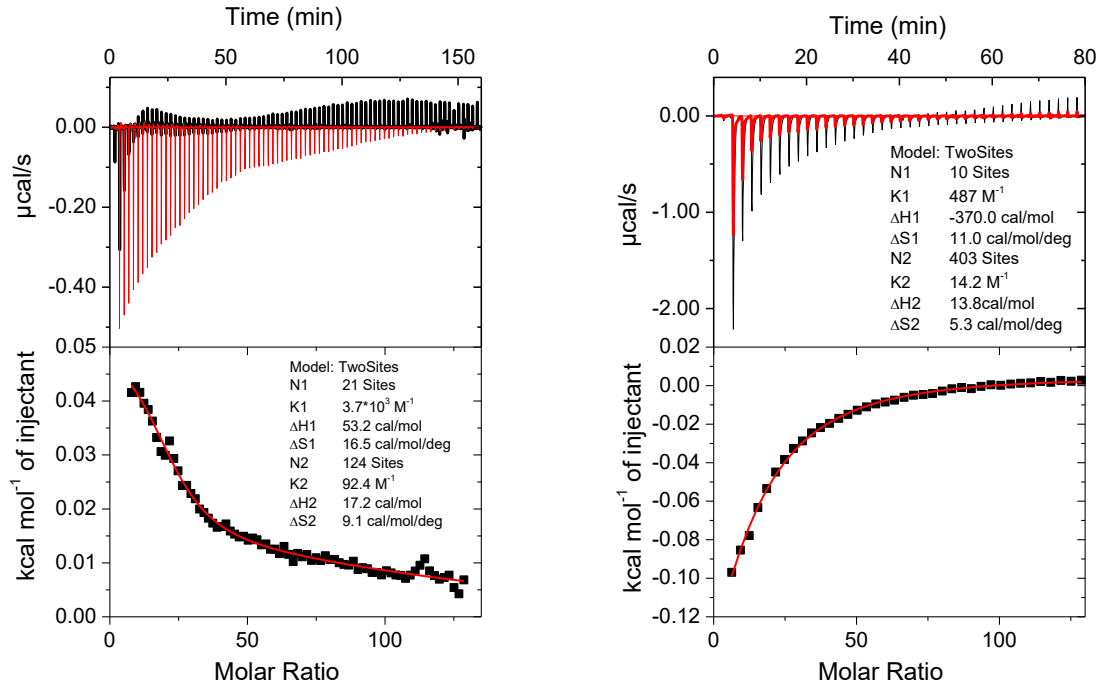

a **b**

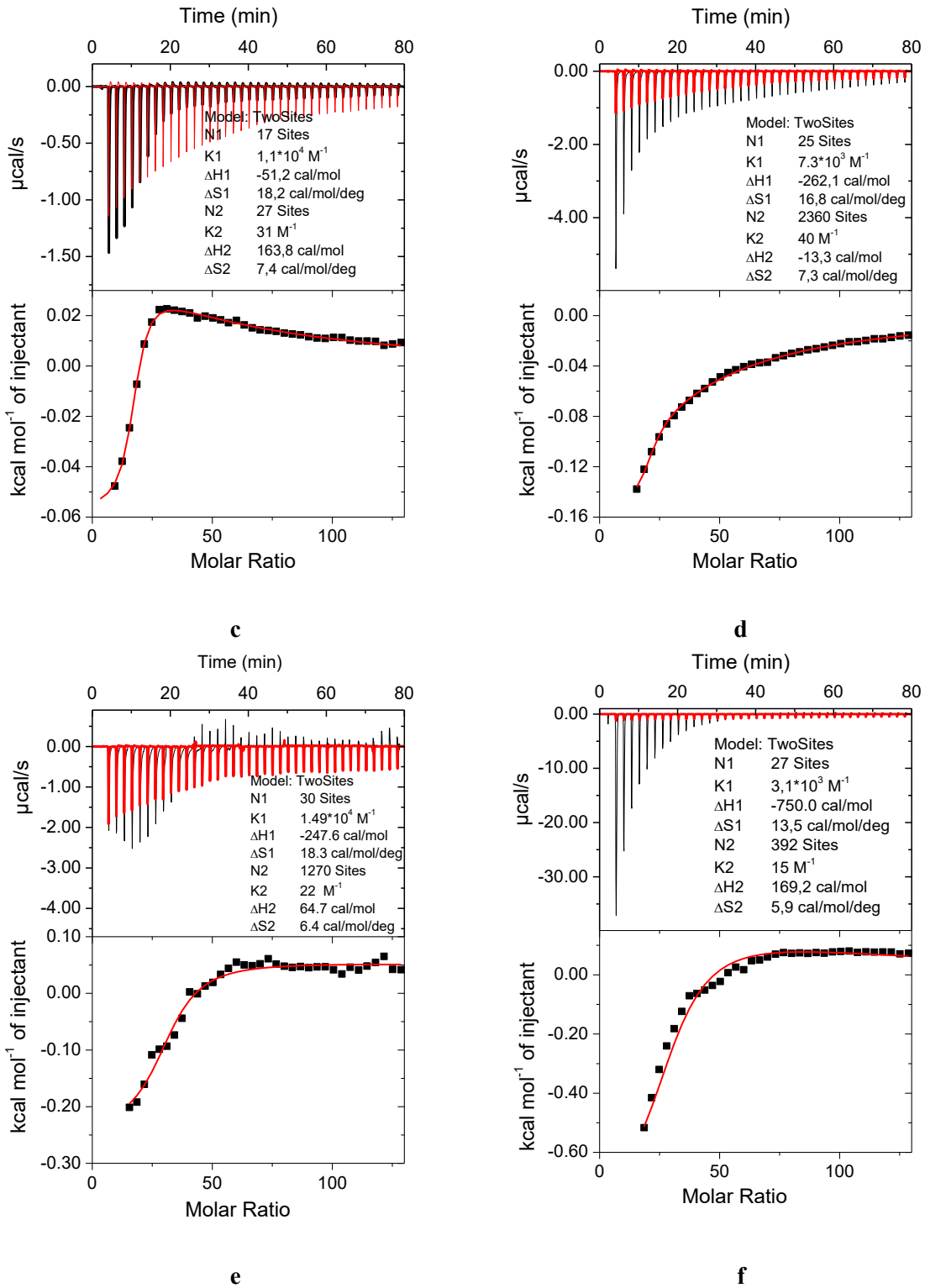

Figure S39. Titration of the **E3** (**pDEA**) solution in ultrapure water with PBS (**a**,**c**,**e**) and FBS (**b**,**d**,**f**) respectively; 293 K (**a**,**b**), 301 K (**c**,**d**) and 313 K (**e**,**f**). Upper graph – heat flux as a function of time; red line – titration of PBS or FBS, respectively, into ultrapure water; black line – titration into polymer solution. Lower graph – integrated heat per 1 mol of titrant (scatter); fit to the two independent binding sites model (line).

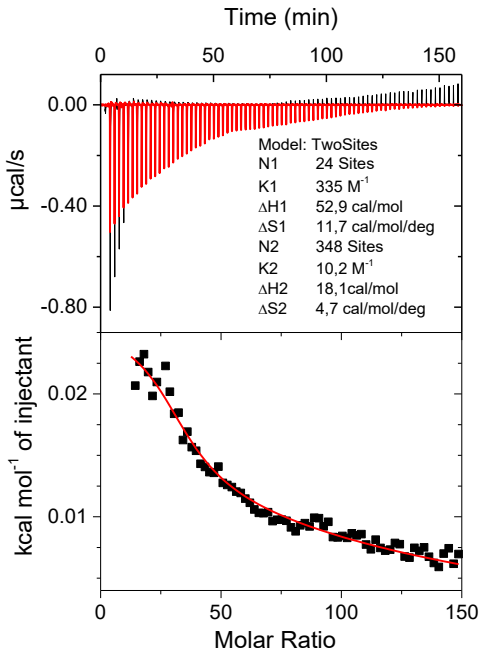
Time (min)
µcal/s
kcal mol^{-1} of injectant
Molar Ratio
Model: TwoSites
N1 24 Sites
K1 335 M^{-1}
ΔH1 52,9 cal/mol
ΔS1 11,7 cal/mol/deg
N2 348 Sites
K2 10,2 M^{-1}
ΔH2 18,1cal/mol
ΔS2 4,7 cal/mol/deg

a

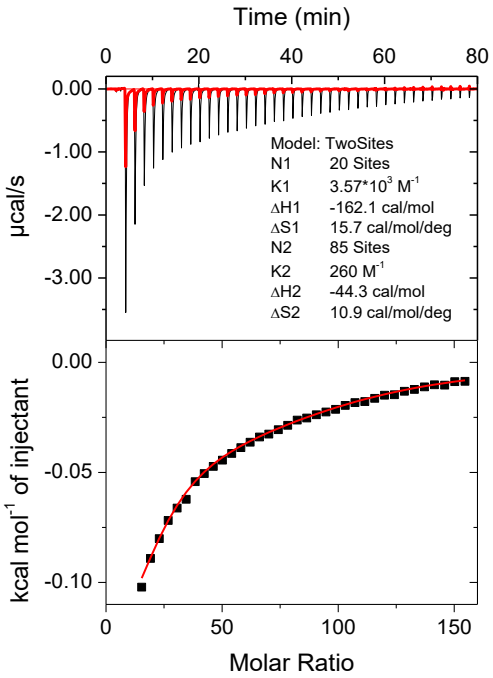
Time (min)
µcal/s
kcal mol^{-1} of injectant
Molar Ratio
Model: TwoSites
N1 20 Sites
K1 3.57*10^{3} M^{-1}
ΔH1 -162.1 cal/mol
ΔS1 15.7 cal/mol/deg
N2 85 Sites
K2 260 M^{-1}
ΔH2 -44.3 cal/mol
ΔS2 10.9 cal/mol/deg

b

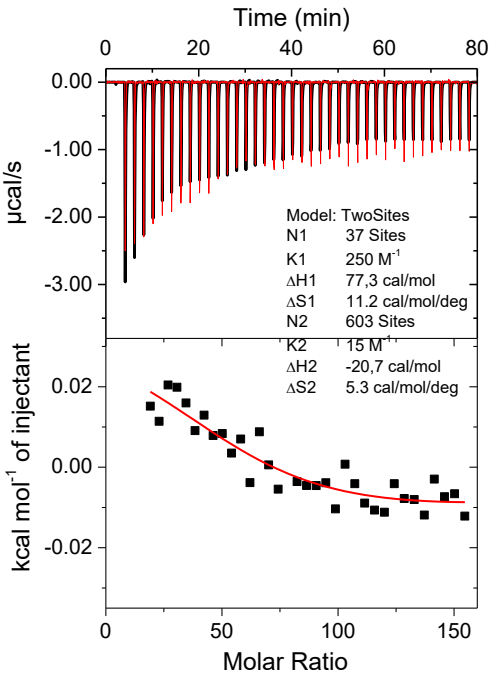
Time (min)
µcal/s
kcal mol^{-1} of injectant
Molar Ratio
Model: TwoSites
N1 37 Sites
K1 250 M^{-1}
ΔH1 77,3 cal/mol
ΔS1 11.2 cal/mol/deg
N2 603 Sites
K2 15 M^{-1}
ΔH2 -20,7 cal/mol
ΔS2 5.3 cal/mol/deg

c

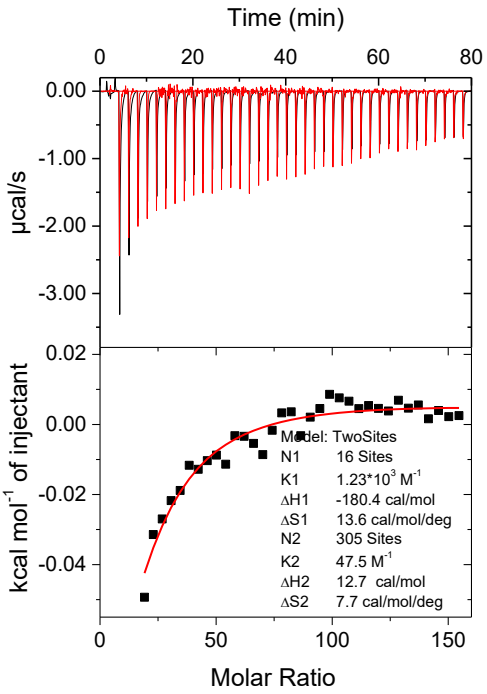
Time (min)
µcal/s
kcal mol^{-1} of injectant
Molar Ratio
Model: TwoSites
N1 16 Sites
K1 1.23*10^{3} M^{-1}
ΔH1 -180.4 cal/mol
ΔS1 13.6 cal/mol/deg
N2 305 Sites
K2 47.5 M^{-1}
ΔH2 12.7 cal/mol
ΔS2 7.7 cal/mol/deg

d

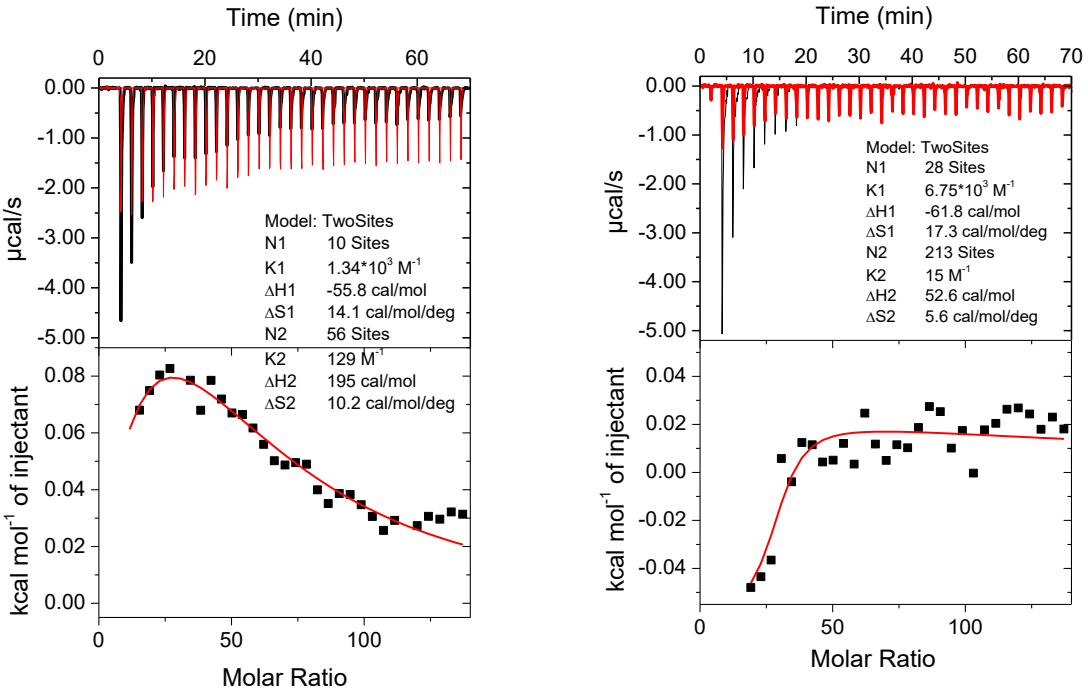

e **f**

Figure S40. Titration of the **P3** (**pAP**) solution in ultrapure water with PBS (**a**,**c**,**e**) and FBS (**b**,**d**,**f**) respectively; 293 K (**a**,**b**), 323 K (**c**,**d**) and 333 K (**e**,**f**). Upper graph – heat flux as a function of time; red line – titration of PBS or FBS, respectively into ultrapure water; black line – titration into polymer solution. Lower graph – integrated heat per 1 mol of titrant (scatter); fit to the two independent binding sites model (line).

The titration isotherms of complex shape consist of heat effects originating from (**i**) "pseudo-binding" event and (**ii**) non-linear heat of mixing. Therefore, we fitted the cumulated reaction heat as a function of titrant-to-analyte molar ratio to **two** independent binding sites model (one Wiseman isoterm[S13] for each effect, both **i** and **ii**). Because the concentration of the titrant (PBS or FBS) is unknown (as these mixtures contain many compounds in various concentrations), we chose an arbitrary value 162.7 mM (ionic strength of PBS) for **both** PBS and FBS. Reaction enthalpy, as an independent fitting parameter, was then normalized to the analyte concentration (polymer). The remaining fitting parameters (stoichiometry n, binding constant K_a) are affected by the titrant-to-analyte molar ratio and, therefore, not included in the results.

The fitting parameters for the second binding site (**ii**) were:
a) $K_{a1} \gg K_{a2}$
b) $\Delta H_1 > \Delta H_2$

S7.2. ITC – enthalpies of F3, I3, E3, and P3

Table S7. Concentrations and pH of polymer solutions; enthalpy Δ*H* (J/mol of monomer) of mixing of polymer solutions with PBS and FBS at various temperatures

Sample	**F3 (pDFEA)**						**I3 (pNIPAM)**						**E3 (pDEA)**						**P3 (pAP)**					
Conc. (mM)*	0.213						0.221						0.267						0.216					
pH in H_2O**	≈ 4.9						≈ 4.6						≈ 4.0						≈ 5.5					
Titrant	**PBS**			**FBS**			**PBS**			**FBS**			**PBS**			**FBS**			**PBS**			**FBS**		
***T*, K**	**293**	**301**	**323**	**293**	**301**	**323**	**293**	**303**	**313**	**293**	**303**	**313**	**293**	**301**	**313**	**293**	**301**	**313**	**293**	**323**	**333**	**293**	**323**	**333**
Δ*H*, (J/mol)	−73.9	-100.7	−394.4	−86.7	−57.9	−559.6	4.9	9.1	113.1	−14.2	≈ 0.0	19.5	15.8	−12.3	−105.4	−52.5	−92.9	−287.2	14.4	32.3	−6.3	−36.7	−32.6	−19.6
transition conc. (mM)***	17.4	13.4	17.5	9.3	8.8	16.3	11.0	11.0	19.0	21.1	N/A	21.2	9.7	7.0	14.6	8.9	11.6	17.3	12.3	16.3	20.0	12.0	14.6	8.1
transition conc. (mg/mL)******	1.0	0.8	1.0	3.0	2.9	5.3	0.6	0.6	1.1	6.9	N/A	6.9	0.5	0.4	0.8	2.9	3.8	5.6	0.7	0.9	1.1	3.9	4.8	2.6

* polymer concentration in the analyte solution

** pH of aqueous solution of polymer, 10 mg/mL

*** concentration of titrant (PBS or FBS) in units of ionic strength of PBS solution, determined from the coordinate on the *x*-axis (molar ratio) on **Figures S37** to **40**.

**** concentration of titrant in mg/mL

S7.3. ITC - titration of benzoic acid

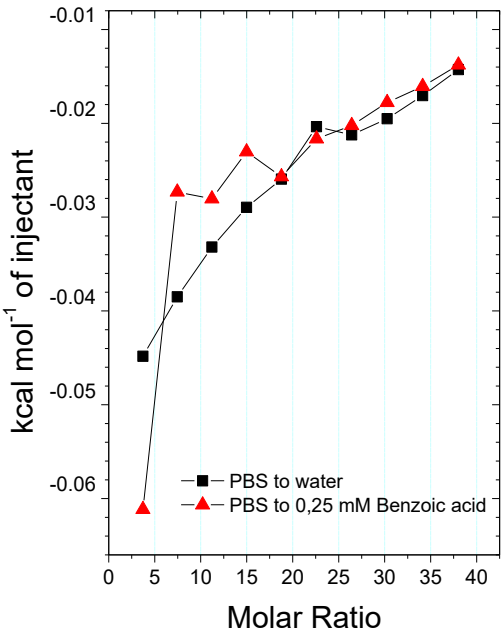

a

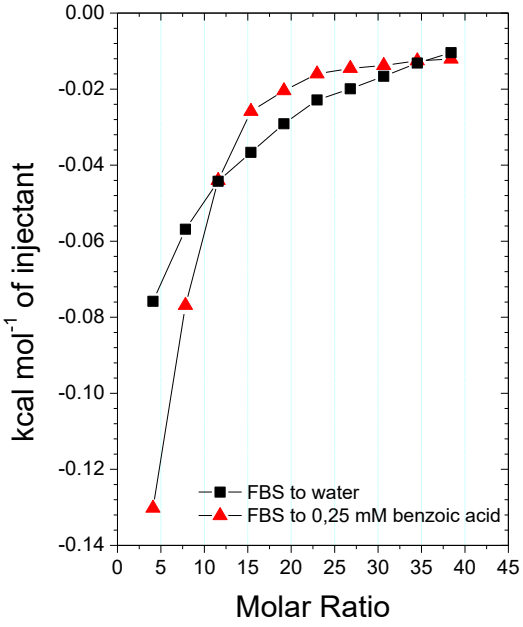

b

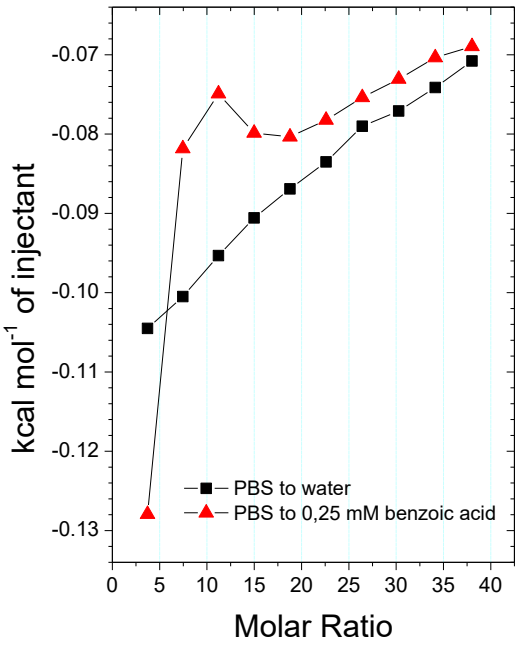

c

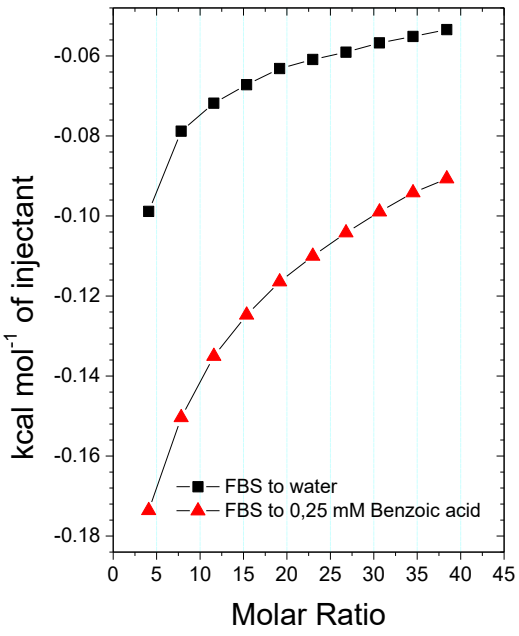

d

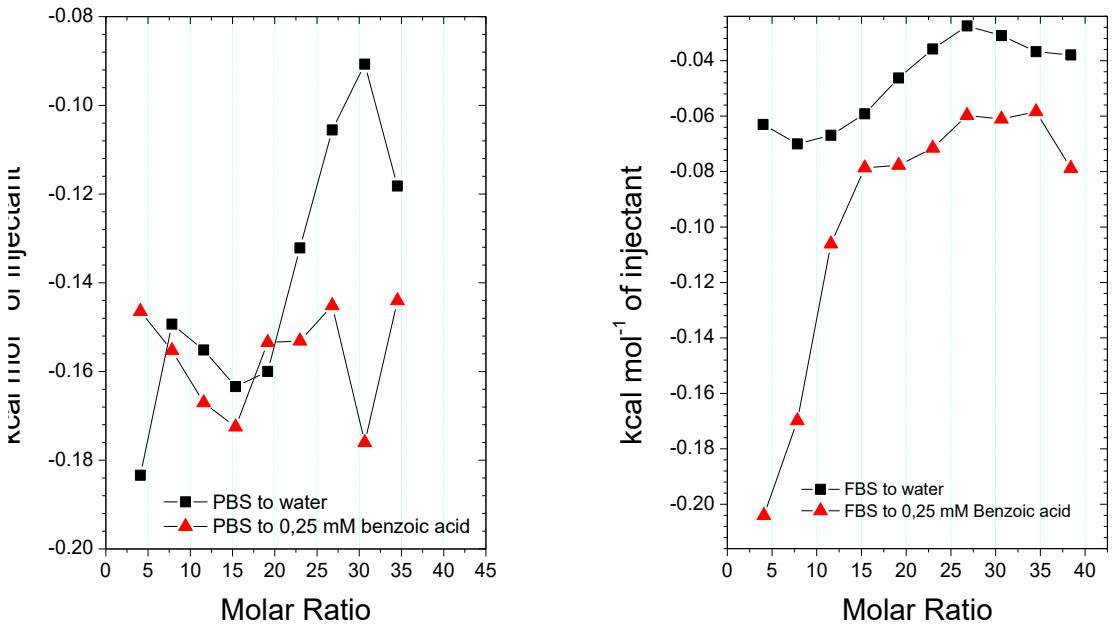

e **f**

Figure S41. ITC isotherms of the titration of the solution of benzoic acid (0.25 mM) with PBS (**a**, **c**, **e**) and FBS (**b**, **d**, **f**) at 293 K (**a**, **b**), 313 K(**c**, **d**) and 333 K (**e**, **f**).

S7.3. ITC – titration of polymers F1 and F2

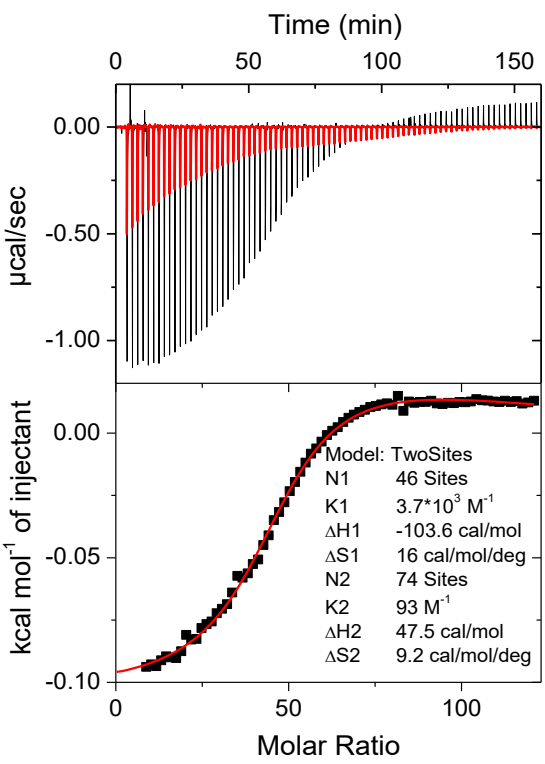

a

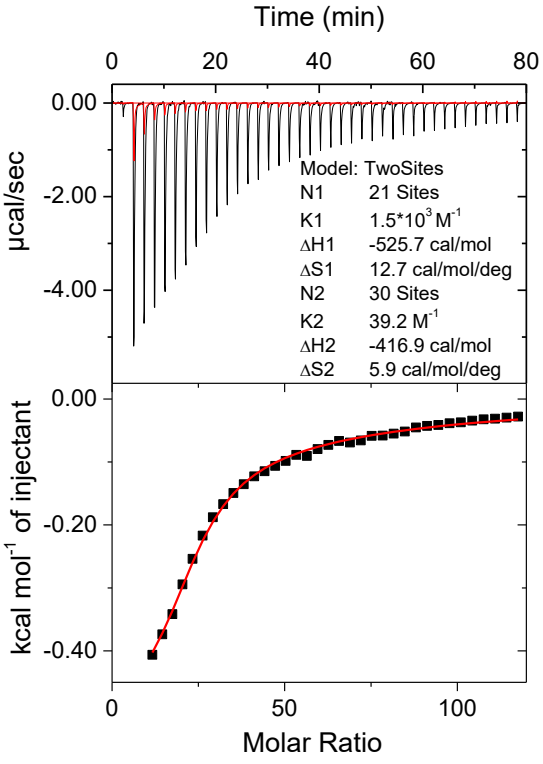

b

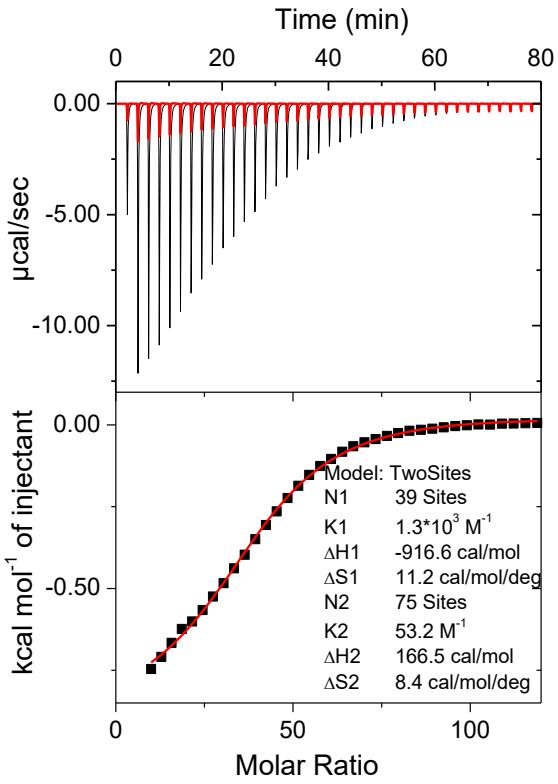

c

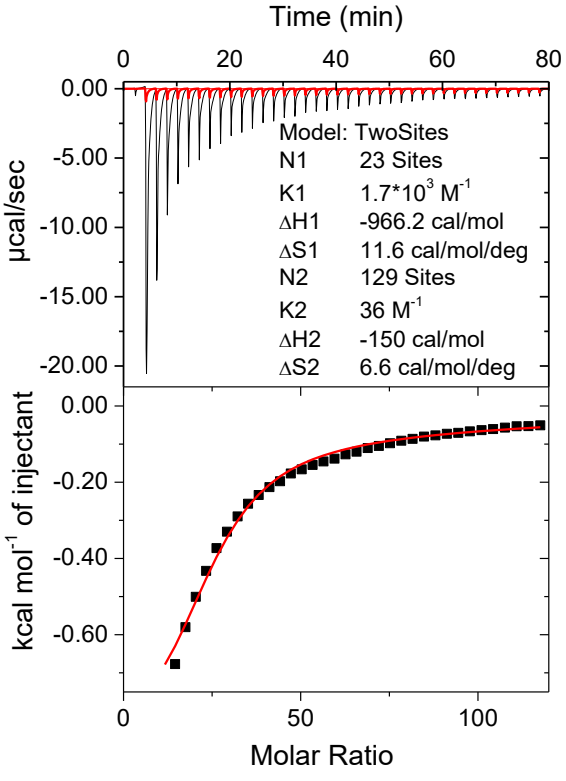

d

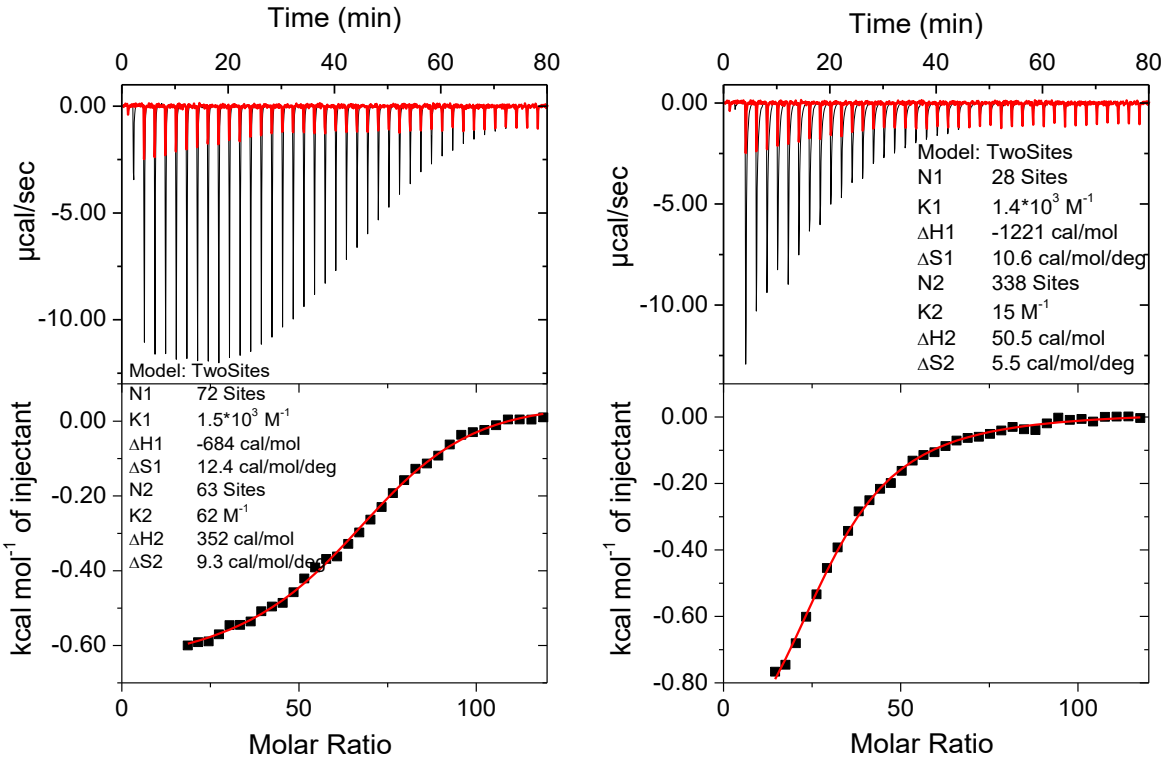

e **f**

Figure S42. Titration of the **F2** (**pDFEA**) solution in ultrapure water with PBS (**a**,**c**,**e**) and FBS (**b**,**d**,**f**) respectively; 293 K (**a**,**b**), 305 K (**c**,**d**) and 323 K (**e**,**f**). Upper graph – heat flux as a function of time; red line – titration of PBS or FBS, respectively into ultrapure water; black line – titration into polymer solution. Lower graph – integrated heat per 1 mol of titrant (scatter); fit to the two independent binding sites model (line).

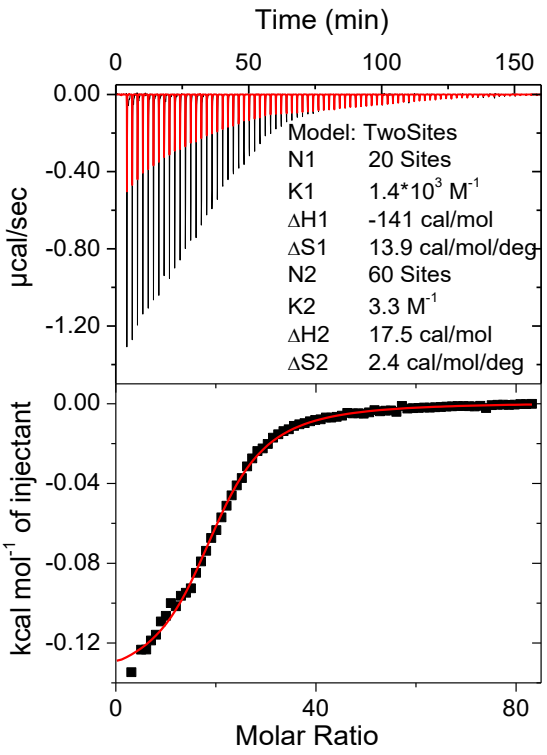
Time (min)
µcal/sec
kcal mol-1 of injectant
Molar Ratio
Model: TwoSites
N1 20 Sites
K1 1.4*10^3 M^-1
ΔH1 -141 cal/mol
ΔS1 13.9 cal/mol/deg
N2 60 Sites
K2 3.3 M^-1
ΔH2 17.5 cal/mol
ΔS2 2.4 cal/mol/deg

a

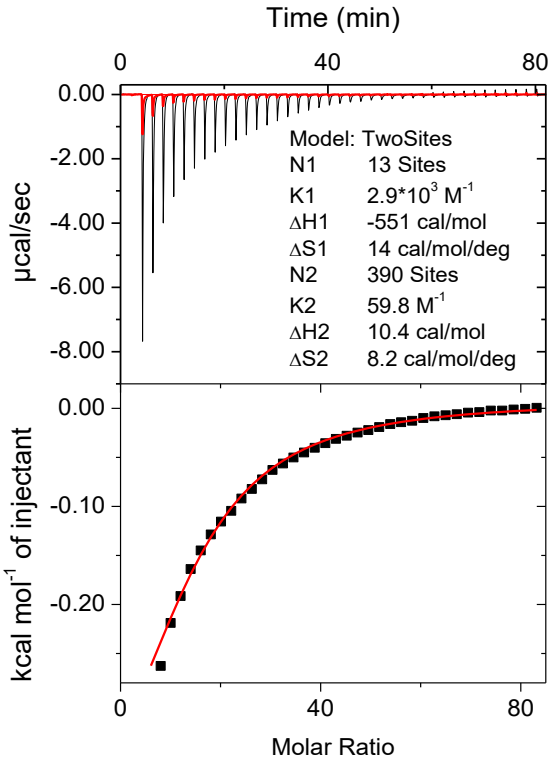
Time (min)
µcal/sec
kcal mol-1 of injectant
Molar Ratio
Model: TwoSites
N1 13 Sites
K1 2.9*10^3 M^-1
ΔH1 -551 cal/mol
ΔS1 14 cal/mol/deg
N2 390 Sites
K2 59.8 M^-1
ΔH2 10.4 cal/mol
ΔS2 8.2 cal/mol/deg

b

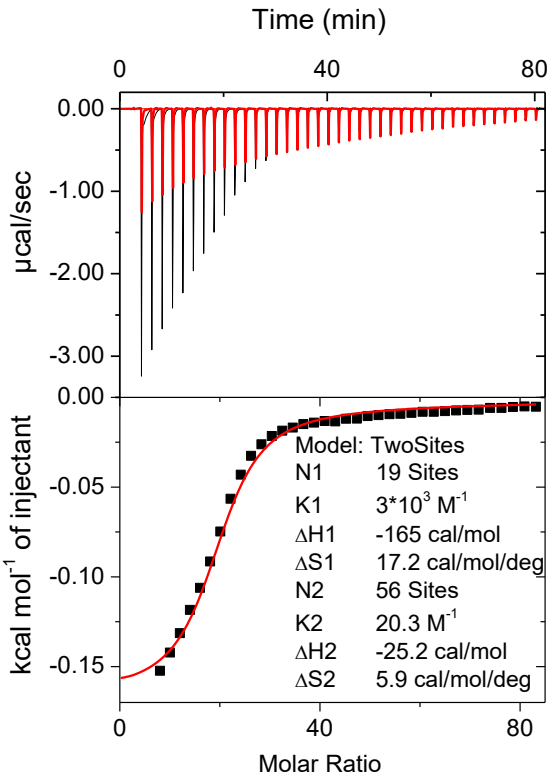
Time (min)
µcal/sec
kcal mol-1 of injectant
Molar Ratio
Model: TwoSites
N1 19 Sites
K1 3*10^3 M^-1
ΔH1 -165 cal/mol
ΔS1 17.2 cal/mol/deg
N2 56 Sites
K2 20.3 M^-1
ΔH2 -25.2 cal/mol
ΔS2 5.9 cal/mol/deg

c

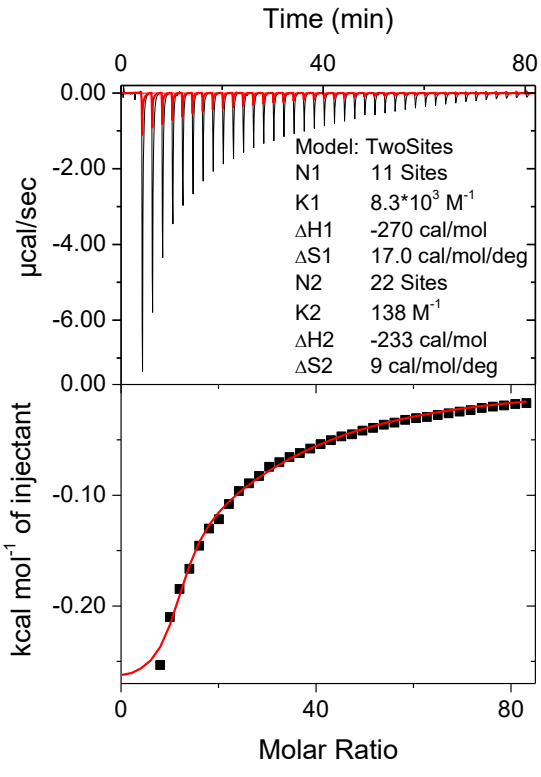
Time (min)
µcal/sec
kcal mol-1 of injectant
Molar Ratio
Model: TwoSites
N1 11 Sites
K1 8.3*10^3 M^-1
ΔH1 -270 cal/mol
ΔS1 17.0 cal/mol/deg
N2 22 Sites
K2 138 M^-1
ΔH2 -233 cal/mol
ΔS2 9 cal/mol/deg

d

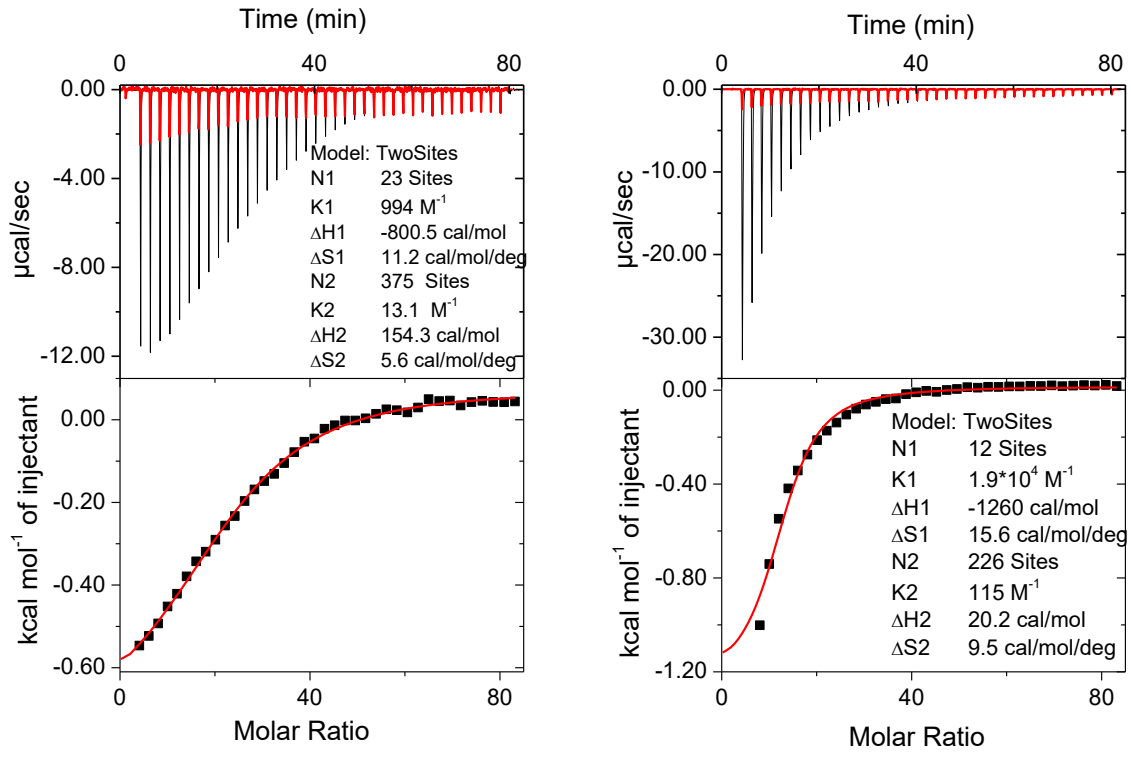

e **f**

Figure S43. Titration of the **F1** (**pDFEA**) solution in ultrapure water with PBS (**a**,**c**,**e**) and FBS (**b**,**d**,**f**) respectively; 293 K (**a**,**b**), 298 K (**c**,**d**) and 323 K (**e**,**f**). Upper graph – heat flux as a function of time; red line – titration of PBS or FBS, respectively into ultrapure water; black line – titration into polymer solution. Lower graph – integrated heat per 1 mol of titrant (scatter); fit to the two independent binding sites model (line).

S7.4. ITC – enthalpies of F1, F2, and F3

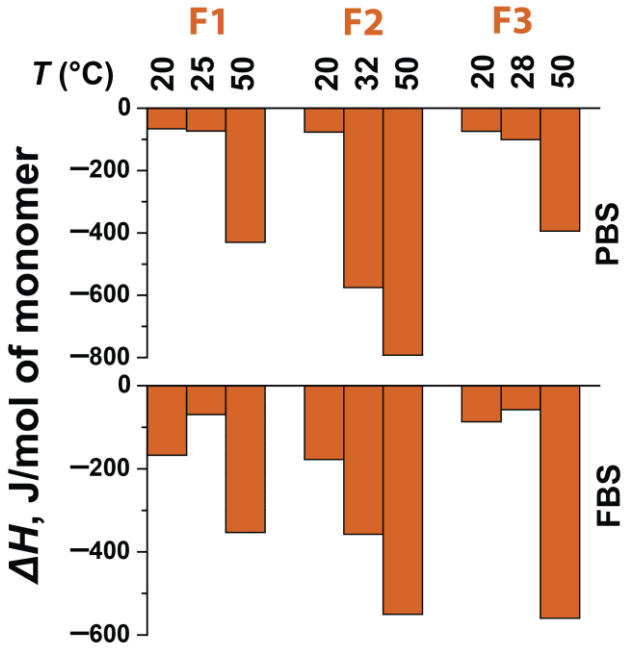

Figure S44. Enthalpy of titration of 10 mg/mL **F1**, **F2** and **F3** solutions with PBS and FBS, normalised to 1 mol of monomer units at three different temperatures with PBS (top) and FBS (bottom). The values of enthalpies are shown in **Table S8**.

We assessed the effect of the polymer molar weight on the enthalpy of aggregation of **pDFEA**. Under all conditions, the **pDFEA** aggregation was exothermic, possibly caused by strong interactions (due to hydrogen bonding of CF_2H moieties[S14]). The interaction of **pDFEA** and PBS or FBS was more exothermic at high (50 °C) than at low (20 °C) temperatures, most likely due to the salting-out effect and subsequent aggregation. Furthermore, adding FBS to the solution of the non-aggregated polymer was always more exothermic than adding only PBS, thus indicating the formation of **pDFEA**-protein complexes. Adding FBS to aggregated polymer was in some cases (**F1**, **F2**) less and in others more (**F3**) exothermic than adding only PBS. The differences in enthalpy of aggregation between **F1**, **F2**, and **F3** in PBS can be ascribed to different the architecture of the particles (as discussed in the Manuscript).

While the reaction enthalpy in both PBS and FBS can be ascribed to changes in polymer solvation, polymer interactions with ions and aggregation, the reaction enthalpy in FBS can be also ascribed to protein-polymer interactions.

Table S8. Concentrations and pH of polymer solutions; enthalpy ΔH (J/mol of monomer) of mixing of polymer solutions with PBS and FBS at various temperatures

Sample	**F1 (pDFEA)**						**F2 (pDFEA)**						**F3 (pDFEA)**					
Conc. (mM)*	0.413						0.284						0.213					
pH in H_2O**	≈ 4.9						≈ 4.8						≈ 4.9					
Titrant	**PBS**			**FBS**			**PBS**			**FBS**			**PBS**			**FBS**		
***T*, K**	**293**	**298**	**323**	**293**	**298**	**323**	**293**	**305**	**313**	**293**	**305**	**313**	**293**	**301**	**293**	**301**	**293**	**301**
ΔH, (J/mol)	−65.9	−73.3	-430.4	−167.4	−69.4	−353.4	−76.7	−575.3	-792.5	−177.7	−357.6	−550.2	−1.23	−2.59	−1.23	−2.59	−1.23	−2.59
transition conc. (mM)***	12.0	10.1	18.1	11.6	10.9	8.7	17.8	17.03	24.6	10.9	10.9	13.1	17.4	13.4	17.4	13.4	17.4	13.4
transition conc. (mg/mL)******	0.7	0.6	1.0	3.8	3.6	2.8	1.0	0.9	1.4	3.6	3.6	4.3	1.0	0.8	1.0	0.8	1.0	0.8

* polymer concentration in the analyte solution

** pH of aqueous solution of polymer, 10 mg/mL

*** concentration of titrant (PBS or FBS) in units of ionic strength of PBS solution, determined from the coordinate on the *x*-axis (molar ratio) on **Figures S41** to **43**.

**** concentration of titrant in mg/mL

S8. Dynamic light scattering data

At a low temperature, almost all study polymers showed a population of unimers (approximately 5 nm), which formed larger aggregates with the increase in temperature. In some samples, we detected a small number of large assemblies (in the order of hundreds of nanometres), even below the T_{CP}s, which had remained undetected by turbidimetry. These 'pre-aggregation' molecular assemblies confirmed our previous observations.[S15–S17] However, large particles scatter light in DLS at a higher intensity than small particles (the scattering intensity is proportional to R_h^3),[S18] so the concentration of large particles is substantially lower than our DLS data suggest.

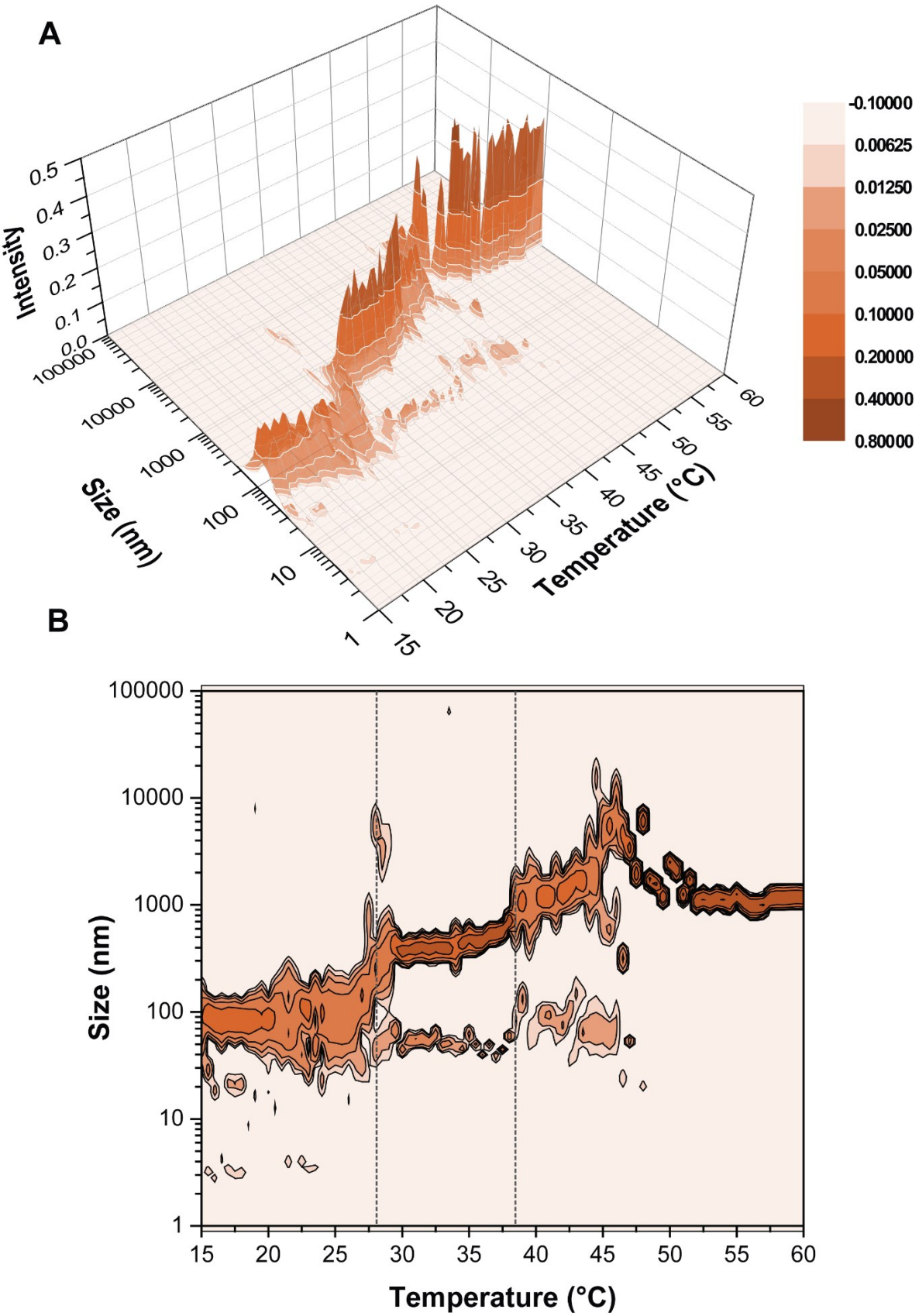

Figure S45. Size distributions of molecular assemblies of polymer **F1** (10 mg/mL in PBS) as a function of temperature; depicted as 3D plot (**A**) and contour graph (**B**). T_{CP1} (dashed lines) was assigned to 28 °C, T_{CP2} was assigned to 38 °C.

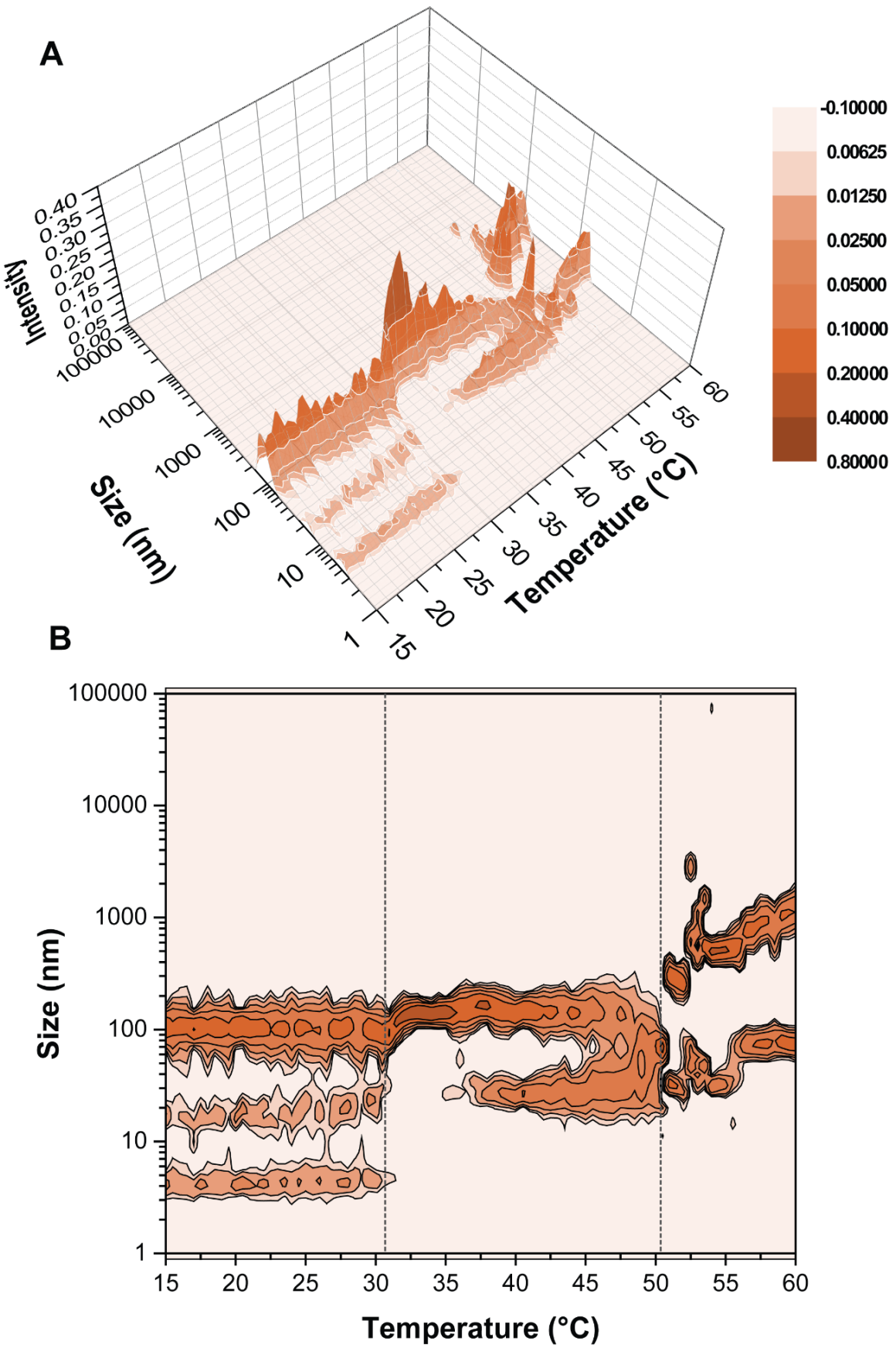

Figure S46. Size distributions of molecular assemblies of polymer **F2** (10 mg/mL in PBS) as a function of temperature; depicted as 3D plot (**A**) and contour graph (**B**). T_{CP1} (dashed lines) was assigned to 31 °C, T_{CP2} was assigned to 50 °C.

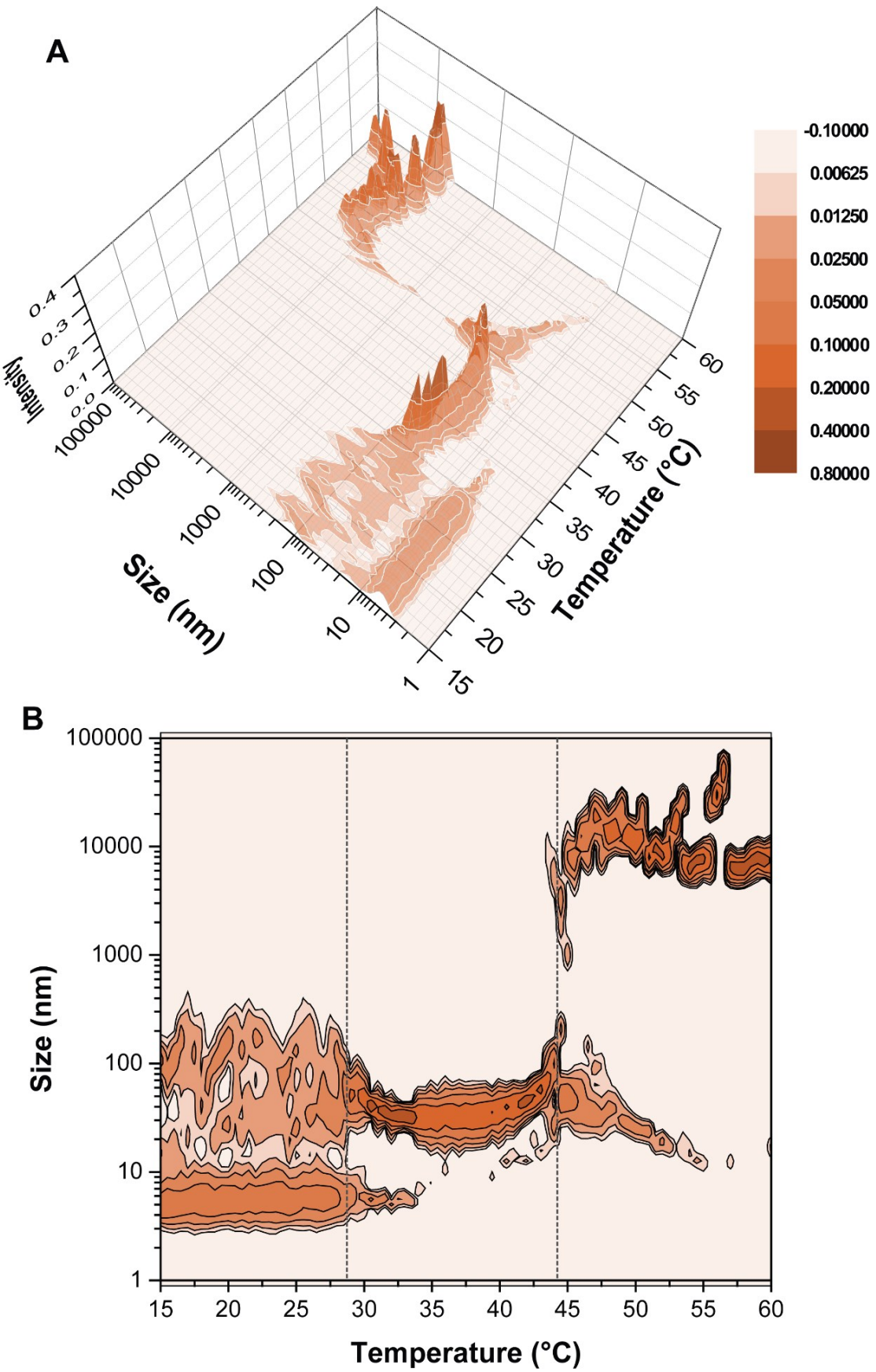

Figure S47. Size distributions of molecular assemblies of polymer **F3** (10 mg/mL in PBS) as a function of temperature; depicted as 3D plot (**A**) and contour graph (**B**). T_{CP1} (dashed lines) was assigned to 28 °C, T_{CP2} was assigned to 44 °C.

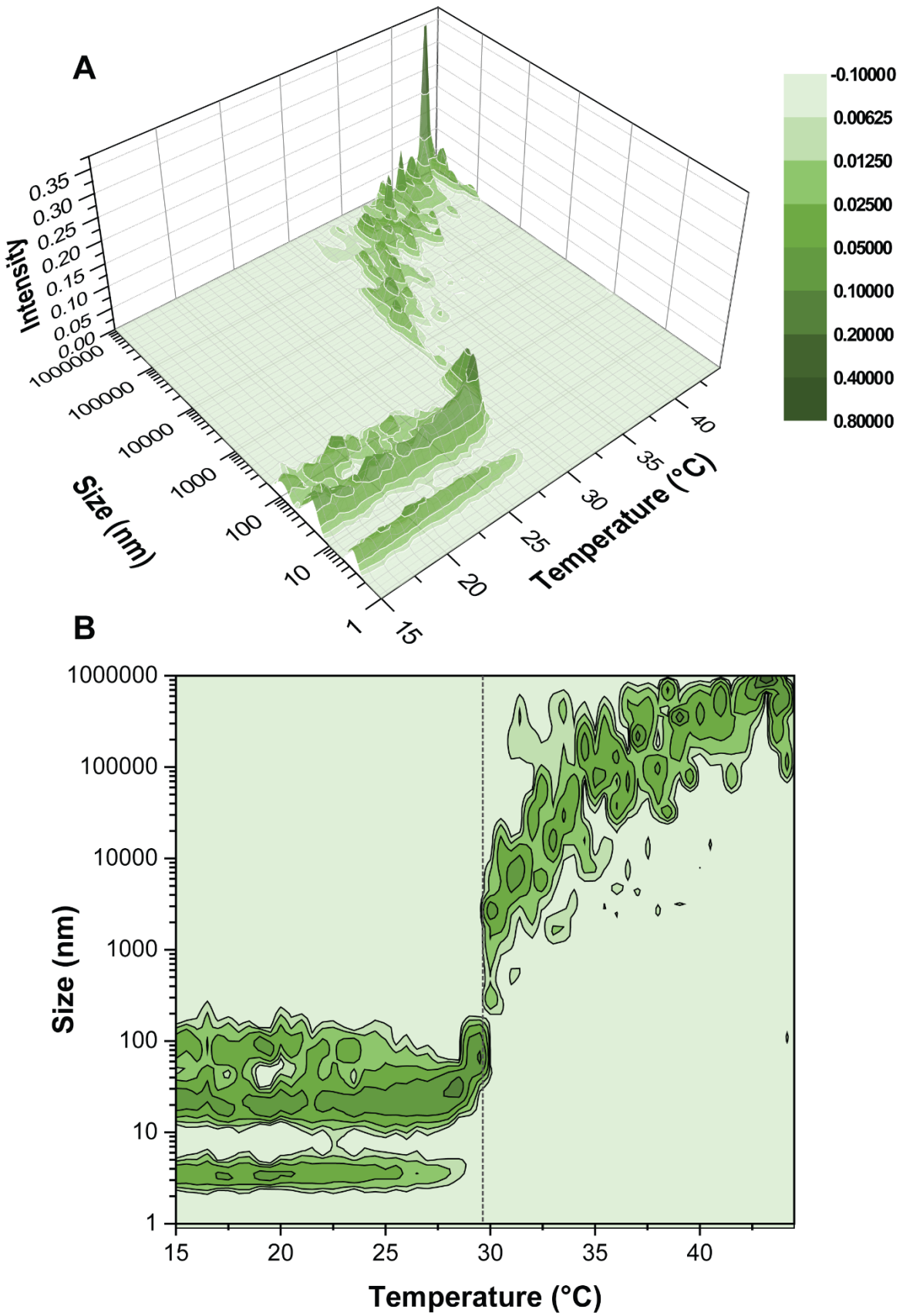

Figure S48. Size distributions of molecular assemblies of polymer **I1** (10 mg/mL in PBS) as a function of temperature; depicted as 3D plot (**A**) and contour graph (**B**). T_{CP} (dashed line) was assigned to 30 °C. The measurement stopped prematurely because the size of the aggregates exceeded the detection limit.

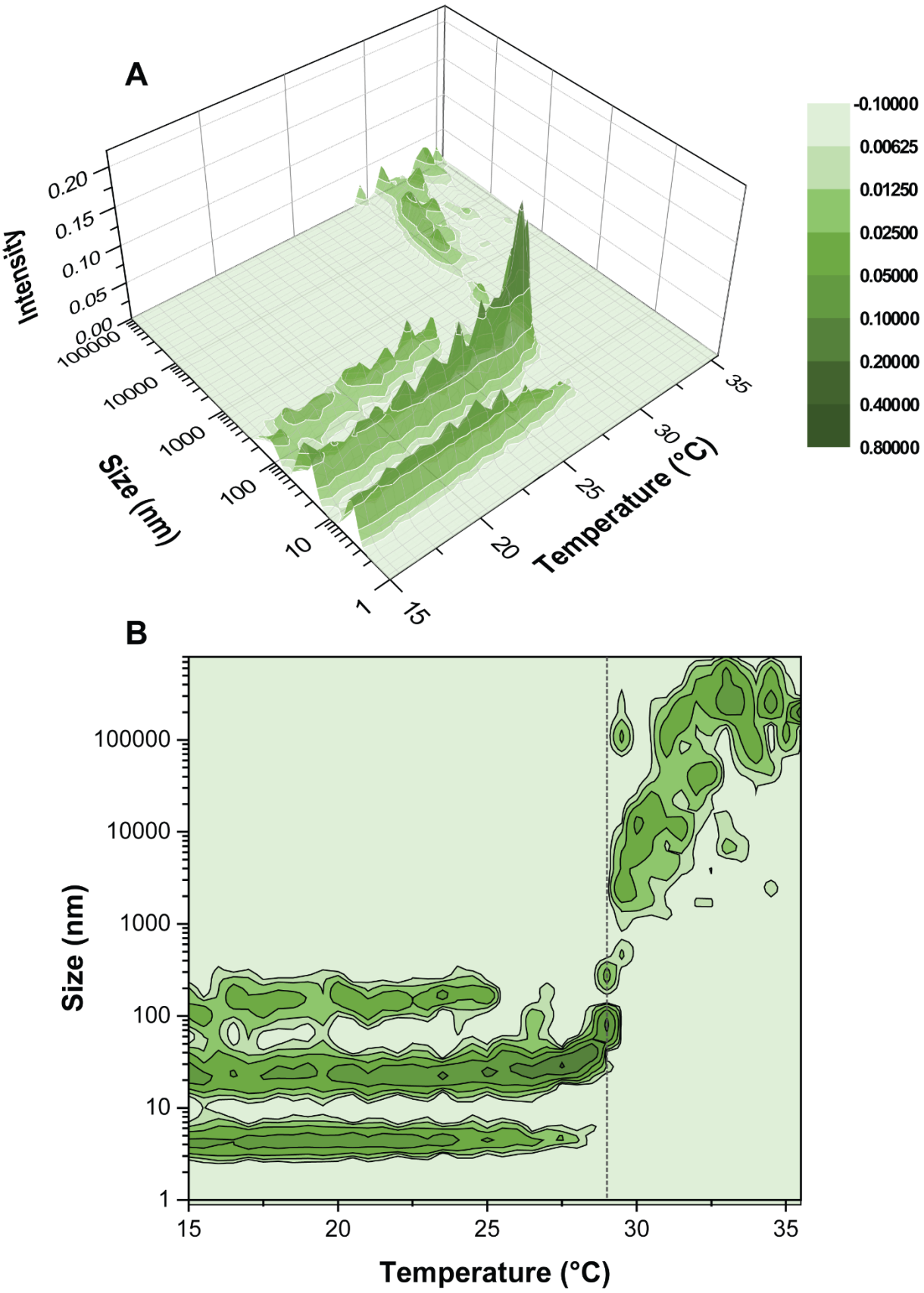

Figure S49. Size distributions of molecular assemblies of polymer **I2** (10 mg/mL in PBS) as a function of temperature; depicted as 3D plot (**A**) and contour graph (**B**). T_{CP} (dashed line) was assigned to 29 °C. The measurement stopped prematurely because the size of the aggregates exceeded the detection limit.

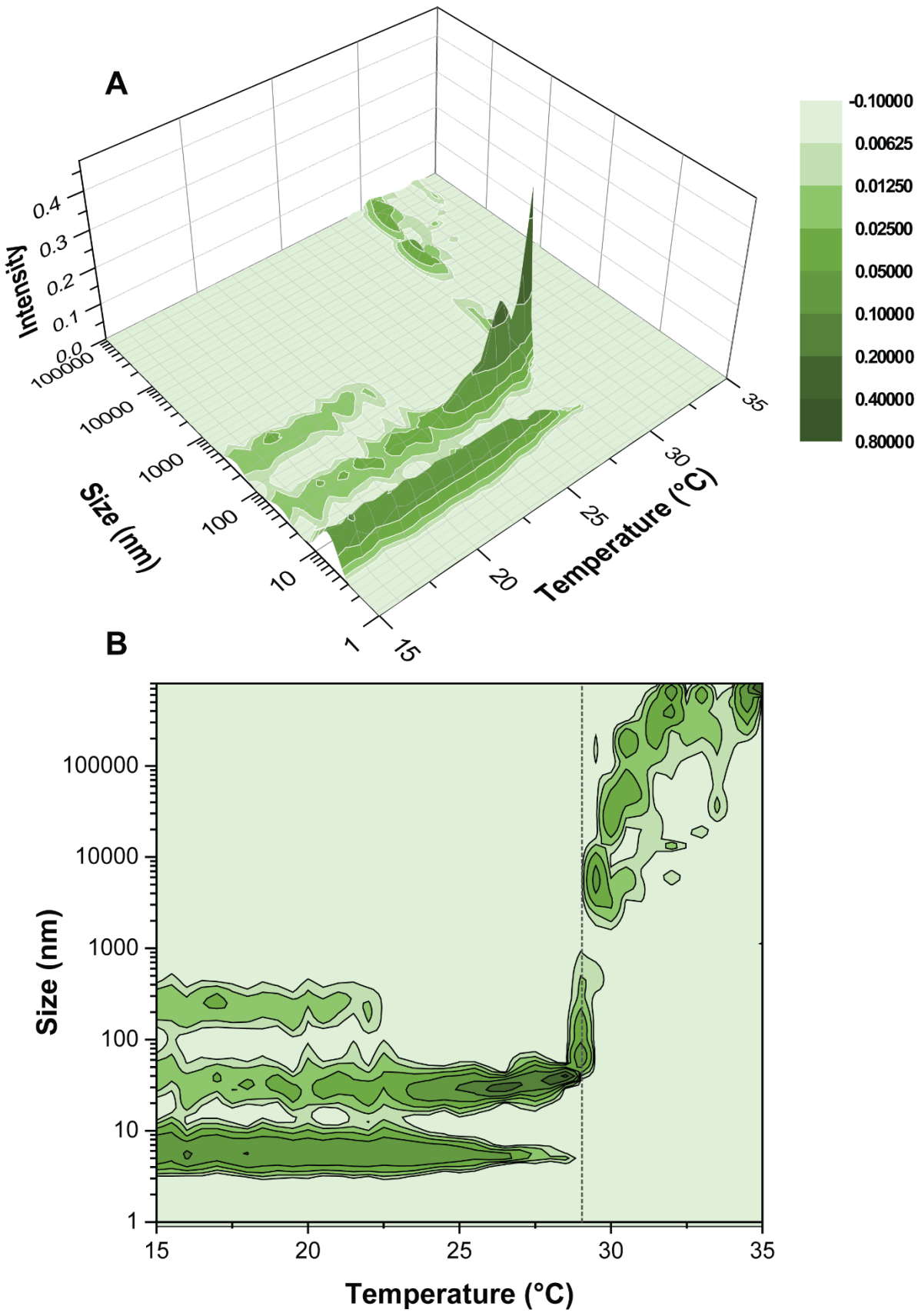

Figure S50. Size distributions of molecular assemblies of polymer **I3** (10 mg/mL in PBS) as a function of temperature; depicted as 3D plot (**A**) and contour graph (**B**). T_{CP} (dashed line) was assigned to 29 °C. The measurement stopped prematurely because the size of the aggregates exceeded the detection limit.

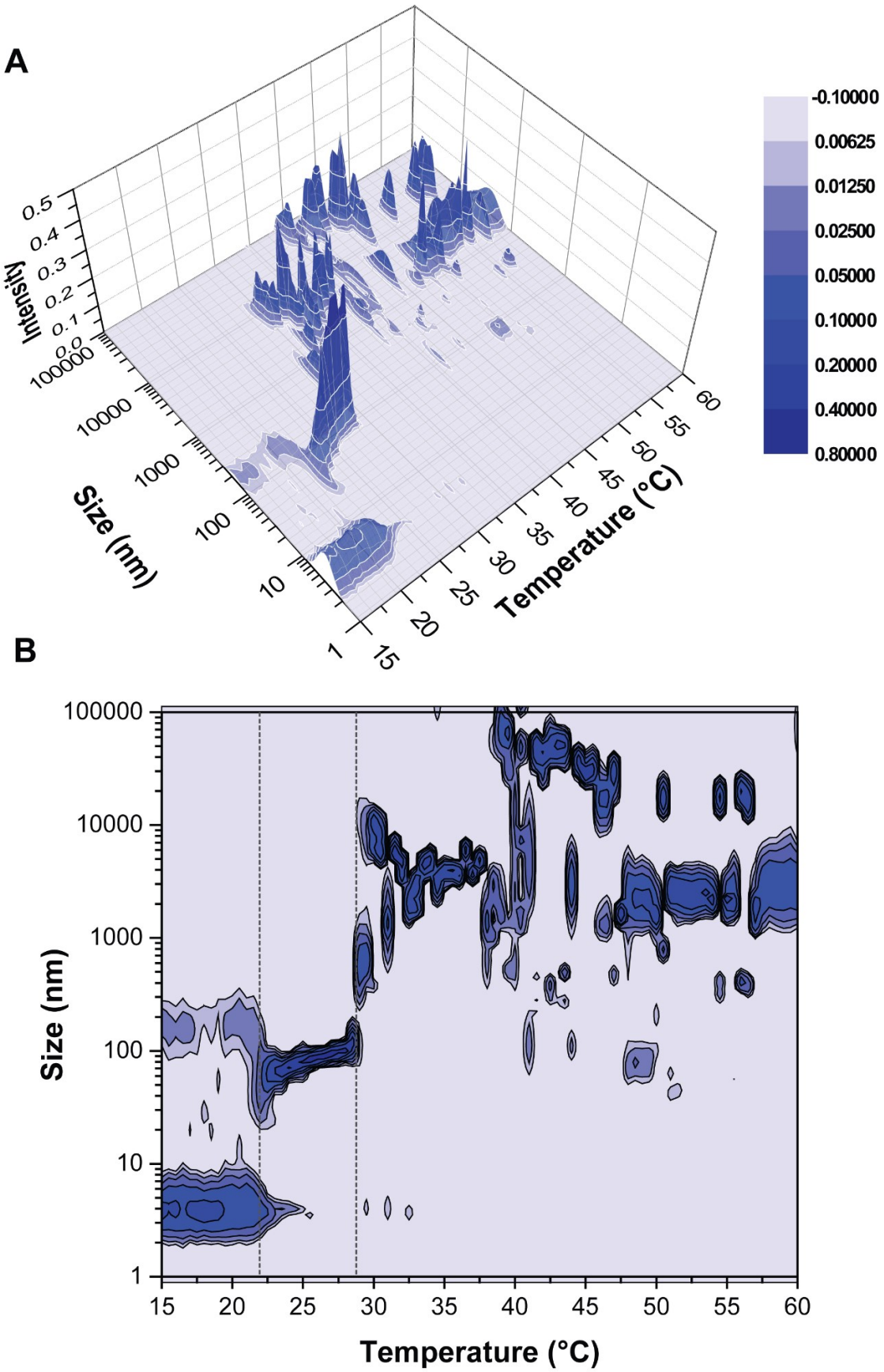

Figure S51. Size distributions of molecular assemblies of polymer **E1** (10 mg/mL in PBS) as a function of temperature; depicted as 3D plot (**A**) and contour graph (**B**). T_{CP1} (dashed lines) was assigned to 22 °C, T_{CP2} was assigned to 28 °C.

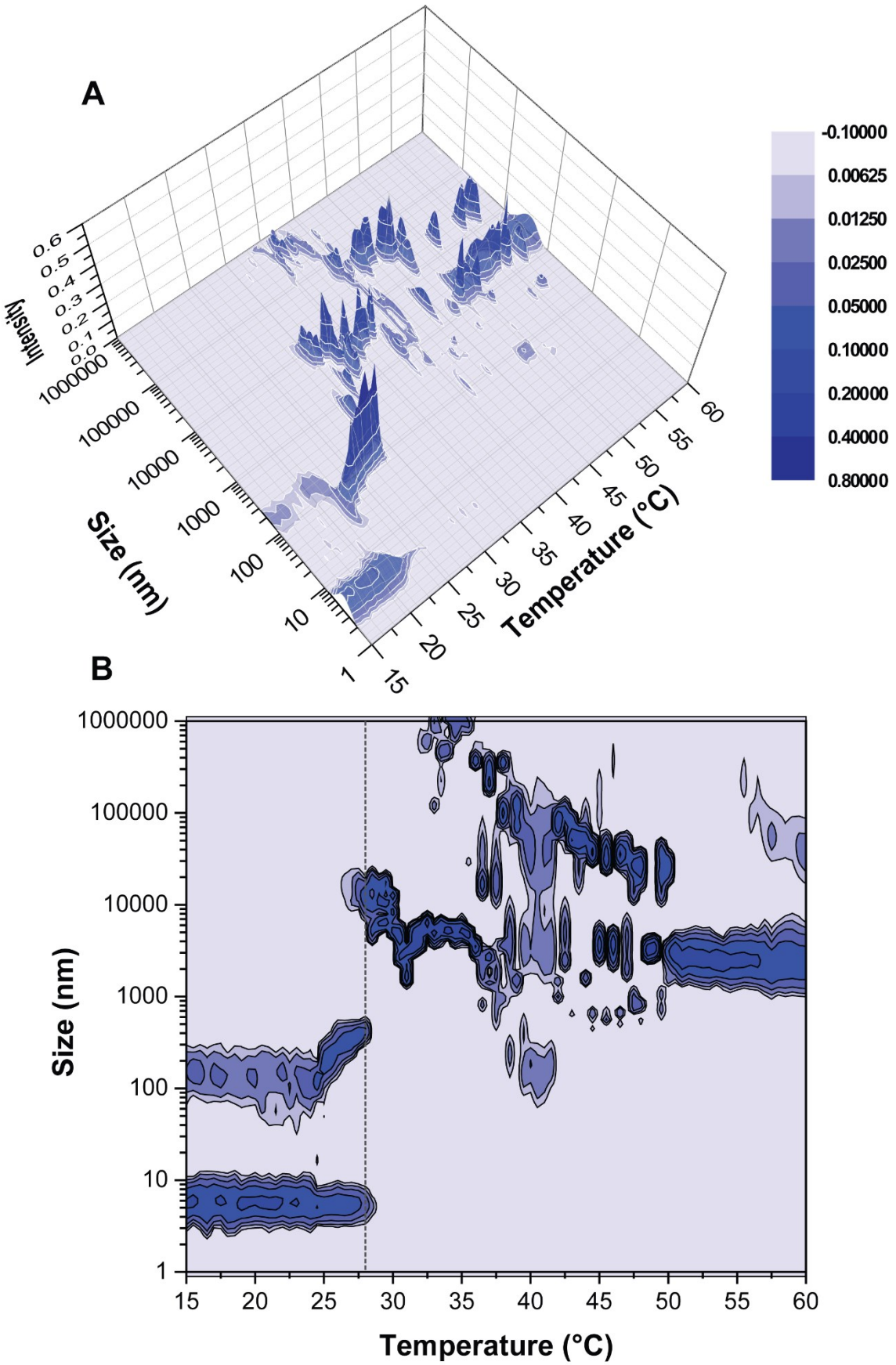

Figure S52. Size distributions of molecular assemblies of polymer **E2** (10 mg/mL in PBS) as a function of temperature; depicted as 3D plot (**A**) and contour graph (**B**). T_{CP} (dashed line) was assigned to 28 °C. The measurement stopped prematurely because the size of the aggregates exceeded the detection limit.

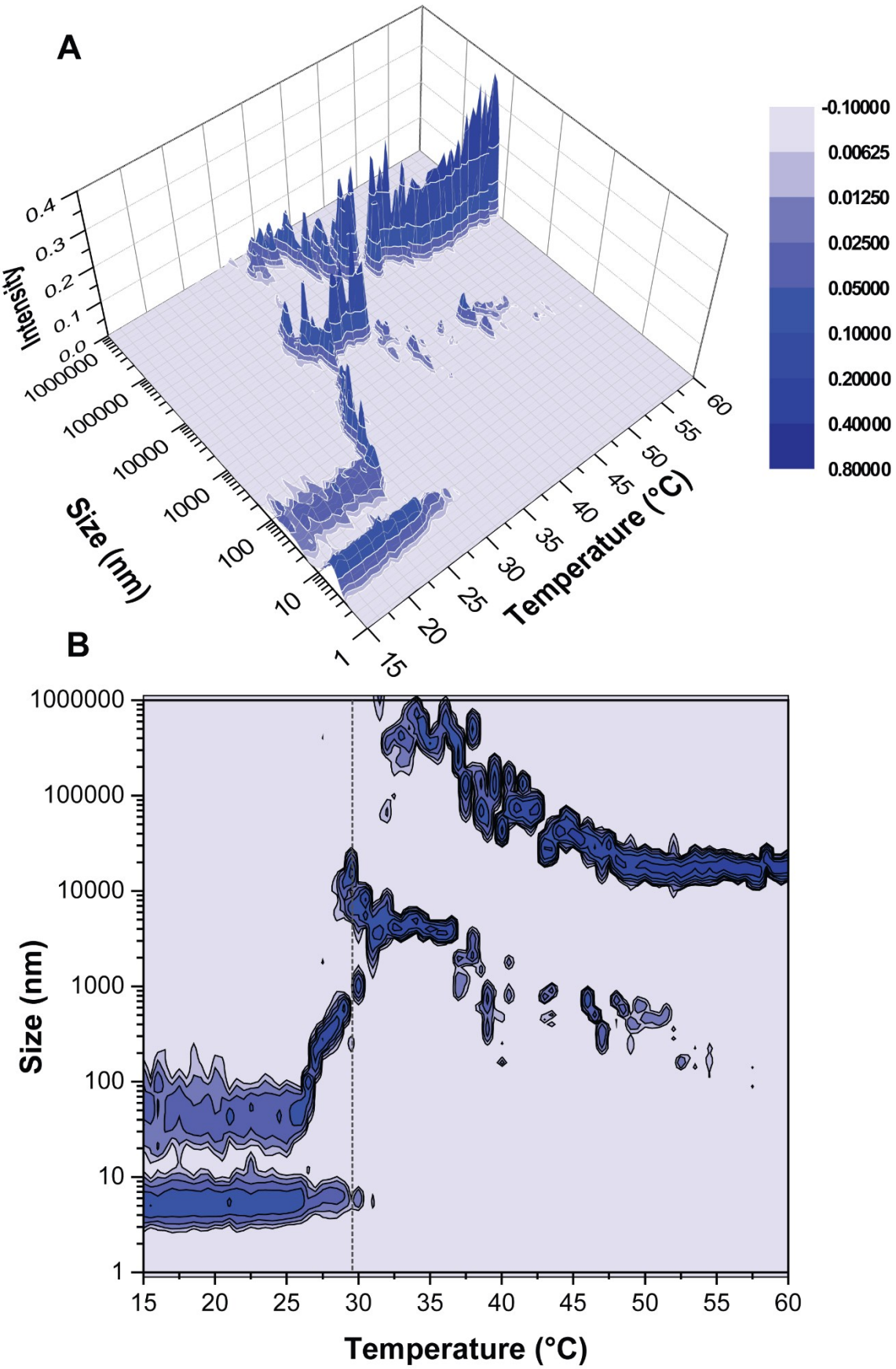

Figure S53. Size distributions of molecular assemblies of polymer **E3** (10 mg/mL in PBS) as a function of temperature; depicted as 3D plot (**A**) and contour graph (**B**). T_{CP} (dashed line) was assigned to 29 °C. The measurement stopped prematurely because the size of the aggregates exceeded the detection limit.

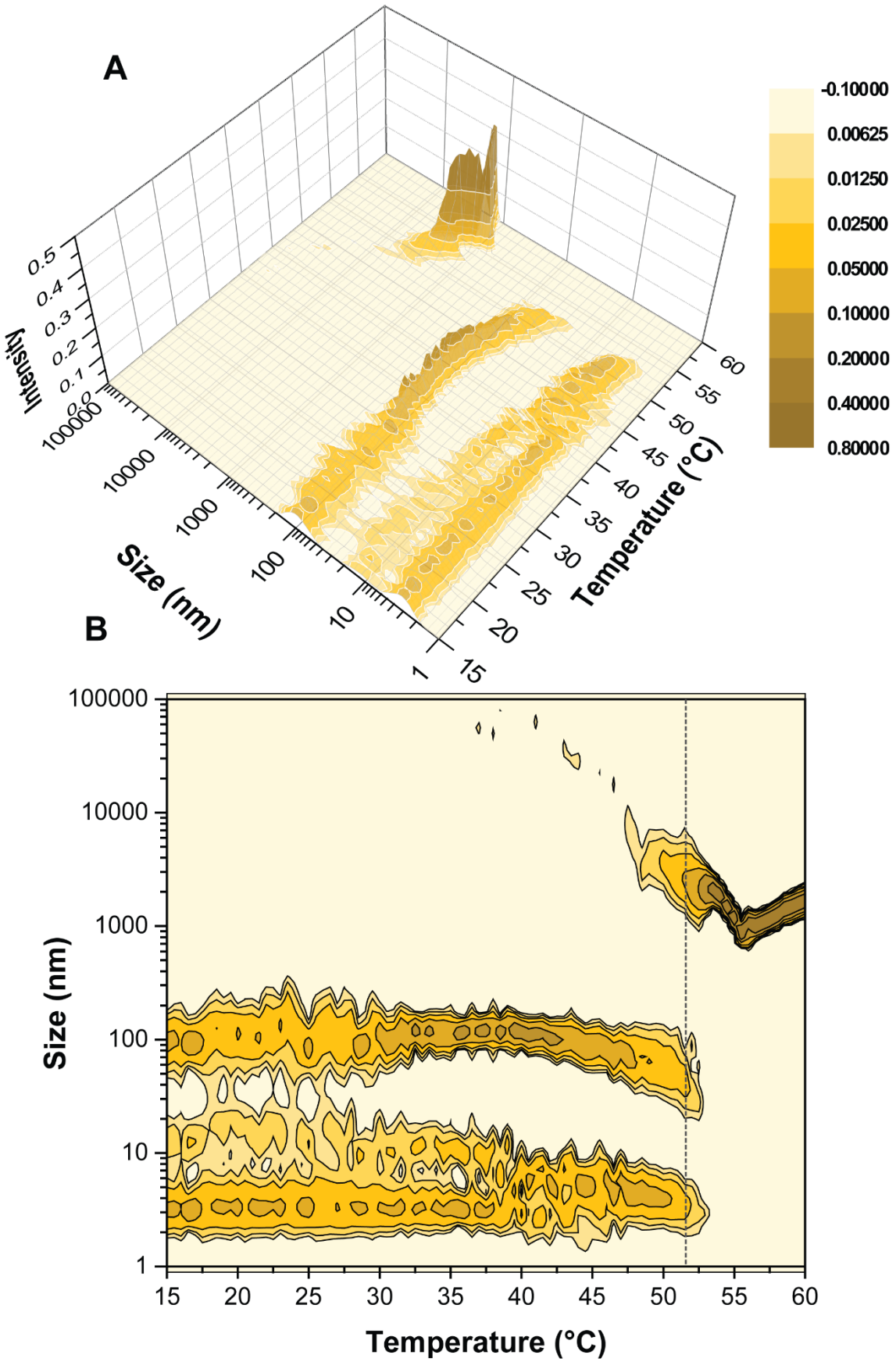

Figure S54. Size distributions of molecular assemblies of polymer **P1** (10 mg/mL in PBS) as a function of temperature; depicted as 3D plot (**A**) and contour graph (**B**). T_{CP} (dashed line) was assigned to 52 °C. The measurement stopped prematurely because the size of the aggregates exceeded the detection limit.

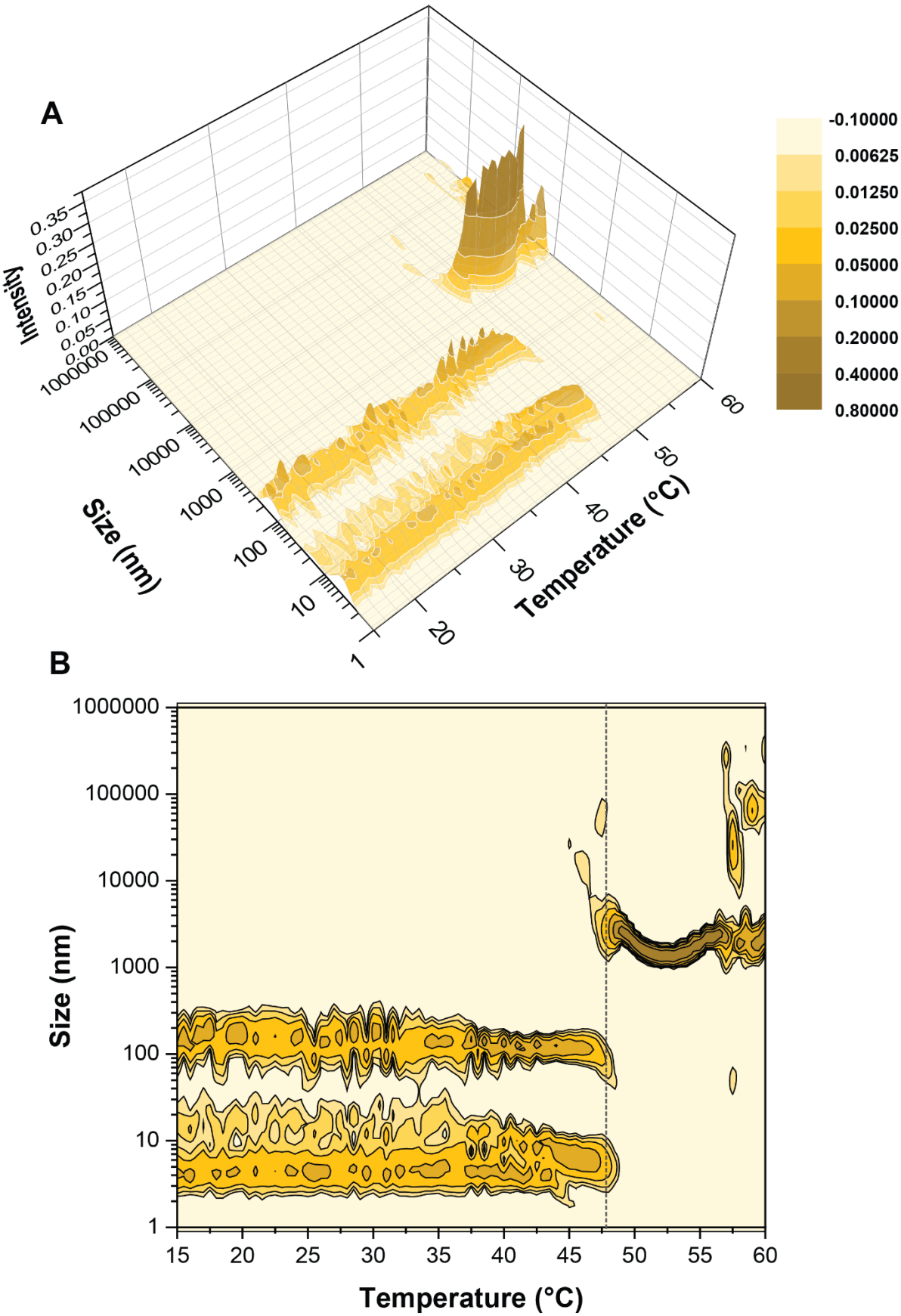

Figure S55. Size distributions of molecular assemblies of polymer **P2** (10 mg/mL in PBS) as a function of temperature; depicted as 3D plot (**A**) and contour graph (**B**). T_{CP} (dashed line) was assigned to 48 °C. The measurement stopped prematurely because the size of the aggregates exceeded the detection limit.

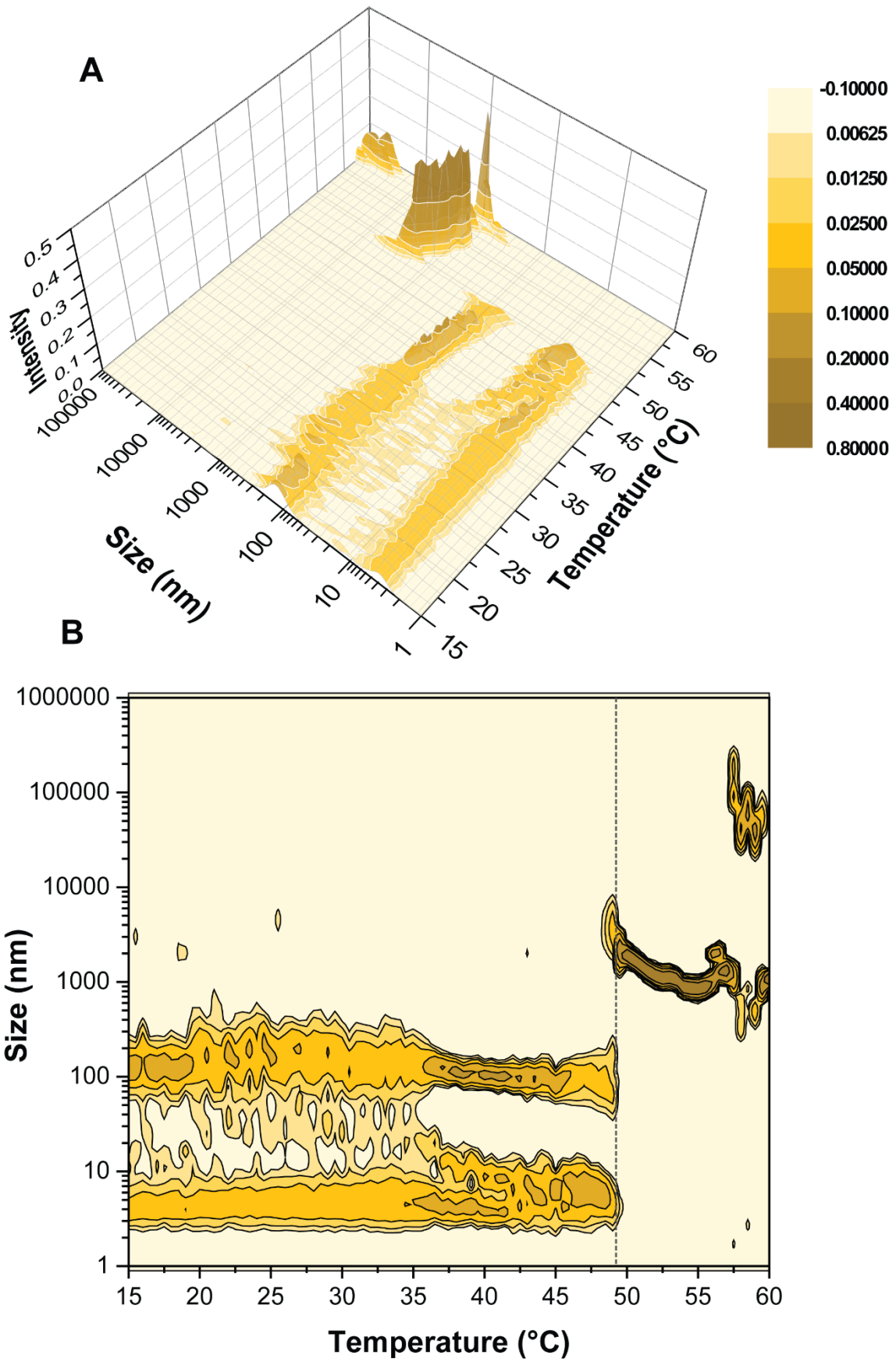

Figure S56. Size distributions of molecular assemblies of polymer **P3** (10 mg/mL in PBS) as a function of temperature; depicted as 3D plot (**A**) and contour graph (**B**). T_{CP} (dashed line) was assigned to 49 °C. The measurement stopped prematurely because the size of the aggregates exceeded the detection limit.

S9. Refractive index increment (d*n*/d*c*)

Brookhaven Instruments Corp.
Differential Refractometer Software Ver. 5.32

Date: Jul 29, 2021
Time: 10:54:38

Sample ID **F1, PBS**
Operator ID **PC**
Notes

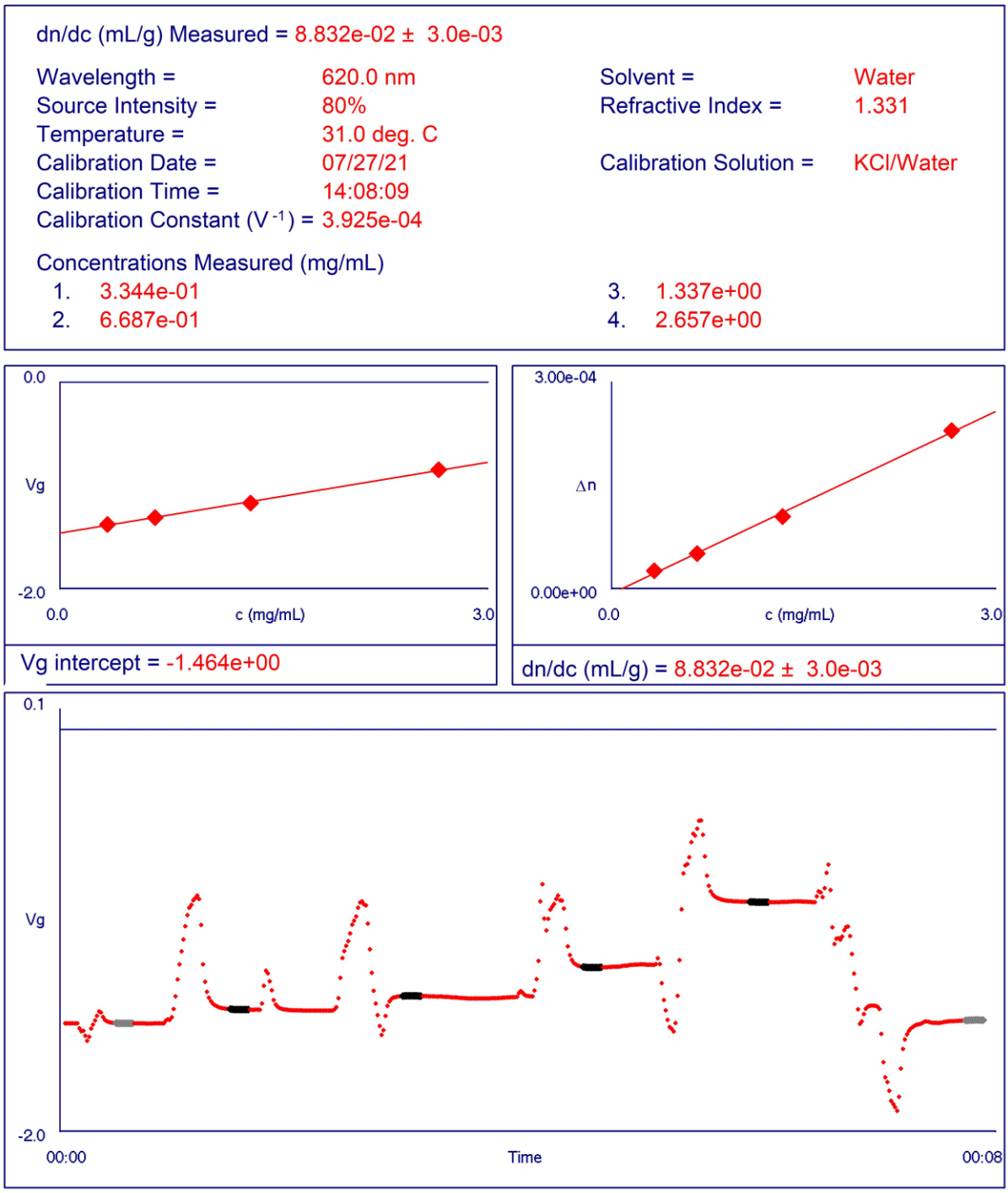

Figure S57. Refractive index increment (d*n*/d*c*) measurement report of **F1** (**pDFEA**) in PBS

Brookhaven Instruments Corp.
Differential Refractometer Software Ver. 5.32

Date: Jul 29, 2021
Time: 11:06:16

Sample ID **F2, PBS**
Operator ID **PC**
Notes

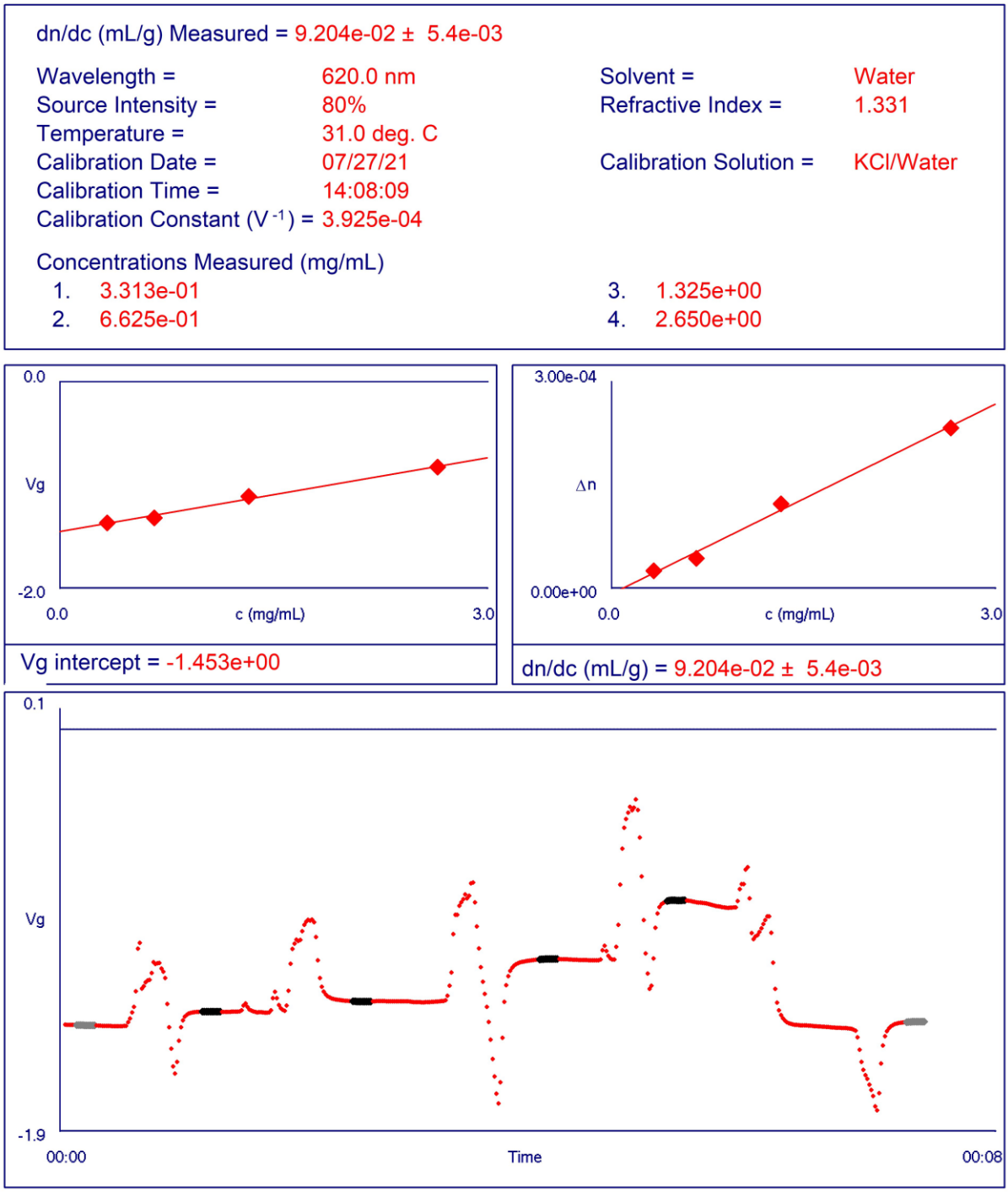

Figure S58. Refractive index increment (d*n*/d*c*) measurement report of **F2** (**pDFEA**) in PBS

Brookhaven Instruments Corp.
Differential Refractometer Software Ver. 5.32

Date: Jul 29, 2021
Time: 11:15:27

Sample ID **F3, PBS**
Operator ID **PC**
Notes

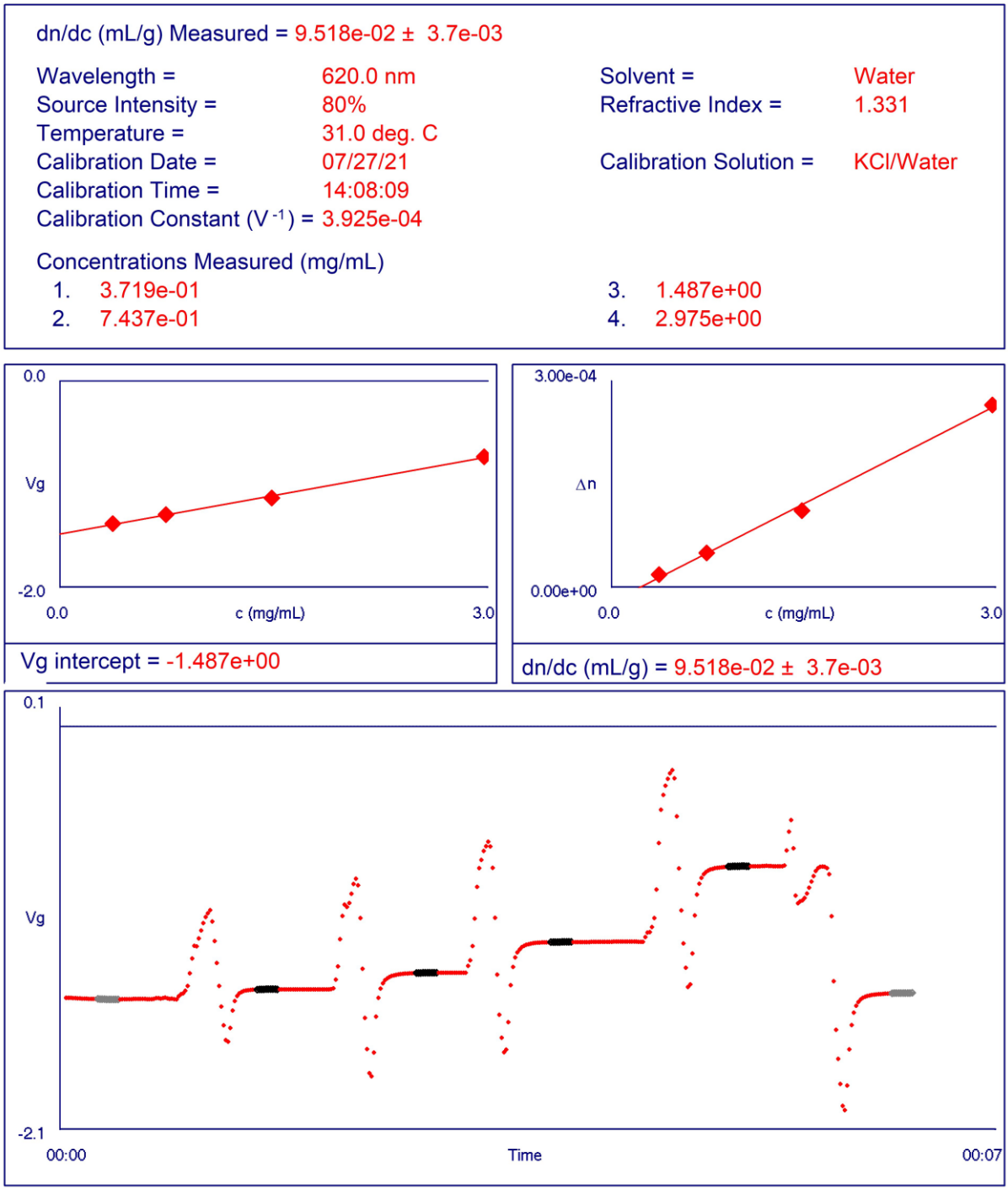

Figure S59. Refractive index increment (d*n*/d*c*) measurement report of **F3** (**pDFEA**) in PBS

Brookhaven Instruments Corp.
Differential Refractometer Software Ver. 5.32

Date: Jul 29, 2021
Time: 12:14:20

Sample ID **I1, PBS**
Operator ID **PC**
Notes

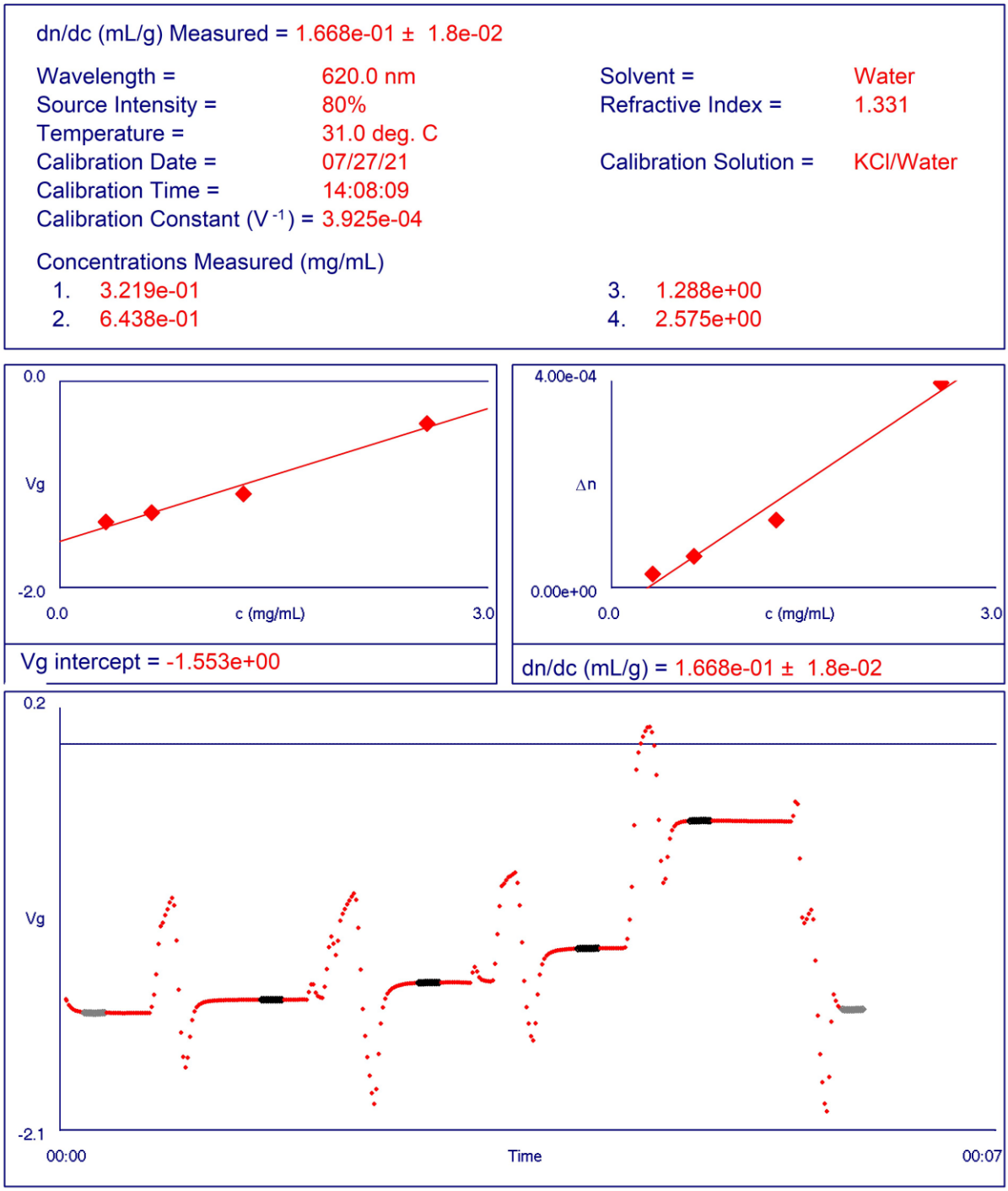

Figure S60. Refractive index increment (d*n*/d*c*) measurement report of **I1** (**pNIPAM**) in PBS

Brookhaven Instruments Corp.
Differential Refractometer Software Ver. 5.32

Date: Jul 29, 2021
Time: 12:26:10

Sample ID **I2, PBS**
Operator ID **PC**
Notes

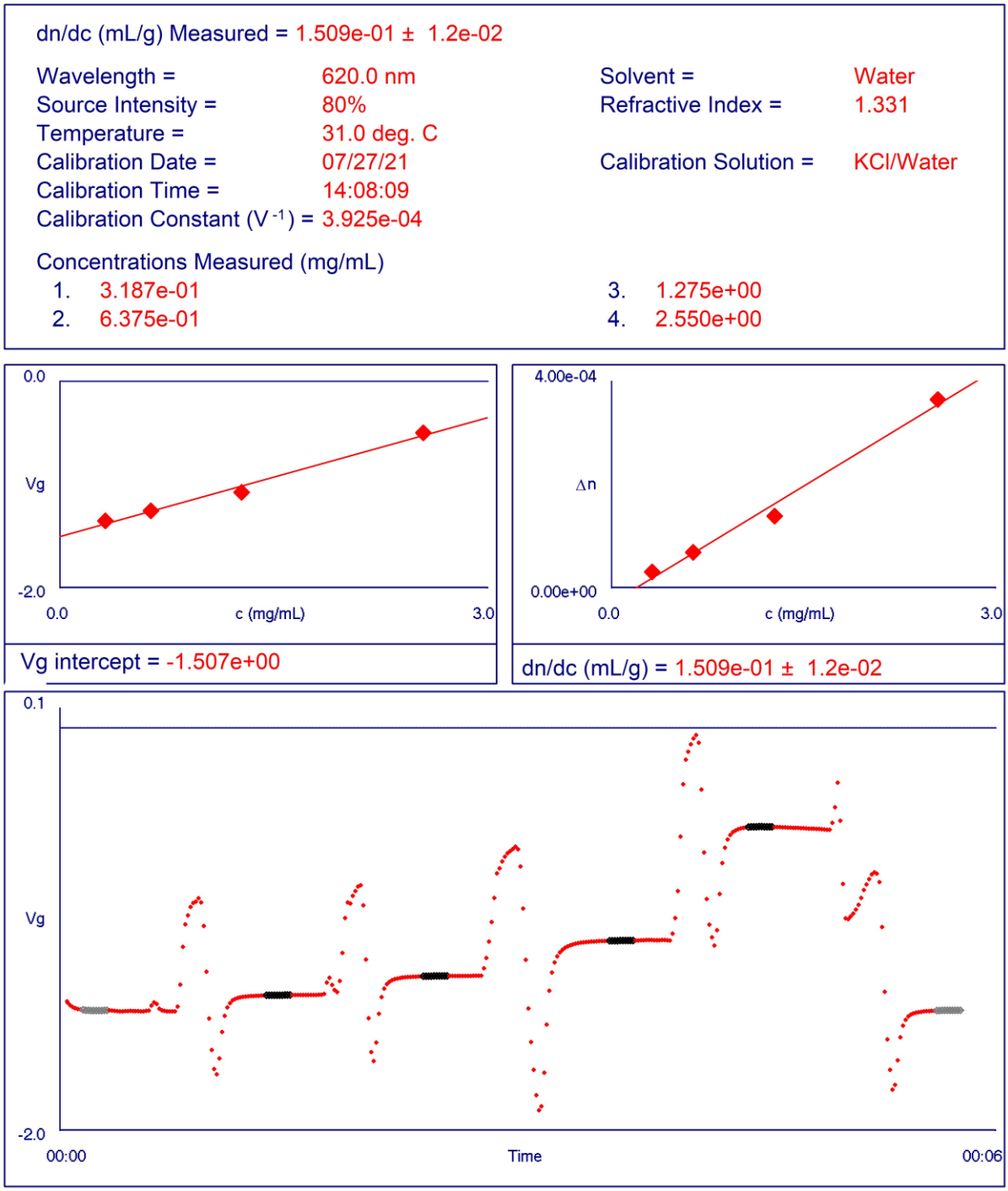

Figure S61. Refractive index increment (d*n*/d*c*) measurement report of **I2** (**pNIPAM**) in PBS

Brookhaven Instruments Corp.
Differential Refractometer Software Ver. 5.32

Date: Jul 29, 2021
Time: 12:33:07

Sample ID **I3, PBS**
Operator ID **PC**
Notes

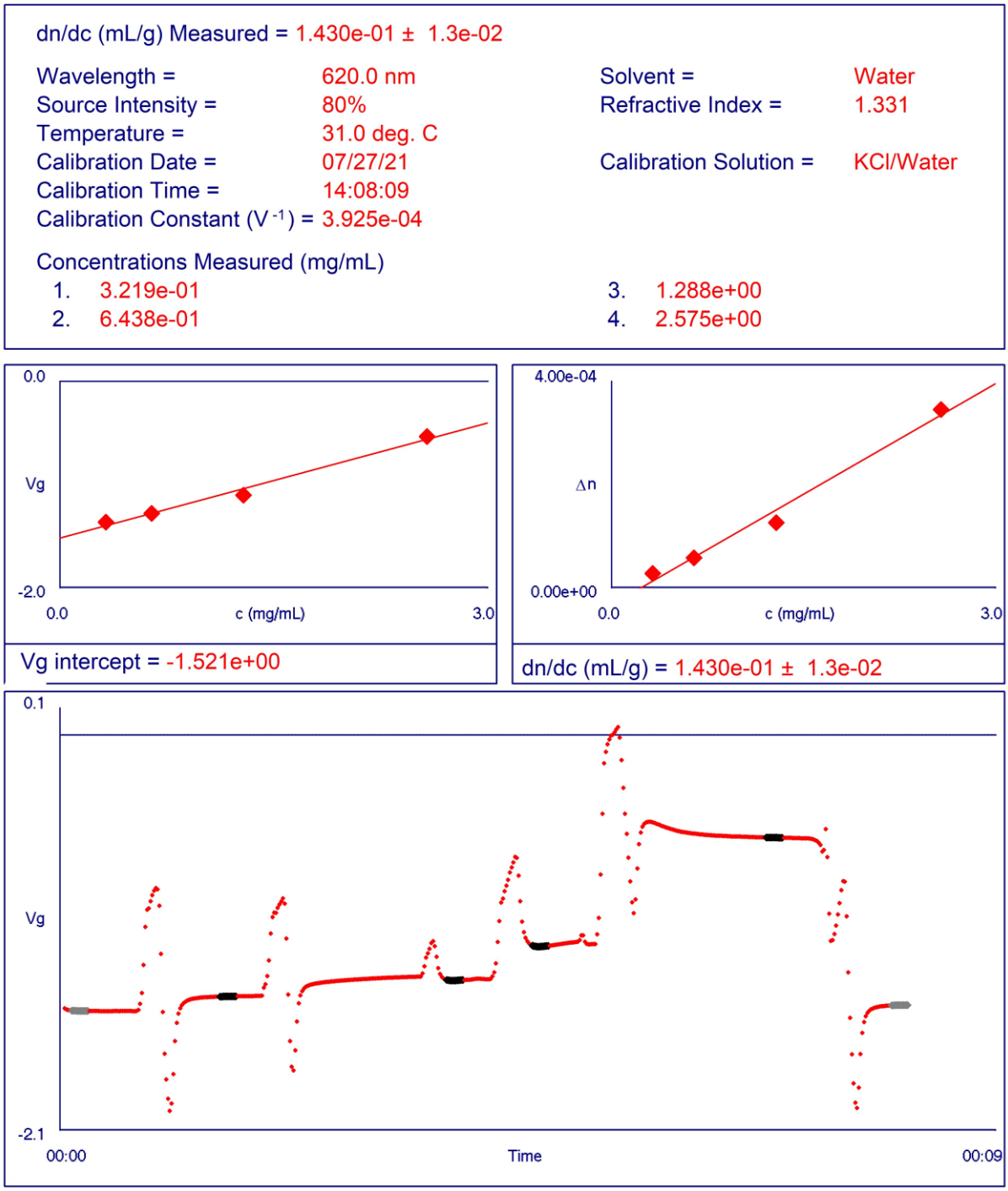

Figure S62. Refractive index increment (d*n*/d*c*) measurement report of **I3** (**pNIPAM**) in PBS

Brookhaven Instruments Corp.
Differential Refractometer Software Ver. 5.32

Date: Jul 30, 2021
Time: 11:08:22

Sample ID **E1, PBS**
Operator ID **PC**
Notes

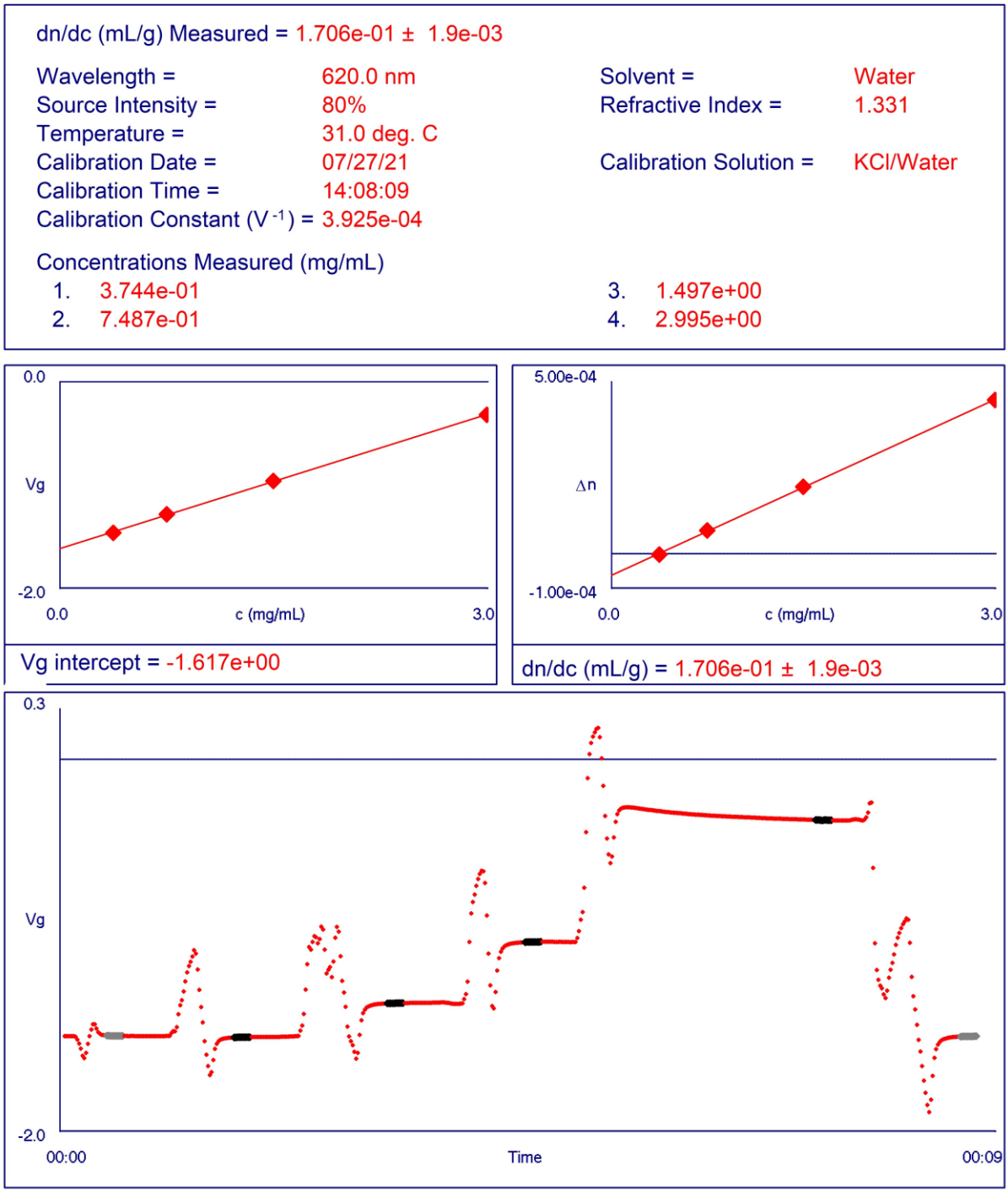

Figure S63. Refractive index increment (d*n*/d*c*) measurement report of **E1** (**pDEA**) in PBS

Brookhaven Instruments Corp.
Differential Refractometer Software Ver. 5.32

Date: Jul 29, 2021
Time: 11:55:03

Sample ID **E2, PBS**
Operator ID **PC**
Notes

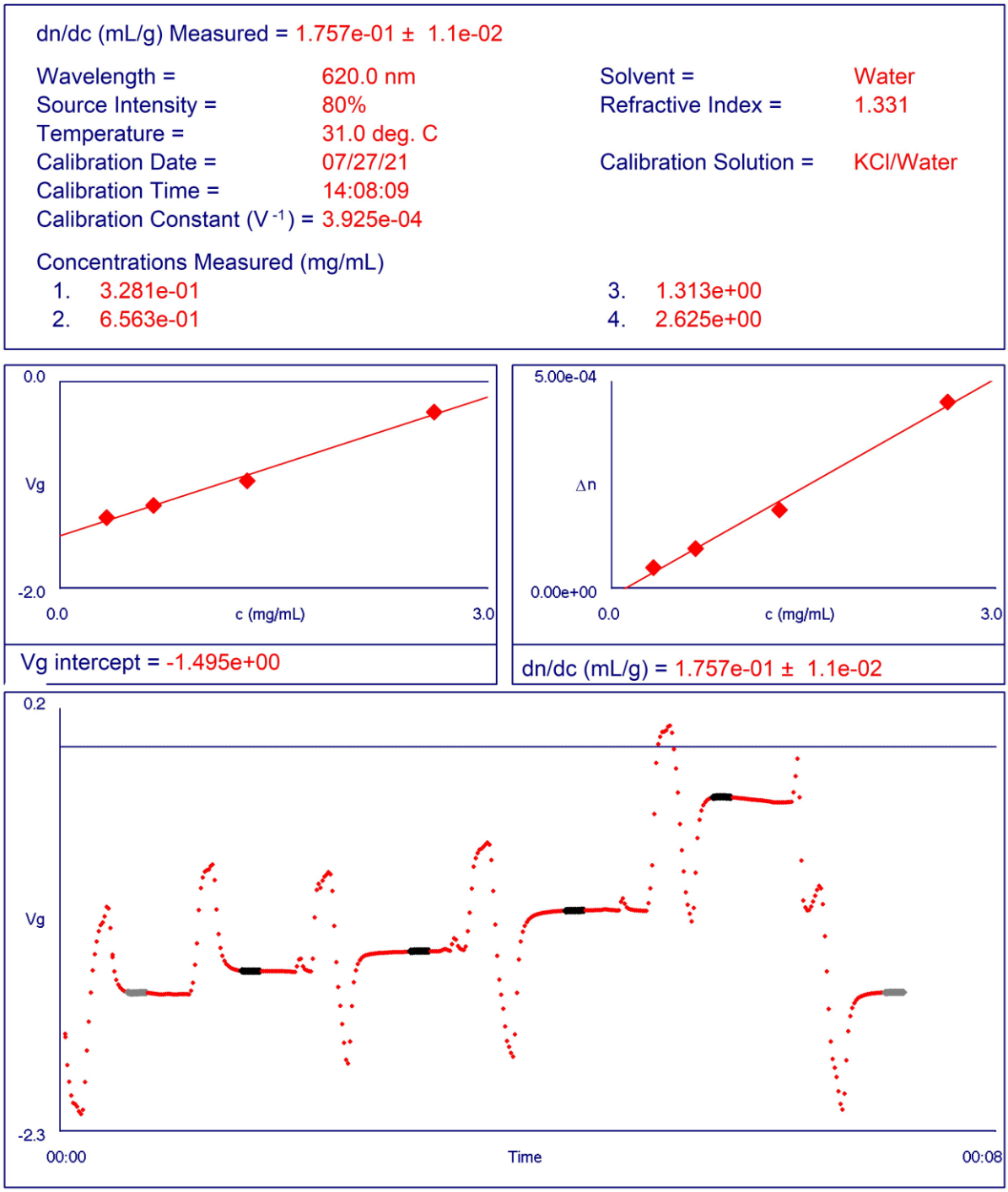

Figure S64. Refractive index increment (d*n*/d*c*) measurement report of **E2** (**pDEA**) in PBS

Brookhaven Instruments Corp.
Differential Refractometer Software Ver. 5.32

Date: Jul 30, 2021
Time: 11:18:11

Sample ID **E3, PBS**
Operator ID **PC**
Notes

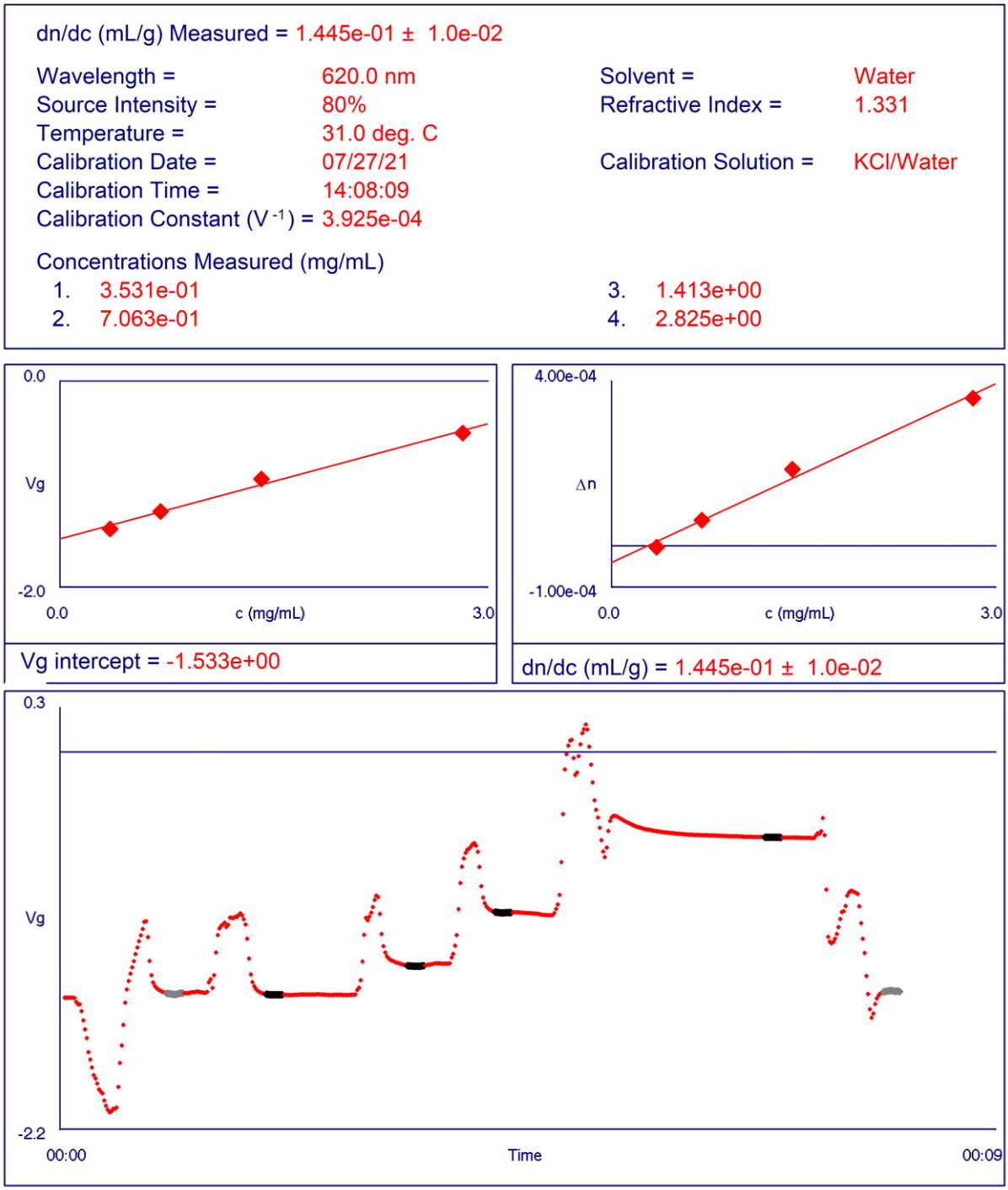

Figure S65. Refractive index increment (d*n*/d*c*) measurement report of **E3** (**pDEA**) in PBS

Brookhaven Instruments Corp.
Differential Refractometer Software Ver. 5.32

Date: Jul 30, 2021
Time: 11:28:37

Sample ID **P1, PBS**
Operator ID **PC**
Notes

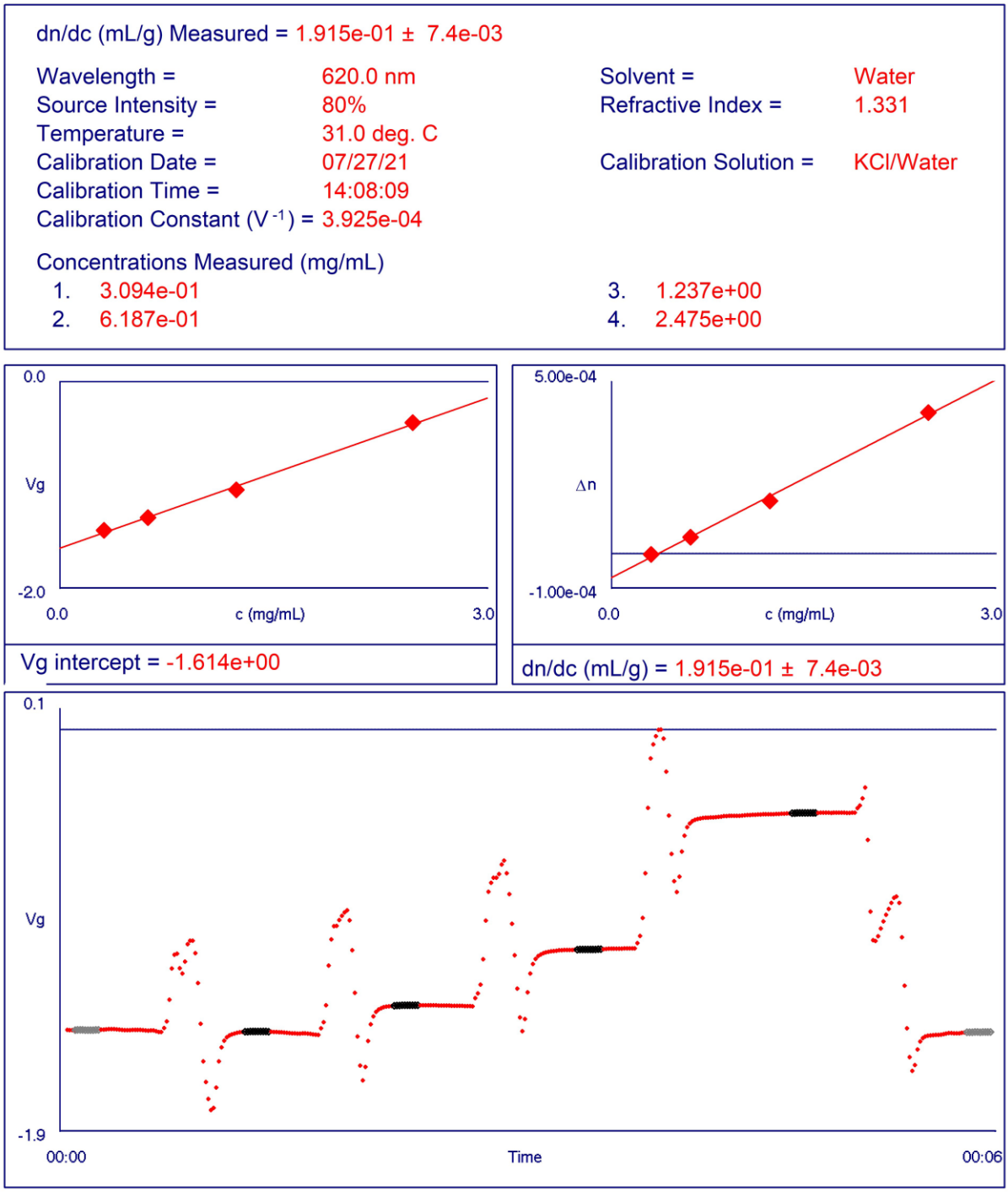

Figure S66. Refractive index increment (d*n*/d*c*) measurement report of **P1** (**pAP**) in PBS

Brookhaven Instruments Corp.
Differential Refractometer Software Ver. 5.32

Date: Jul 29, 2021
Time: 12:59:10

Sample ID **P2, PBS**
Operator ID **PC**
Notes

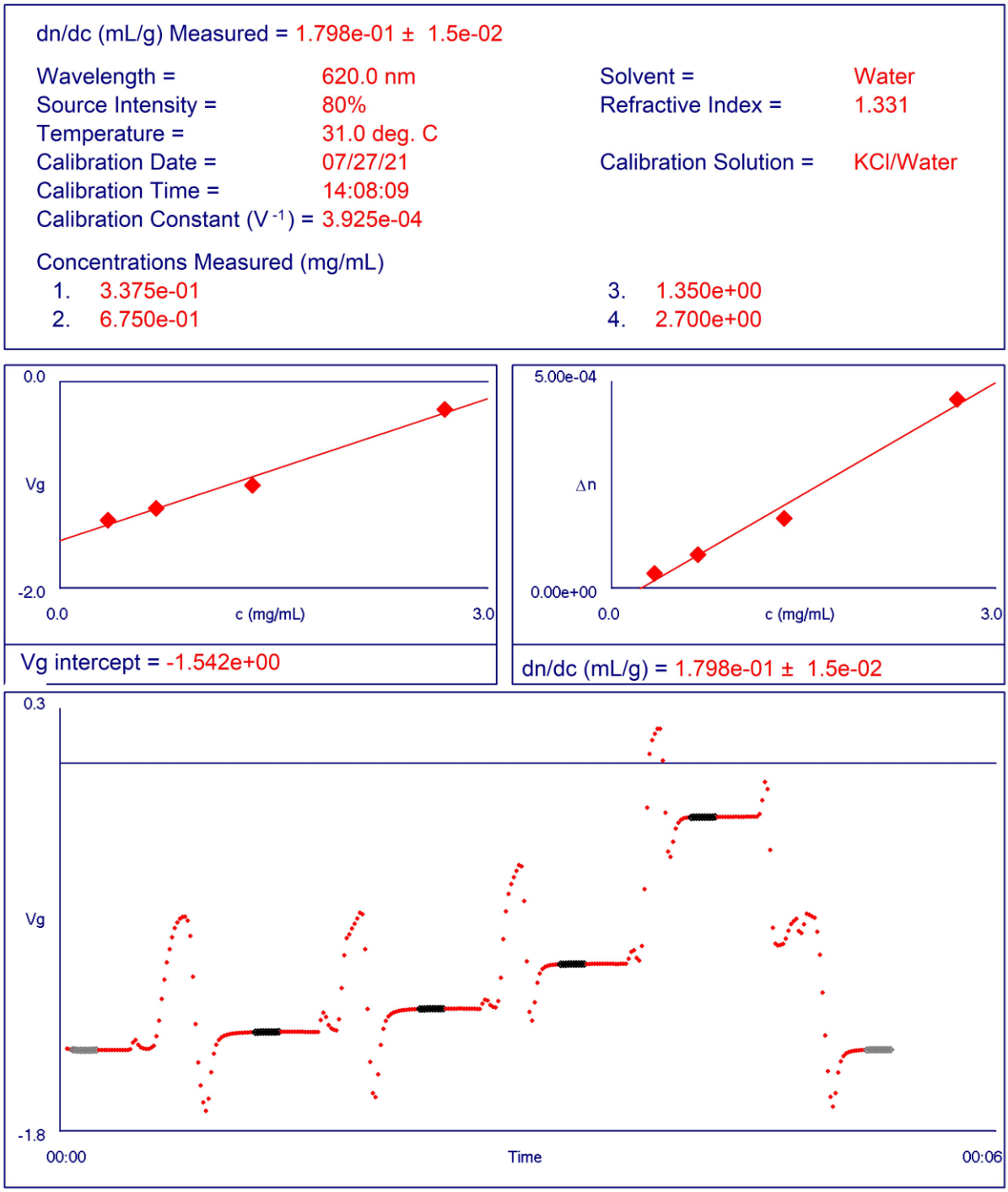

Figure S67. Refractive index increment (d*n*/d*c*) measurement report of **P2** (**pAP**) in PBS

Brookhaven Instruments Corp.
Differential Refractometer Software Ver. 5.32

Date: Jul 29, 2021
Time: 13:05:54

Sample ID **P3, PBS**
Operator ID **PC**
Notes

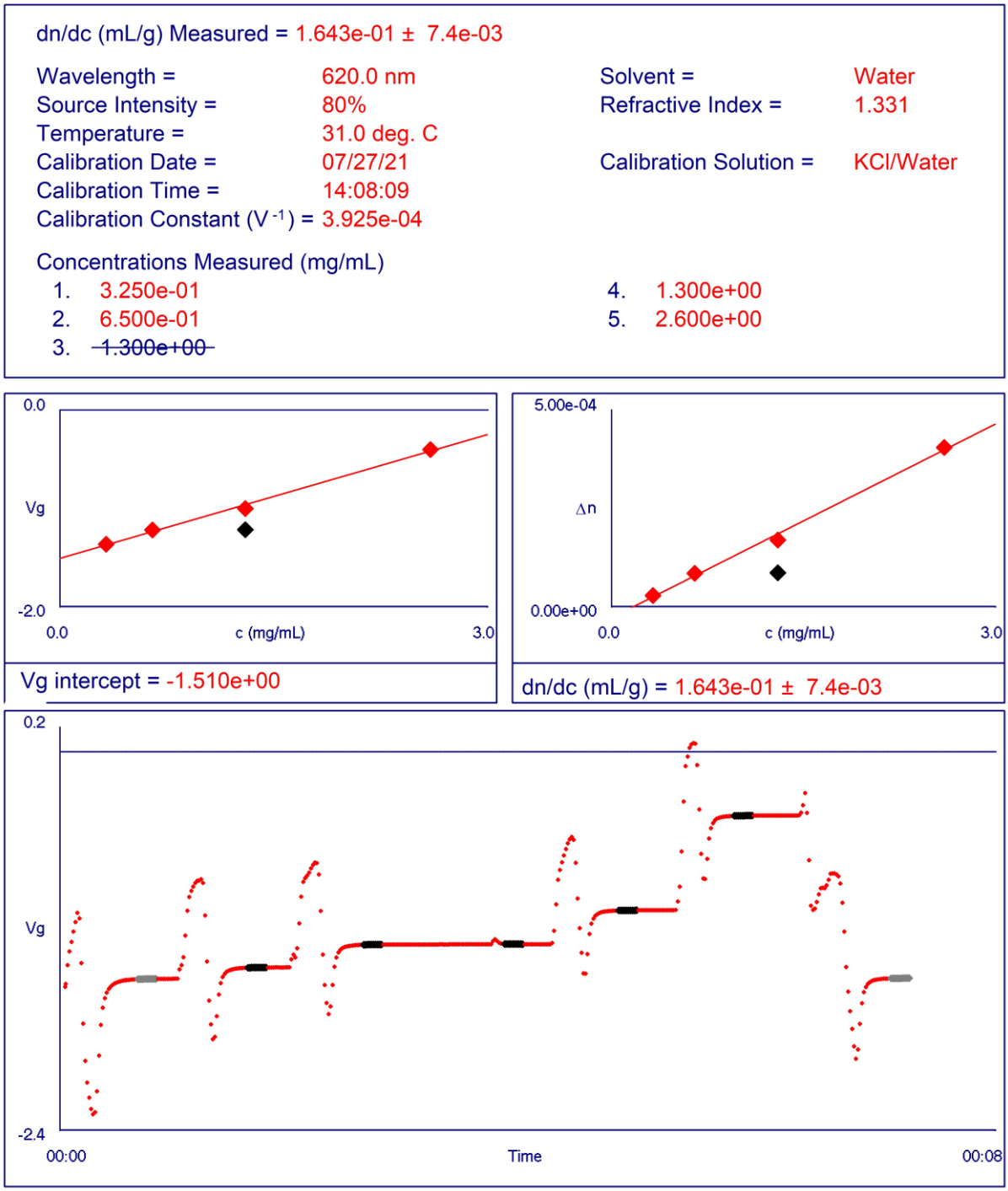

Figure S68. Refractive index increment (d*n*/d*c*) measurement report of **P2** (**pAP**) in PBS

S10. Additional information

S10.1. Heating/cooling cycles of turbidimetry

Some polymers (particularly **pDFEA** and **pDEA**) tend to coalesce into large particles, which may sink, float, or stick to the cuvette. Coalescence is observed in some heating cycles (see, *e.g.*, **Figure S30**): initially small polymer aggregates are formed, and transmittance decreases. However, upon further heating, these small polymer aggregates may coalesce into large assemblies and (in some cases) move out of the detection area. As a result, transmittance increases again. In some samples, the coalesced assemblies occasionally and temporarily obscure the light beam and thus cause fluctuations in transmittance (caused by sample stirring).

Coalescence and polymer sticking/ floating do not prevent us from determining T_{CP} in the heating cycle: T_{CP} is defined by the initial polymer aggregation. For this reason, such a T_{CP} measurement is well reproducible (inter-run variation was mostly within 0.2 °C; see **Figure 3**). Conversely, T_{CP} measurements during the cooling cycle were unreliable – the polymer may behave as intended but may also float away from the laser beam or stick to the glass and thus hinder proper reading (the T_{CP} values in the cooling cycle varied more than 15 °C). We were unsure whether transmittance increased because the polymer aggregates dissolved or because they moved away from the light beam. Therefore, we decided to disregard these values and focus only on the T_{CP} determined during the heating cycle. The cooling cycle in turbidimetry was used merely as a regeneration phase for subsequent heating cycles; the samples remained at 10 °C for 30 minutes, which reliably ensured that all residual polymer aggregates dissolved.

S10.2. Structure-to-properties relationship

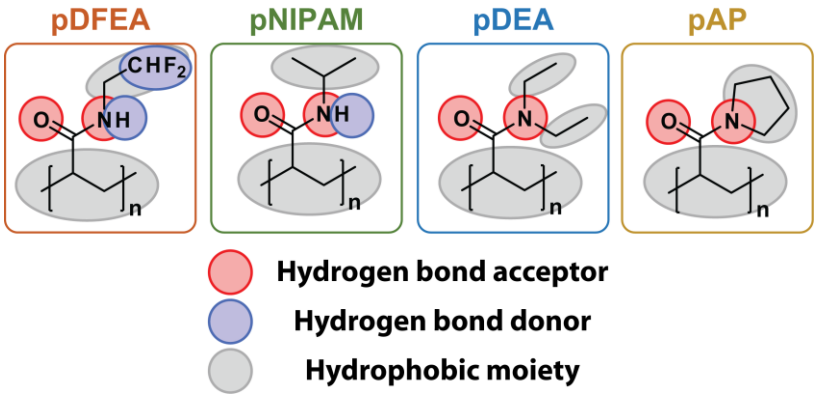

Scheme S2. Hydrogen bond acceptors, donors, and hydrophobic moieties in the molecules.

Zhao *et al*. [S19] suggested, that LCST-type thermoresponsive polymers must be hydrophilic (negative ΔH_m) and that the entropy of mixing (ΔS_m) must be negative as well (see **Scheme S3**). T_{CP} can then be calculated according to **Equation 1**.

$$T_{CP} = \frac{\Delta H_m}{\Delta S_m} \quad (1)$$

The ΔH_m of a polymer correlates with its hydrophilicity. Some researchers rank the hydrophilicity of polymers according to their T_{CP}.[S20] Therefore, the rank of hydrophobicity of the study polymers would be as follows:

pAP ≫ pNIPAM ≈ pDEA > pDFEA

Nevertheless, this approach is most suitable for ranking hydrophilicity of *similar* copolymers (*i.e.* those with *similar* molecular moieties, *e.g.* alkyls). However, **pDFEA** contains -CF_2H moiety, which is somewhat lipophilic, but can also form hydrogen bonds,[S14] decreasing the enthalpy of aggregation and

potentially lowering the T_{CP}. Therefore, we chose a different approach to rank the hydrophilicity of the polymers.

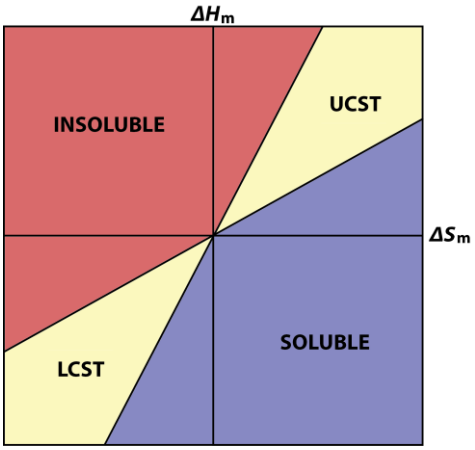

Scheme S3. A thermodynamic map showing the solubility and solution properties of polymers in water, redrawn according to [S19].

Zhao *et al.*[S19] suggests ranking the hydrophilicity of polymers according to the enthalpy of mixing (ΔH_m) of the alkanes (corresponding to the hydrophobic moiety) with water. We were unable to find mixing enthalpy of 1,1-difluoroethane with water in the literature, but the mixing enthalpy should inversely correlate with the solubility of the corresponding alkanes in water, enabling us to estimate the ranks of hydrophilicities of study polymers. The concentration of saturated 1,1-difluoroethane aqueous solution is 50 to 80 mmol/l (0 °C),[S21,S22] ethane 4.2 mmol/l (0 °C),[S22] propane 3.5 mmol/l (4 °C),[S22] and butane 3.1 mmol/l (3 °C).[S22] In this approach, we consider only the "hydrophilicity" of the substituent, and we disregard the effect of ligands on the hydrophilicity of the rest of the acrylamide (due to changes of electron densities on NH). Because 1,1-difluoroethane has (by far) the highest aqueous solubility of all corresponding alkanes, we rank **pDFEA** as the most hydrophilic (contrary to the rank suggested by method in [S20]). Both **pDEA** and **pAP** are di-substituted acrylamides; therefore, we rank them as the least hydrophilic. The cyclic structure of the **pAP** side chain will, however, be more compact, thereby shielding the hydrophilic amide less and being more hydrophilic than pDEA. This approach would suggest the following rank of hydrophilicities of polymers: [note1]

pDFEA ≫ pNIPAM > pAP > pDEA

As shown in the ITC results, **pDFEA** has strong intramolecular interactions, which decrease the aggregation enthalpy, possibly due to its intramolecular hydrogen bonds.[S14] These hydrogen bonds may explain the strong interactions of **pDFEA** with proteins as well.

The ΔS_m is hard to estimate from commonly available material quantities as it is strongly related to the release of 'high energy' hydrating water molecules. In line with this statement, the more hydrophilic **pAP** has a higher T_{CP} as **pDEA** as the hydration ΔS_m will be similar based on the presence of a tertiary amide (**Scheme S2**). Despite the higher hydrophilicity of **pNIPAM** and **pDFEA**, these polymers have a lower T_{CP} than **pAP**, which can be ascribed to the higher ΔS_m resulting from a more efficient hydration thanks to the secondary amide groups (both **pNIPAM** and **pDFEA**) and to the difluoroalkyl group (**pDFEA**).

[note 1] **pDEA** contains two ethyls; therefore, it is considered less hydrophilic than **pNIPAM**. Its monoethyl analogue (poly(ethyl-*N*-acrylamide) would be more hydrophilic than **pNIPAM**; and its T_{CP} is ≈ 73 °C.[S19]

S10.3. Detection of terminal moiety

Detecting these terminal moieties in polymers with M_w around/ above 25 kg/mol is notoriously difficult because of their very low content, broad peaks, noise and trace contaminants (see NMR spectra in ESI).[S23] The terminal CH_3O moiety provides ^{1}H NMR signals at ≈ 3.5-3.6 ppm, and -CH_2CH_2- (from acrylate) provides NMR signals at 2.6 to 2.8 ppm.[S5,S24] Unfortunately, these signals are often partly masked by broad peaks from solvents or polymers (NCH_2, 3.2 to 3.9 ppm; acrylamide peak at ≈ 2.3 ppm; see NMR spectra in ESI). Nevertheless, we remeasured ^{1}H NMR spectra of all polymers in higher concentrations and with a higher number of scans (256 scans), now added to ESI as raw files (available for inspection). We were able to detect signals of terminal -CH_2CH_2-, most pronounced in polymers **F1** and **P1**, where the content of end-moiety is the highest and the end-moiety signals are not masked by polymer signals (**Figure S69**). Therefore, the signals of terminal -CH_2CH_2- serve as an indirect evidence of terminal -$CH_2CH_2COOCH_3$ moiety. The remaining peaks in this region can be attributed to low-molecular weight contaminants (mostly solvents; their peaks are narrow, but the overall integral is low).

We measured ^{1}H-NMR spectra in MeOH-4d solutions because polymers dissolve in MeOH, whose residual peak is found at 3.31 ppm, whereas the peak of water is at 4.78 ppm;[S9] therefore, MeOH does not mask these terminal peaks. DMSO-6d has a peak at 2.50 ppm, and water has a peak at 3.33 ppm; thus, the peaks of these solvents would mask the peaks of interest.[9]

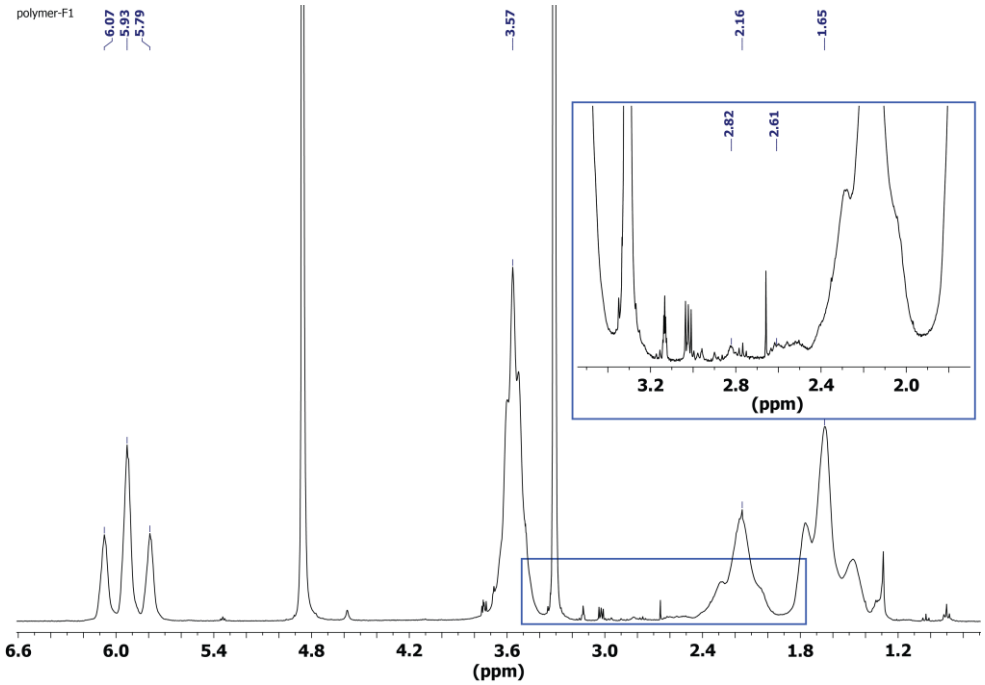

Figure S69. ^{1}H NMR of polymer **F1** in MeOH-4d showing the peaks at 2.6 and 2.8 ppm, corresponding to terminal CH_2CH_2 moieties.[S5,S24] The CH_3O- moiety remained masked by other peaks.

S11. List of used abbreviations and symbols

Abbreviation	**Explanation**
^{1}H NMR	^{1}H nuclear magnetic resonance
^{1}H-^{13}C HSQC-edit NMR	^{1}H-^{13}C multiplicity edited, heteronuclear single quantum coherence spectroscopy nuclear magnetic resonance
^{13}C{^{1}H} NMR	^{13}C nuclear magnetic resonance with ^{1}H decoupling
^{19}F NMR	^{19}F nuclear magnetic resonance
ACVA	4,4'-[(E)-diazenediyl]bis(4-cyanopentanoic acid)
c_x	molar concentration of compound x
ca.	*circa*, approximately
Corp.	corporation
CPT	cloud point temperature
CTA	chain transfer agent
CA	California, state of the USA
D	content of deuterium of all hydrogen atoms (*e.g.* 'in 99.80% D')
d	doublet (in NMR)
dd	doublet of doublets (in NMR)
ddd	doublet of doublets of doublets (in NMR)
d*n*/d*c*	specific refractive index increment
DLS	dynamic light scattering
DMF	dimethylformamide
DSC	differential scanning calorimetry
DMSO	dimethyl sulfoxide
DMSO-6d	perdeuterated dimethyl sulfoxide
E	poly[(*N*,*N*-diethyl)acrylamide]
E$_1$	poly[(*N*,*N*-diethyl)acrylamide], lowest M_w (see **Table 1**)
E$_2$	poly[(*N*,*N*-diethyl)acrylamide], medium M_w (see **Table 1**)
E$_3$	poly[(*N*,*N*-diethyl)acrylamide], highest M_w (see **Table 1**)
F	poly[(*N*-2,2-difluoroethyl)acrylamide]
F$_1$	poly[(*N*-2,2-difluoroethyl)acrylamide], lowest M_w (see **Table 1**)
F$_2$	poly[(*N*-2,2-difluoroethyl)acrylamide], medium M_w (see **Table 1**)
F$_3$	poly[(*N*-2,2-difluoroethyl)acrylamide], highest M_w (see **Table 1**)
FBS	foetal bovine serum (fetal bovine serum in US english)
e.g.	*exempli gratia*, for example
GA UK	Grantová agentura UK (the Charles University Grant Agency)
HSQC	heteronuclear single quantum coherence spectroscopy
I	poly[(*N*-isopropyl)acrylamide]
I$_1$	poly[(*N*-isopropyl)acrylamide], lowest M_w (see **Table 1**)
I$_2$	poly[(*N*-isopropyl)acrylamide], medium M_w (see **Table 1**)
I$_3$	poly[(*N*-isopropyl)acrylamide], highest M_w (see **Table 1**)
i.e.	*id est*; that is
Inc.	incorporation; legal concept of company in the USA
ITC	isothermal titration calorimetry
J	spin-spin coupling constant (J-coupling constant, spin-spin coupling)
LCST	lower critical solution temperature
LFT	lattice fluid theory
LFT-HB	lattice fluid theory with hydrogen bonding correction
NMR	nuclear magnetic resonance
m	multiplet (in NMR)
m_x	mass of compound x

Abbreviation	**Explanation**
MA	Massachusetts, state of the USA
MALS	multiangle light scattering
MeHQ	4-methoxyphenol (mequinol, 4-hydroxyanisole)
MeOH	methanol
MeOH-4d	perdeuterated methanol
MiliQ/MilliQ water	ultrapure water
M_n	number-average molar mass
M_w	weight-average molar mass
n	refractive index
n_x	molar amount of compound x
N/A	not applicable (not available)
No.	number
NY	New York, state of the USA
norm.	normalized
P	poly[(*N*-acryloyl)pyrrolidine]
$\mathbf{P_1}$	poly[(*N*-acryloyl)pyrrolidine], lowest M_w (see **Table 1**)
$\mathbf{P_2}$	poly[(*N*-acryloyl)pyrrolidine], medium M_w (see **Table 1**)
$\mathbf{P_3}$	poly[(*N*-acryloyl)pyrrolidine], highest M_w (see **Table 1**)
PDI	(poly)dispersity index ($Đ_M = M_n/M_w$)
pH	potential of hydrogen
pAP	poly[(*N*-acryloyl)pyrrolidine]
PBS	phosphate saline buffer
pDFEA	poly[(*N*-2,2-difluoroethyl)acrylamide]
pDEA	poly[(*N*,*N*-diethyl)acrylamide]
pNIPAM	poly[(*N*-isopropyl)acrylamide]
ppm	parts per million
$PrNH_2$	propylamine, *n*-propylamine
®	registered trademark (Lanham Trademark Act of 1946)
RI	refractive index
RT	room temperature
rpm	revolutions per minute
RAFT	reversible addition−fragmentation chain-transfer polymerisation
SAXS	small-angle X-ray scattering
SD	standard deviation
SEC	size exclusion chromatography
s.r.o.	private limited company in legal structure of the Czech Republic
T_{CP}	cloud point temperature
t	triplet (in NMR)
TCEP	3,3′,3″-phosphanetriyltripropanoic acid
THF	tetrahydrofuran; oxolane
™	unregistered trademark symbol (Lanham Trademark Act of 1946)
tt	triplet of triplets (in NMR)
tdd	triplet of doublets of doublet (in NMR)
UK	United Kingdom of Great Britain and Northern Ireland
USA	United States of America
UV-vis	ultraviolet/visible light
V_x	volume of compound x
v/v	volume fraction, volume per volume
WA	Washington, state of the USA

Abbreviation	**Explanation**
WAXS	wide-angle X-ray scattering
ΔH	change of enthalpy
ΔH_m	mixing enthalpy
ΔS_m	mixing entropy
$Đ_M$	dispersity index, defined as M_w/M_n
λ	wavelength

S12. Author contributions and Contributor Roles Taxonomy (CRediT)

S12.1. Contributor Roles Taxonomy (CRediT)

Kristýna Kolouchová (K.K.) - Investigation, Methodology, Data curation, Writing – original draft, Writing – review & editing, Visualization, Project administration
Volodymyr Lobaz (V.L.) - Investigation, Methodology, Validation, Formal analysis, Writing – original draft, Data curation
Hynek Beneš (H.B.) - Investigation, Methodology, Data curation
Victor R. de la Rosa (V.R.R.) - Investigation, Methodology, Writing – review & editing
David Babuka (D.B.) - Investigation, Methodology, Data curation, Software
Pavel Švec (P.Šv.) - Validation, Data curation, Methodology, Writing – review & editing
Peter Černoch (P.Č.) - Investigation
Martin Hrubý (M.H.) - Resources, Validation, Funding acquisition, Writing – review & editing
Richard Hoogenboom (R.H.) - Validation, Methodology, Writing – review & editing, Resources, Funding acquisition, Supervision
Petr Štěpánek (P.Št.) – Validation, Methodology, Writing – review & editing
Ondřej Groborz (O.G.) – Conceptualization, Supervision, Methodology, Data curation, Investigation, Formal analysis, Visualization, Project administration, Writing – original draft, Writing – review & editing, Funding acquisition, Resources, Software

S12.2. Author contributions

O.G. conceived the presented idea, K.K. synthesized the monomers, K.K., O.G. synthesized, modified, purified, and characterized the polymers (SEC, NMR). K.K. and V.R.R. measured and evaluated T_{CP} as a function of polymer temperature. V.L. and H.B. measured and evaluated calorimetry data. D.B. collected and evaluated DLS. P.Č. measured the d*n*/d*c* of study polymers. K.K., O.G., V.L., R.H., P.Št., M.H., D.B., H.B., and P.Šv. were involved in methodology design. K.K., O.G., V.L., R.H., P.Št., M.H., D.B., H.B., and P.Šv evaluated the measured data; O.G., K.K., and R.H. have proposed the study strategies, validated data, and formulated the conclusions of the study. M.H., R.H., O.G. and P.Št. and have secured the resources for this study, M.H., O.G. and R.H. have secured its funding. O.G. supervised the project, K.K. and O.G. controlled the project management and administration. O.G. and K.K wrote major parts of the manuscript, R.H., V.R.R., P.Šv, M.H., and P.Št. wrote and/ or reviewed parts of the manuscript.

S13. Additional supplementary files

Processed dynamic light scattering data (DLS data; size of polymer assemblies as a function of solution temperature) can be found in **d1py00843a1.rar** file on the **web of the journal**.

Both processed and non-processed NMR spectra of all polymers can be found in **d1py00843a2.rar** file on the **web of the journal**. The file contains ^{1}H, ^{13}C{^{1}H}, ^{19}F, and ^{1}H-^{13}C multiplicity-edited HSQC NMR spectra of acryloyl pyrrolidine (**AP-momomer**), *N*-(2,2-difluoroethyl)acrylamide (**DFEA-momomer**), poly[(*N*-acryloylpyrrolidine)] (**pAP**), poly[*N*-(2,2-difluoroethyl)acrylamide] (**pDFEA**), poly[(*N*-isopropylacrylamide)] (**pNIPAM**), poly[(*N*-diethylacrylamide)] (**pDEA**) (both processed, as seen in ESI, and non-processed data files). Additionally, this file contains ^{1}H NMR raw spectra of all polymers.

Processed size exclusion chromatograms (SEC traces) can be found in **d1py00843a4.rar** file on the **web of the journal**.

S14. References

S1 K. Tanaka, Y. Hagiwara and K. Noguchi, Rhodium-Catalyzed Regio- and Enantioselective Intermolecular [4+2] Carbocyclization of 4-Alkynals with *N*,*N*-Dialkyl Acrylamides, *Angew. Chem. Int. Ed.*, 2005, **44**, 7260–7263, 10.1002/anie.200502380

S2 J. M. Bak, K.-B. Kim, J.-E. Lee, Y. Park, S. S. Yoon, H. M. Jeong and H. Lee, Thermoresponsive fluorinated polyacrylamides with low cytotoxicity, *Polym. Chem.*, 2013, **4**, 2219–2223, 10.1039/C2PY20747H

S3 J. Chiefari, Y. K. (Bill) Chong, F. Ercole, J. Krstina, J. Jeffery, T. P. T. Le, R. T. A. Mayadunne, G. F. Meijs, C. L. Moad, G. Moad, E. Rizzardo and S. H. Thang, Living Free-Radical Polymerization by Reversible Addition−Fragmentation Chain Transfer: The RAFT Process, *Macromolecules*, 1998, **31**, 5559–5562, 10.1021/ma9804951

S4 A. D. McNaught and A. Wilkinson, *IUPAC. Compendium of Chemical Terminology*, Blackwell Scientific Publications, Oxford, 2nd ed., 1997, 10.1351/goldbook

S5 C. Zhou, M. A. Hillmyer and T. P. Lodge, Micellization and Micellar Aggregation of Poly(ethylene-*alt*-propylene)-*b*-poly(ethylene oxide)-*b*-poly(*N*-isopropylacrylamide) Triblock Terpolymers in Water, *Macromolecules*, 2011, **44**, 1635–1641, 10.1021/ma102786q

S6 J. A. Burns, J. C. Butler, J. Moran and G. M. Whitesides, Selective Reduction of Disulfides by Tris(2-carboxyethyl)phosphine, *J. Org. Chem.*, 1991, **56**, 2648–2650, 10.1021/jo00008a014

S7 J. Schleucher, M. Schwendinger, M. Sattler, P. Schmidt, O. Schedletzky, S. J. Glaser, O. W. Sørensen and C. Griesinger, A general enhancement scheme in heteronuclear multidimensional NMR employing pulsed field gradients, *J. Biomol. NMR*, 1994, **4**, 301–306, 10.1007/BF00175254

S8 L. Kay, P. Keifer and T. Saarinen, Pure absorption gradient enhanced heteronuclear single quantum correlation spectroscopy with improved sensitivity, *J. Am. Chem. Soc.*, 1992, **114**, 10663–10665, 10.1021/ja00052a088

S9 H. E. Gottlieb, V. Kotlyar and A. Nudelman, NMR Chemical Shifts of Common Laboratory Solvents as Trace Impurities, *J. Org. Chem.*, 1997, **62**, 7512–7515, 10.1021/jo971176v

S10 R. Dulbecco and M. Vogt, Plaque formation and isolation of pure lines of poliomyelitis viruses, *J. Exp. Med.*, 1954, **99**, 167–182, 10.1084/jem.99.2.167

S11 Q. Zhang, C. Weber, U. S. Schubert and R. Hoogenboom, Thermoresponsive polymers with lower critical solution temperature: from fundamental aspects and measuring techniques to recommended turbidimetry conditions, *Mater. Horiz.*, 2017, **4**, 109–116, 10.1039/C7MH00016B

S12 J. Jakeš, Regularized Positive Exponential Sum (REPES) Program - A Way of Inverting Laplace Transform Data Obtained by Dynamic Light Scattering, *Collect. Czechoslov. Chem. Commun.*, 1995, **60**, 1781–1797, 10.1135/cccc19951781

S13 T. Wiseman, S. Williston, J. F. Brandts and L.-N. Lin, Rapid measurement of binding constants and heats of binding using a new titration calorimeter, *Anal. Biochem.*, 1989, **179**, 131–137, 10.1016/0003-2697(89)90213-3

S15 Y. Zafrani, D. Yeffet, G. Sod-Moriah, A. Berliner, D. Amir, D. Marciano, E. Gershonov and S. Saphier, Difluoromethyl Bioisostere: Examining the "Lipophilic Hydrogen Bond Donor" Concept, *J. Med. Chem.*, 2017, **60**, 797–804, 10.1021/acs.jmedchem.6b01691

S16 C. Zhao, Z. Ma and X. X. Zhu, Rational design of thermoresponsive polymers in aqueous solutions: A thermodynamics map, *Prog. Polym. Sci.*, 2019, **90**, 269–291, 10.1016/j.progpolymsci.2019.01.001

S14 M. M. Bloksma, D. J. Bakker, C. Weber, R. Hoogenboom and U. S. Schubert, The Effect of Hofmeister Salts on the LCST Transition of Poly(2-oxazoline)s with Varying Hydrophilicity, *Macromol. Rapid Commun.*, 2010, **31**, 724–728, 10.1002/marc.200900843

S17 A. L. Horvath, *Halogenated Hydrocarbons: Solubility-Miscibility with Water*, CRC Press, 1982, 978-0-8247-1166-5

S18 S. H. Yalkowsky, *Handbook of Aqueous Solubility Data*, CRC Press, 2nd edn., 2003, 978-0-203-49039-6

S19 J. U. Izunobi and C. L. Higginbotham, Polymer Molecular Weight Analysis by ^{1}H NMR Spectroscopy, *J. Chem. Educ.*, 2011, **88**, 1098–1104, 10.1021/ed100461v

S20 X.-P. Qiu and F. M. Winnik, Facile and Efficient One-Pot Transformation of RAFT Polymer End Groups via a Mild Aminolysis/Michael Addition Sequence, *Macromol. Rapid Commun.*, 2006, **27**, 1648–1653, 10.1002/marc.200600436

S21 D. Babuka, K. Kolouchová, O. Groborz, Z. Tošner, A. Zhigunov, P. Štěpánek and M. Hrubý, Internal Structure of Thermoresponsive Physically Crosslinked Nanogel of poly[*N*-(2-hydroxypropyl)methacrylamide]-block-poly[*N*-(2,2-difluoroethyl)acrylamide], Prominent ^{19}F MRI Tracer, *Nanomaterials*, 2020, **10**, 2231, 10.3390/nano10112231

S22 D. Babuka, K. Kolouchova, M. Hruby, O. Groborz, Z. Tosner, A. Zhigunov and P. Stepanek, Investigation of the internal structure of thermoresponsive diblock poly(2-methyl-2-oxazoline)-*b*-poly[N-(2,2-difluoroethyl)acrylamide] copolymer nanoparticles, *Eur. Polym. J.*, 2019, **121**, 109306, 10.1016/j.eurpolymj.2019.109306

S23 K. Kolouchova, O. Sedlacek, D. Jirak, D. Babuka, J. Blahut, J. Kotek, M. Vit, J. Trousil, R. Konefał, O. Janouskova, B. Podhorska, M. Slouf and M. Hruby, Self-Assembled Thermoresponsive Polymeric Nanogels for ^{19}F MR Imaging, *Biomacromolecules*, 2018, **19**, 3515–3524, 10.1021/acs.biomac.8b00812

S24 P. Štěpánek, in *Dynamic Light Scattering*, ed. W. Brown, Clarendon Press, Oxford, 1993, p. 760, 978-0-19-853942-1